Final Report

Field Study of Recycled Concrete Aggregate in French Drain

FDOT Contract No.: BDV24-977-19

Prepared by:

Boo Hyun Nam, Ph.D.
Principal Investigator

Adam Lane Perez, M.S.
Graduate Research Assistant

Jinwoo An, Ph.D.
Postdoctoral Research Associate

and

Manoj Chopra, Ph.D.
Faculty Co-Investigator

Department of Civil, Environmental, and Construction Engineering
University of Central Florida
4000 Central Florida Blvd.
Orlando, FL 32816-2450

Submitted to:

Office of Construction
State of Florida Department of Transportation
605 Suwannee Street, MS30
Tallahassee, FL 32399-0450

January, 2019

DISCLAIMER

The opinions, findings, and conclusions expressed in this publication are those of the authors and not necessarily those of the Florida Department of Transportation or the U.S. Department of Transportation.

UNIT CONVERSION

ENGLISH TO METRIC			METRIC TO ENGLISH		
LENGTH (APPROXIMATE)			**LENGTH (APPROXIMATE)**		
1 inch (in)	=	2.5 centimeters (cm)	1 millimeter (mm)	=	0.04 inch (in)
1 foot (ft)	=	30 centimeters (cm)	1 centimeter (cm)	=	0.4 inch (in)
1 yard (yd)	=	0.9 meter (m)	1 meter (m)	=	3.3 feet (ft)
1 mile (mi)	=	1.6 kilometers (km)	1 meter (m)	=	1.1 yards (yd)
			1 kilometer (km)	=	0.6 mile (mi)
AREA (APPROXIMATE)			**AREA (APPROXIMATE)**		
1 square inch (sq in, in^2)	=	6.5 square centimeters (cm^2)	1 square centimeter (cm^2)	=	0.16 square inch (sq in, in^2)
1 square foot (sq ft, ft^2)	=	0.09 square meter (m^2)	1 square meter (m^2)	=	1.2 square yards (sq yd, yd^2)
1 square yard (sq yd, yd^2)	=	0.8 square meter (m^2)	1 square kilometer (km^2)	=	0.4 square mile (sq mi, mi^2)
1 square mile (sq mi, mi^2)	=	2.6 square kilometers (km^2)	10,000 square meters (m^2)	=	1 hectare (ha) = 2.5 acres
1 acre = 0.4 hectare (he)	=	4,000 square meters (m^2)			
MASS - WEIGHT (APPROXIMATE)			**MASS - WEIGHT (APPROXIMATE)**		
1 ounce (oz)	=	28 grams (gm)	1 gram (gm)	=	0.036 ounce (oz)
1 pound (lb)	=	0.45 kilogram (kg)	1 kilogram (kg)	=	2.2 pounds (lb)
1 short ton = 2,000 pounds (lb)	=	0.9 tonne (t)	1 tonne (t)	=	1,000 kilograms (kg)
				=	1.1 short tons
VOLUME (APPROXIMATE)			**VOLUME (APPROXIMATE)**		
1 teaspoon (tsp)	=	5 milliliters (ml)	1 milliliter (ml)	=	0.03 fluid ounce (fl oz)
1 tablespoon (tbsp)	=	15 milliliters (ml)	1 liter (l)	=	2.1 pints (pt)
1 fluid ounce (fl oz)	=	30 milliliters (ml)	1 liter (l)	=	1.06 quarts (qt)
1 cup (c)	=	0.24 liter (l)	1 liter (l)	=	0.26 gallon (gal)
1 pint (pt)	=	0.47 liter (l)			
1 quart (qt)	=	0.96 liter (l)			
1 gallon (gal)	=	3.8 liters (l)			
1 cubic foot (cu ft, ft^3)	=	0.03 cubic meter (m^3)	1 cubic meter (m^3)	=	36 cubic feet (cu ft, ft^3)
1 cubic yard (cu yd, yd^3)	=	0.76 cubic meter (m^3)	1 cubic meter (m^3)	=	1.3 cubic yards (cu yd, yd^3)
TEMPERATURE (EXACT)			**TEMPERATURE (EXACT)**		
[(x-32)(5/9)] °F	=	y °C	[(9/5) y + 32] °C	=	x °F

TECHNICAL REPORT DOCUMENTATION PAGE

1. Report No.	2. Government Accession No.	3. Recipient's Catalog No.
4. Title and Subtitle Field Study of Recycled Concrete Aggregate in French Drain		5. Report Date January, 2019
		6. Performing Organization Code
7. Author(s) Boo Hyun Nam, Adam Lane Perez, Jinwoo An, and Manoj Chopra		8. Performing Organization Report No.
9. Performing Organization Name and Address University of Central Florida 4000 Central Florida Blvd. Orlando, FL 32816-2450		10. Work Unit No. (TRAIS)
		11. Contract or Grant No. BDV24-977-19
12. Sponsoring Agency Name and Address Office of Construction State of Florida Department of Transportation 605 Suwannee Street, MS30 Tallahassee, FL 32399-0450		13. Type of Report and Period Covered Final Report February 2016 – January 2019
		14. Sponsoring Agency Code

15. Supplementary Notes
Mr. John Shoucair of the State Materials Office at the Florida Department of Transportation served as the project manager for this project.

16. Abstract
A field study of recycled concrete aggregate (RCA) in French drains was conducted to evaluate in situ exfiltration drainage performance of RCA as a pipe backfill material. The project was aimed at: (i) developing field test protocols to measure the exfiltration drainage performance of the RCA French drain, (ii) long-term monitoring (12 months in this study) of the field drainage behaviors of RCA French drains, and (iii) investigation of clogging buildup in the drains over time. Four French drains were designed and constructed with different aggregate type and condition, which involve limestone, RCA 'as is', RCA with 2% fines, and RCA with 4% fines. Field and laboratory tests were conducted. First, the flow rate and discharge rate of French drains were monitored for 12 months to evaluate the short- and long-term performances of RCA French drains. Second, permittivity testing was conducted on the geotextile samples taken from the four French drains after 12 months of field conditioning. Third, visual inspection inside the pipes was conducted at 3, 6, 9, and 12 months. Lastly, X-ray diffraction (XRD) tests were conducted on RCA field models, which were embedded underground for 6, 12, and 18 months to identify re-cementation and calcite precipitation.

The results of laboratory and field tests indicated that the drainage performance of RCA French drain is mainly controlled by soil conditions (e.g., groundwater table, permeability of surrounding soils, etc.) and the amounts of excessive fines in the drain system; however, the aggregate type is not a critical factor affecting exfiltration drainage performance. Therefore, it was concluded that RCA in French drains performs similarly to limestone and causes no significant reduction in exfiltration drainage performance.

17. Key Word	18. Distribution Statement
Recycled Concrete Aggregate, French drain, Drainage, Fines, Flow rate, Permeability, and Clogging	No restrictions.

19. Security Classif. (of this report)	20. Security Classif. (of this page)	21. No. of Pages	22. Price
Unclassified.	Unclassified.	141	

Form DOT F 1700.7 (8-72) Reproduction of completed page authorized

ACKNOWLEDGEMENTS

This research was funded by the Research and Development Office of the Florida Department of Transportation (FDOT). Mr. John Shoucair of the FDOT State Materials Office served as the project manager and provided the overall direction for the project.

EXECUTIVE SUMMARY

Recycled concrete aggregate (RCA) is often used as a replacement for virgin aggregate in road foundations, embankments, hot mix asphalt, and Portland cement concrete; however, its applications to exfiltration drainage systems such as French drains is still not common due to unknown field performance and no materials specification of RCA as sub-drainage materials. In this project, a full-scale study of RCA French drains was conducted to evaluate their in situ exfiltration drainage performance with time. The project was aimed at: (i) development of field test protocols to measure the field drainage performance of full-scale RCA French drain, (ii) long-term monitoring (12 month in this study) of the drainage performance and clogging buildup in the in situ RCA French drain systems, and (iii) evaluation of long-term chemical reaction (e.g., calcite precipitation, re-cementation) in RCAs, as a potential source of clogging.

Four outdoor full-scale French drain systems were designed and constructed. Limestone (as control) and RCA ('as is', 2% fines, and 4% fines) were used as pipe backfill materials. A sensing system (e.g., piezometers, flow meter, pipe camera, etc.) was used to measure and monitor the drainage performance and clogging buildup of the drains with time. In addition, in situ RCA field models were prepared to evaluate long-term geochemical reaction such as re-cementation and calcite precipitation in RCAs. The four different aggregate types were embedded underground and then conditioned for 6, 12, or 18 months.

The following field and laboratory tests were then conducted. First, flow rate and discharge rate of the French drains were regularly measured for 12 months to evaluate the field drainage performances of RCA French drain over time. The flow rate was measured by a constant-head infiltration testing method, and the discharge rate was monitored with instrumented piezometers over 24 hours after the water supply was stopped. Second, geotextiles were excavated from the four French drains after 12 months, and the permittivity was measured. Third, X-ray diffraction (XRD) was conducted on those in situ RCA field models with different times to identify the change in re-cementation and calcite precipitation.

The results of field tests indicated that the drainage performance of RCA French drain was mainly controlled by in situ soil conditions (e.g., groundwater table, permeability of surrounding soils, etc.) and the amounts of excessive fines in the drain system; however, the aggregate type was not a critical factor affecting exfiltration drainage performance. Upon a camera inspection of the French drain systems, it was concluded that no surrounding aggregate or precipitation deposited into the pipes. The permittivity test results indicate that RCA with 4% fines shows higher reduction in permittivity measurement after 12-month field conditioning. In addition, RCA with 2% fines and limestone (2.2% fines) drains have similar values of permittivity probably due to a similar amount of fines content. The result of XRD analysis showed a trend that more fines created a higher level of calcite; however, the total amount of calcite precipitation may not be significant in RCA drains. It was concluded that the use of RCA in French drains did not cause a noticeable reduction in the exfiltration drainage performance compared to virgin limestone.

TABLE OF CONTENTS

LIST OF FIGURES

LIST OF TABLES

1. INTRODUCTION

1.1. Problem Statement

In November 2010, FDOT modified Section 901 of its Standard Specifications for Road and Bridge Construction, allowing the use of reclaimed concrete aggregate (RCA) from sources other than FDOT projects. Before the modification, RCA was only allowable in the use of nonstructural concrete applications. RCA was also only allowed in hot bituminous mixtures if it was derived from a concrete mix which was produced and placed in accordance with applicable department specifications. After the modification, the allowable uses include pipe backfill under wet conditions, underdrain aggregate, or concrete meeting the requirements of FDOT Section 347.

The reuse of RCA as drainage material, for instance in base and subbase layer, has shown the potential of clogging of filter-fabric. Generally, the presence of fine particles (or "fines" smaller than 75 μm) in the aggregate causes the clogging of filter fabric, rendering the filter inoperable, or significantly reducing its performance efficiency. The use of RCA in pavement base layers has been associated with reductions in filter fabric permittivity and the accumulation of precipitate and other materials in pavement subdrainage systems (Snyder, M., and Bruinsma, J., 1996). The primary performance concern is the deposition of calcite precipitate and other fines in the drainage system (Snyder and Bruinsma, 1996). Some laboratory studies have shown that RCAs can produce significant calcium carbonate (calcite) deposits while virgin aggregates such as gravel and crushed stone do not (Muethel, 1989 and Tamirisa, 1993). In addition, the fines from RCA may pose another risk if they rehydrate in the pores of the filter fabric. Recementaion of RCAs in stockpiles has been reported.

A French drain collects water from the roadway and transfers the water into slotted pipes underground. The water then filters through coarse aggregate and passes out through a permeable filter fabric. Figure 1.1a shows a schematic diagram of French drain having No. 4 RCA as subdrainage aggregate. Despite the clogging potential mentioned above, the reuse of RCA in French drains has recently received a lot of attention because of the requirement of large aggregate in the drain. The required aggregate is No. 4 gradation (see Figure 1.1b) and can minimize the clogging potential. Although extensive studies on the RCA used as base/subbase material and filler materials in PCC and HMA have been conducted, the RCA in French drain applications has not been studied in the US.

In the previous study, a series of laboratory-scale permeability and clogging tests were conducted to evaluate the drainage performance of RCA No. 4 aggregate (Nam et al., 2014). In permeability and clogging tests, the changes of flow rate by the addition of RCA fines (defined as particles smaller than 75 μm) were measured over time. Testing results could provide insights of RCA material characteristics associated with short- and long-term drainage performance. In particular, the influence of RCA fines was clearly observed by reducing the outflow rate over time. These small-scale tests, however, have revealed some limitations summarized as below.

- The permeability testing simulates the only one-dimensional flow.
- A scale effect cannot be avoided because a small permeameter (9-in. diameter) and a large size of aggregates (No. 4 aggregate) were used.
- Calcite precipitation in the clogging test cannot represent in situ condition.

Therefore, it is necessary to setup in situ/full-scale experiments that simulate three-dimensional flow and to make long term monitoring of performance. The measurements and conclusions will be used to develop or modify Specifications for the Use of RCA in French drains.

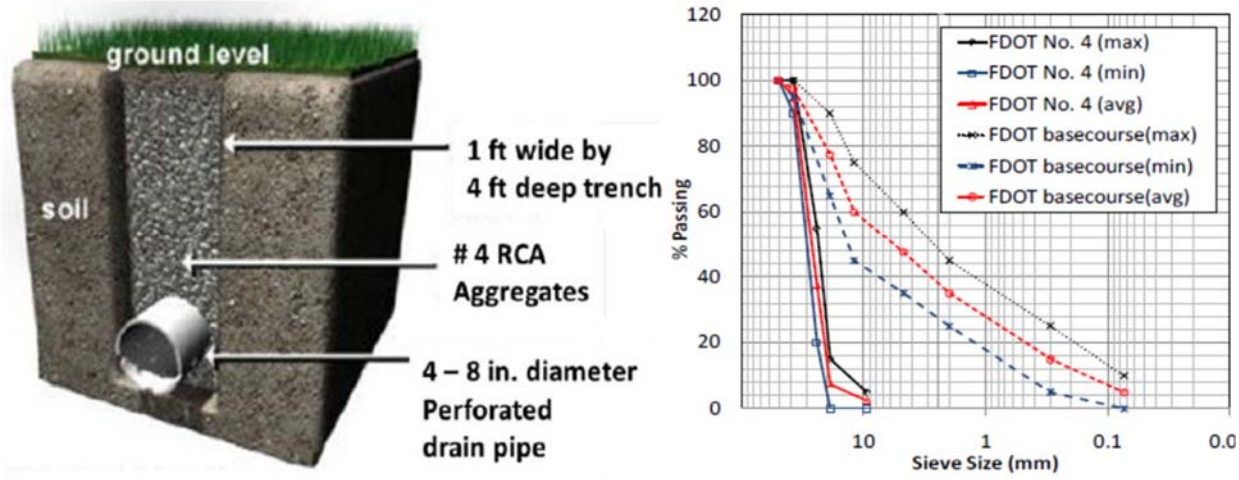

(a) (b)

Figure 1.1: Drainage system with RCA
(Note: (a) schematic diagram of French drain and (b) FDOT No. 4 aggregate gradation)

1.2. Research Objectives

In this study, the researchers proposed construction of in situ, full-scale French drain systems to monitor long term drainage performance, and clogging buildup. As a long-term goal, the researchers investigated the beneficial use of RCAs as sub-drainage material in French drain applications. The objectives of this research on the in situ study of RCA French drain were:

1) to develop field test protocols to measure the field drainage performance of full-scale RCA French drain,
2) to monitor the field exfiltration drainage performance and clogging buildup in the in situ RCA French drain systems, and
3) to evaluate the calcite precipitation and re-cementation in RCAs under in situ environment.

1.3. Organization of Project

The chapters of this report are organized and described as follows:

Chapter 2: This chapter reviews literature of French drain and RCA regarding: 1) Exfiltration Trench (French drain), 2) RCA as drainage material in laboratory-scale experiment, and 3) RCA as drainage material in full-scale or in situ experiment.

Chapter 3: French drain design and construction, including 1) Project site selection, 2) Numerical seepage analysis, 3) Material properties of limestone, RCA and in situ soil, 4) Fine migration test, 5) As-built plans of the field drainage system, and 6) French drain system construction.

Chapter 4: The short- and long-term RCA French drain performance, including 1) Monitored groundwater table depth (GWT), 2) Measured flow rate of French drains, 3) Discharge behavior of French drains by analyzing the data of monitoring wells, 4) Groundwater mounding ana lysis from the data of monitoring wells, 5) Camera inspection of inside perforated pipes, and 6) Geotextile permittivity testing results of the filter Fabric before Installation and after 12 months of field simulation.

Chapter 5: Material characterization, including 1) Material and test description of in situ RCA field model setup, 2) Microstructure analysis using Powder X-ray diffraction (XRD) analysis and 3) Discussion and conclusions on the result of XRD analysis of in situ RCA.

Chapter 6: This chapter presents the conclusion of this research including a summary of the project and results. Recommendations and future work are also summarized.

2. LITERATURE REVIEW

This field study of RCA French drain is a continuation of the previous project (Project Contract No. BDK78 TWO 977-12), entitled as "Evaluating the use of reclaimed concrete aggregate in French drain applications." In-depth literature review on RCA (e.g. production, material properties, applications, etc.) can be found from the technical report (Nam et al. 2014).

2.1. Exfiltration Trench (French drain)

Urban storm water in the United States has been identified as the largest contributor of pollution to coastal waters (Burton and Pitt, 2002). Anthropogenic pollutants mainly produced from traffic related activities are contained in urban storm water runoff. These pollutants include metal elements, suspended solids, inorganic and organic compounds. These contaminates are discharged from urban drainage systems into receiving waters, and notably in especially high concentrations during the "first flush". Parameters that influence the first flush are rainfall intensity, rainfall duration, impervious area and the antecedent dry weather period (Gupta et al. 1996, Wanielista and Yousef 1993, Lee et al 2000). Many researchers have given slightly different definition for what portion of the initial storm water runoff constitutes the "first flush". Wanielista and Yousef (1993) suggested that a significant first flush occurs when 50% of the total cumulative pollutant mass is transported within the first 25% of the total runoff volume, 25/50. Bertrand-Krajewski et al. (1998) established a stricter definition of a significant first flush as the occurrence of 80% of the total contaminates being contained int the first 30% of the total runoff volume, 30/80. Roughly speaking, the initial half inch of storm water runoff may be considered the first flush, because this volume usually caries the highest concentrations of pollutants (Branscome, J., and Tomasello, S. R., 1987).

Exfiltration trenches are used in many urban developments to treat the first flush of storm water runoff. A study by the United States Environmental Protection Agency's Nationwide Urban Runoff Program has shown that heavy metal contained in the run off are removed from the infiltrating waters within the first few centimeters of soil (Nightingale 1989). Unlike detention ponds, exfiltration trenches do not require the use of large land surface areas because they are subterranean structures, which may be a big advantage in dense urban areas. Exfiltration trench systems are similar to French drain systems in that they are both subsurface structures including a perforated pipe, filter material (coarse aggregate), fine drainage materials (sand and pea gravel), and filter fabric. Some drainage fields consist of a series of exfiltration trenches used in conjunction with septic tanks where the effluent from septic tanks are distributed through a drain field and the water exits the perforated pipes and filters through the aggregate, then the treated water is allowed to percolate into the native soil. Exfiltration trenches are especially useful when there is limited land area to devote to storm water management (St. Johns River Management District, 2010). System design must consider such things as existing utilities and infrastructure, building environment (e.g. neighboring basements and foundations), groundwater levels, soil permeability, and economical aspects.
The storage volume of the exfiltration system will depend on the dimensions of the trench and the porosity of the gravel, whereas the exfiltration volume will depend on a multitude of factors. Under

ideal conditions, the exfiltration rate of a single exfiltration trench should depend on surface area of the trench available for exfiltration, geotextile permittivity, soil layer dimensions and permeabilities, presence of any impermeable boundaries close to the French drain, time from beginning of exfiltration, and head difference across the system (Branscome, 1987). Fundamentally, exfiltration system provides stormwater detention and infiltration into the surrounding soils, thus helping to restore the pre-development hydrology (Mikkelsen et al., 1996). They also filter pollutants, therefore improving the quality of urban runoff (Pratt and Powell, 1993).

A notable systemic source of failure for an exfiltration system includes the site itself. Two specific conditions regarding the site for construction of an exfiltration system should be considered. The flow of stormwater can be severely decreased or even stopped if the surrounding soils have a low permeability, or if the location of the construction site has a high groundwater table. In such cases, it is likely that the exfiltration system would have limited effect (Barraud et al., 1999).

Clogging represents the greatest source of failure in exfiltration systems (Galli, 1992; Nozi et al., 1999; Raimbault et al., 1999; Warnaars et al., 1999). The failure of an exfiltration system would best be considered by the flow of stormwater exceeding its storage capacity, as well as certain other types of failure, such as having an adverse effect on the environment or the potential for the surrounding soils to become substantially altered by water retention. In the case of an exfiltration system negatively affecting the environment, the system itself would not create the environmental pollution; however, it could be a factor in spreading or retaining contaminants. When water in the surrounding soils is increased by the presence of an exfiltration system, it could create adverse conditions for the foundations of nearby buildings. Most likely, damage to nearby building foundations would be caused by not adhering to reasonable requirements for buffers associated with the exfiltration system (Alfakih et al., 1999; Argue and Pezzaniti, 2006). The processes that creates clogging can be physical, biological or chemical, with the most common being physical (Bouwer, 2002). The primary cause of clogging is the infiltration of sediments into the system, which become deposited in ways in which the system is unable to remove the material. These sediments ultimately cause a reduction in permeability and porosity within the system, thus sharply decreasing the rate of infiltration.

Several studies have been conducted regarding the overall issues of clogging. As one of studies, a field survey about stormwater exfiltration systems was conducted in the state of Maryland, US in 1986. In this survey by Lindsey et al. (1992), of 207 systems, a majority of which were only around 2 years old, 33% had become unfunctional due to clogs. After repeating the survey again just 4 years later in 1990, it was found that altogether no less than half of the systems had failed. A substantial number of cases exist where pre-treatment practices were employed to mitigate potential clogging, yet the system still failed due to clogging. (Barrett and Taylor, 2004; Bouwer, 2002).

Previous studies from laboratory-scale tests concluded that the location of clogging most likely occurs at the convergence of the soil surrounding the system and the media directly involve with filtration (Pokrajac and Deletic, 2002). The filter media, as a source of clogging, has also been studied, as a common occurrence in various disciplines involving water resources and management,

including urban drainage systems, vertical-flow wetlands (constructed) (Langergraber et al., 2003), recharge basins (Rinck-Pfeiffer et al., 2000), wells for groundwater recharge (Goodrich et al., 1990), drainage layers (Row et al., 2000), and many involving filters for potable water (Reddi et al., 2000), Additional research involving understanding the timeframe for the failure of a system due to clogging was conducted by Ishizaki et al. (1996), with conclusions regarding the type of associated area being impervious to varying degrees. In one case study, the frequency of an overflow event in the exfiltration system was increased due to clogging, though this conclusion by Warnaars et al. (1998) is hardly unexpected. Accounting for an excess of variables as well as a difficulty in controlling the scope of each study makes interpreting the results from the existing research, as well as generalizing effective expectations, problematic and potentially inappropriate. However, there is no guarantee whether the findings from these studies can be transferred to the exfiltration system.

2.2. RCA as Drainage Material

2.2.1. Laboratory-Scale Experiment

The utilization of RCA as pipe backfill or drainage materials in exfiltration trench system has been studied recently from the short- and long- term performance perspective in laboratory-scale experiment. Laboratory-scale experiment regarding RCA is important because it provides insight into cause-and-effect of RCA as a drainage material by demonstrating what outcome occurs when particular factors such as the size of RCA, fine content, and RCA from different sources, etc. are manipulated. Previous studies have investigated the chemical and physical properties and behaviors of RCA as well as, the permeability performance of RCA (Snyder and Bruinsma, 1996, Song et al. 2011, and Nam et al. 2014).

According to recent research studies, drainage performance of a exfiltration drain system can be reduced significantly with certain chemical components of RCA such as unhydrated cement grain, portlandite ($Ca(OH)_2$) and calcite ($CaCO_3$), etc. because these chemical components have a chemical clogging potential of French drain system, especially geotextile. Nam et al. (2014) reports the issue of material variability when RCA is used as a drainage material because chemical components of RCA can significantly vary depending on original source and storage time and environment. The chemical components of RCA differ greatly from those of virgin aggregates primarily due to the existence of mortar attached to the aggregate. The original coarse aggregate type contributes to the amount of mortar content in that, smooth rounded coarse aggregates tend to break apart at the aggregate-mortar interface during the crushing processes. A Canadian study on RCA (Fathifazl, 2008) reported the mortar content of RCA can be as high as 41 percent by volume depending on the original concrete mix proportions and crushing operations. Several studies also reported the problem of re-cementation activity and accumulation of calcium carbonate precipitation of RCA, depositing onto the geotextiles of subsurface drainage systems (Snyder, 1995; Muethel, 1989; Tamirisa, 1993). Kim et al. (2014) investigated the potential of re-

cementation activity of RCA and concluded that relatively old RCA does not contain unhydrated cement grains; thus, no significant re-cementation reactivity. However, as previously mentioned, the chemical and physical properties of RCA can vary depending on original source and storage time and environment. Nam et al. (2014) proposed an accelerated method of calcite precipitation that can be a cause of long-term clogging in RCA drainage systems.

Some studies also pointed out the problem of fine content generated from RCA. The L.A. abrasion of RCA is generally higher than other virgin aggregates because it is a mixture of several different materials such as fine and coarse aggregate and paste. In other words, RCA is heterogeneous, porous and contains residual impurities, thus it can be more vulnerable to abrasion in comparison with other virgin aggregates. Hiller et al. (2011) reports that the gradation of the RCA should be considered, as the amounts of fines in the aggregate can contribute to the clogging potential of the drainage system.

2.2.2. Full-Scale and In Situ Experiment

There is not much research related to full-scale or in situ experiment of RCA as a drainage material in an exfiltration drainage system. However, some states have tested and used RCA as a backfill material in base and subbase layers of pavement. Researchers who used RCA as a backfill material have concluded that RCA shows poor permeability characteristics (Song et al. 2011; Bennert and Maher 2008; Paige-Green 2010). Other studies show that the clogging can be caused by recementation and the accumulation of calcite precipitation (Song et al. 2011; Snyder 1995; Muethel 1989; Tamirisa 1993). The study that was performed by Minnesota Department of Transportation (MnDOT) found that 17 to 84% permittivity loss in geotextile filter fabric over 8 years was a result of calcite precipitation, while the remaining loss was a result of noncarbonate material (RCA fine) (Snyder and Bruinsma 1996) Another study on the Lakeville test beds in 1989 showed that after 3 years 70% of the loss of permittivity in filter fabric was due to calcite while the remaining 30% was due to noncarbonate material (Bruinsma et al. 1997).

The reduction of geotextile permittivity has been an associated issue for the use of RCA as a base course in pavement systems. This is typically because of the accumulation of calcium carbonate precipitation and fines from RCAs, depositing onto the geotextiles of subsurface drainage systems (Snyder, M., and Bruinsma, J., 1996). Therefore, it is essential to develop a full-scale/in situ RCA French drain system to understand the potential for geotextile clogging and to determine possible fines migration. Based on the results of flowrate and discharge behavior of a full-scale/in situ RCA French drain system, the beneficial use of RCAs as a drainage material in French drain application can be well understood.

2.3. Economic and environmental impacts of RCA

Recycling of construction and demolition (C&D) wastes is beneficial from both economic and environmental perspectives. RCA has been considered and reused in the construction sector for various applications because concrete is one of the main C&D wastes streams, as well as the most heavily used material in construction. For the economical aspect, utilizing RCA can not only reduce the consumption of primary (natural) aggregates, which is normally more expensive than RCA, but also the manufacturing process cost. For the environmental aspect, using RCA can reduce the emission of carbon dioxide (CO2), and also save limited landfills and natural resources.

Life Cycle Assessment (LCA) has been performed by many researchers to evaluate the economic and environmental impacts of utilizing RCA on the construction sector. Simion et al. (2013) analyzed the environmental impact of both crushed natural and recycled aggregates by using data from Bundesamt für Umwelt, Wald und Landschaft (BUWAL) 250 and other literatures. They found that using RCA can reduce Global Warming Potential (GWP) seven times lower than natural aggregates. Knoeri et al. (2013) reported that the environmental impacts can be reduced about 70% when recycled aggregates are used instead of conventional aggregates. Estanqueiro et al. (2016) also reported positive impacts of using evaluated the effect of RCA on the environment. Braga et al. (2017) concluded that the use of RCA can noticeably reduce the environmental impacts as well as material costs.

In this section, a literature review on the economic and environmental quantitative comparison between RCA and the conventional aggregate has been investigated and summarized in tables to show quantifiable economic and environmental benefits of recycling RCA in the construction sector. Figures 2.1 and 2.2 show flow charts of the manufacturing processes of natural aggregate and RCA.

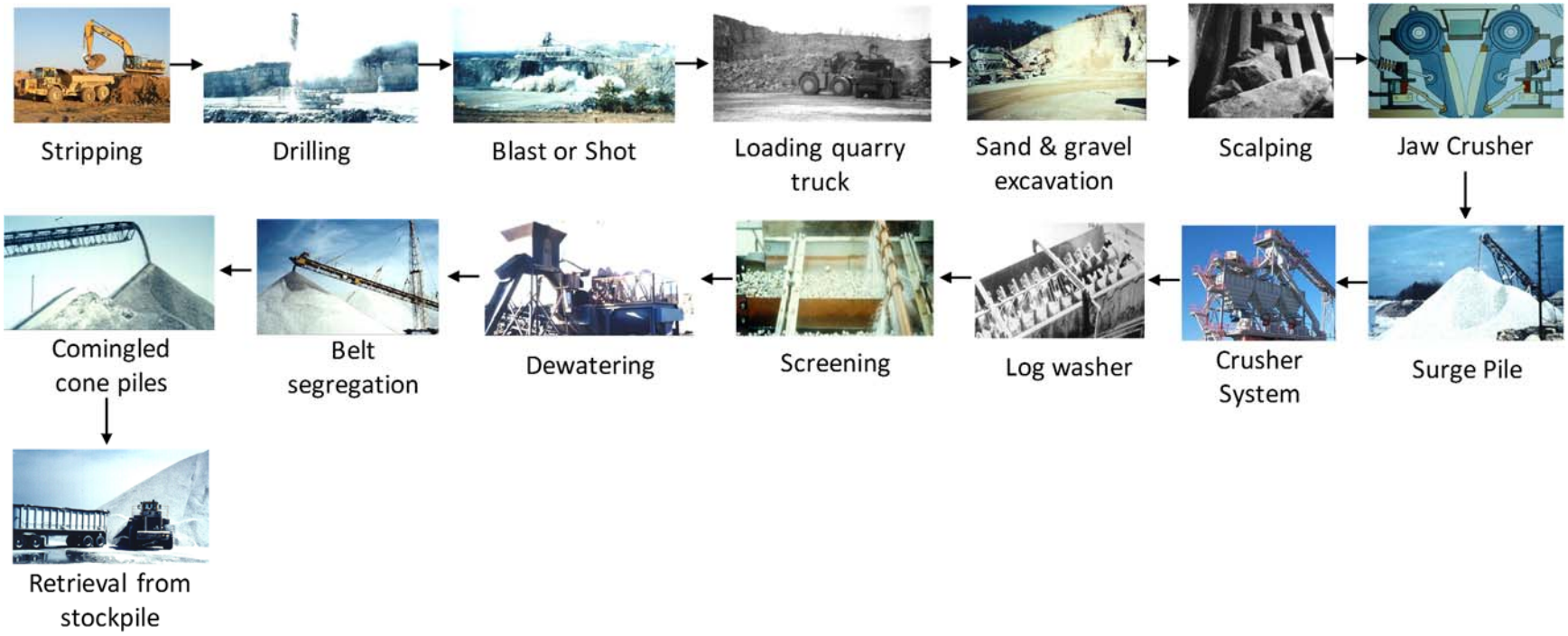

Figure 2.1: Flow chart of conventional aggregate preparation process

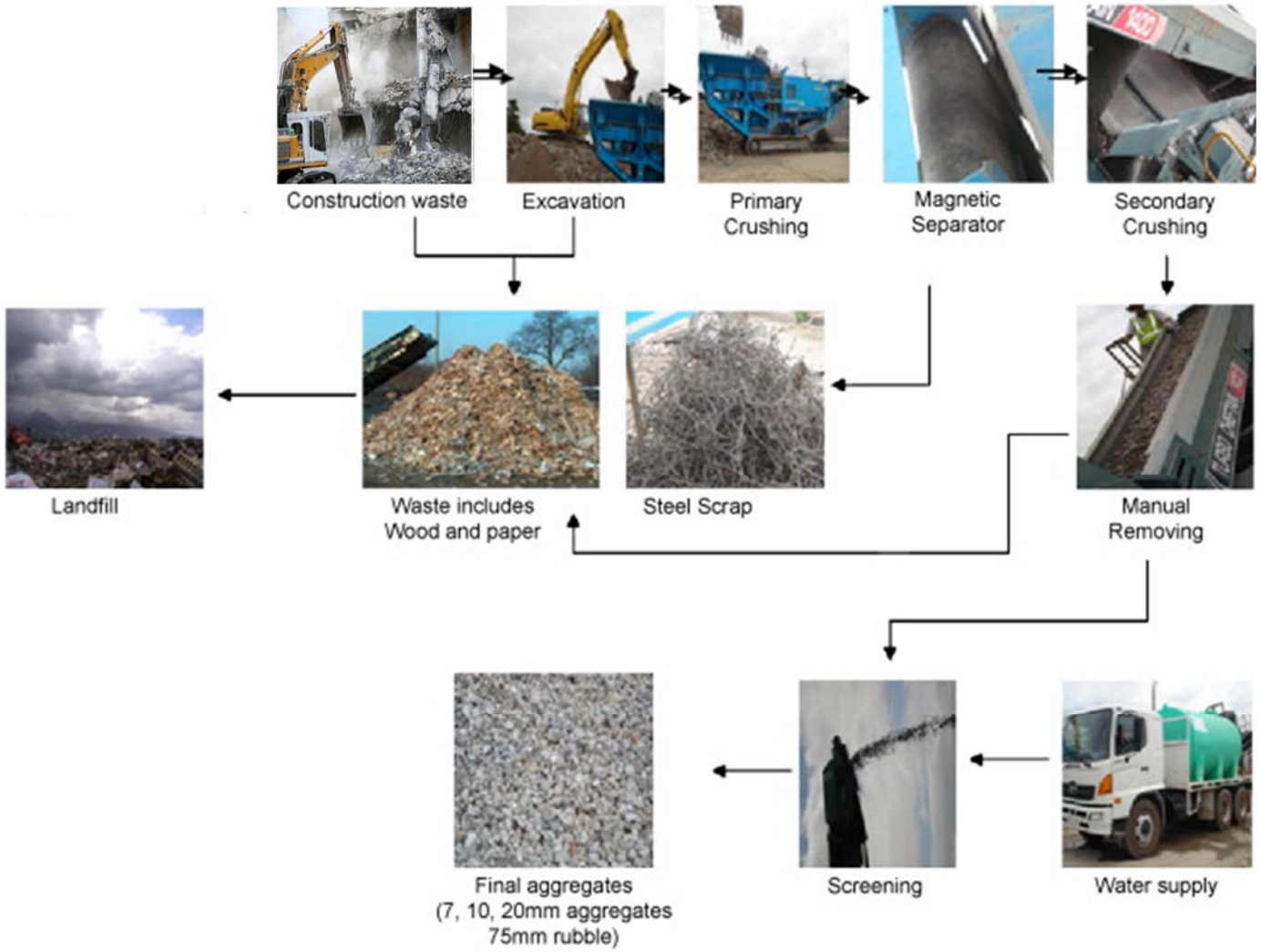

Figure 2.2: Flow chart of RCA preparation process (Tam, V. W. Y., 2008)

Figure 2.1 describes the total process of natural aggregate production from extraction (or stripping) through stockpiling. Figure 2.2 shows the entire process steps of concrete recycling method from construction waste to stockpiling. Based on the flow charts in Figures 2.1 and 2.2, the tools used under each of the aggregate production phase are summarized in Table 2.1. The main sources of CO2 emissions throughout the aggregate production are generated from the combustion of fuels used by on site electricity generators, production equipment and transport vehicles. Atmospheric emissions which include dust emission have multiple sources such as blasting, drilling, crushing and traffic on unpaved road, etc. One of the benefits of using either recycled or secondary aggregate is the reduction of CO2 emissions. As can be seen in Table 2.1, recycled aggregate production uses lesser tools than conventional aggregate production.

Table 2.1: Aggregate Industry corresponding tools regarding carbon footprint (Korre, A. and Durucan, S., 2009)

Aggregate Industry tool	Life cycle phase				
	Extraction	Processing	Restoration	Materials Transfer	Off-site Transfer
Crushed rock tool	√	√	√		
Recycled concrete aggregate tool		√			
Product distribution tool				√	√

Braga et al. (2017) used eight environmental categories, which are abiotic depletion (ADP), global warming (GWP), ozone depletion (ODP), acidification (AP), eutrophication potential (EP), and photochemical ozone creation (POCP) potential, and consumption of primary energy, renewable (PE-Re) and non-renewable (PE-NRe), to compare those environmental measures between conventional aggregate and RCA. Tables 2.2 and 2.3 present the comparison results of those environmental measures. To evaluate the economic impact of reusing RCA, the material costs of limestone, granite aggregates and RCA were also compared. The difference and reduction rate between the conventional aggregates and RCA were also calculated for the comparison. According to the results shown in Tables 2 and 3, the material cost can be reduced up to 47.82% by using RCA instead of the conventional limestone aggregate. As seen also in Tables 2.2 and 2.3, the use of RCA can significantly reduce the environmental impacts. For example, GWP, which is the indicator of CO2 emission, can be reduced 76.31 and 69.52% when RCA replaces limestone and granite aggregates, respectively. In summary, the economic and environmental quantitative comparison between the conventional aggregates and RCA show significant cost and environmental benefits of RCA compared to conventional aggregates and reduces GWP.

Table 2.2: Economic and environmental quantitative comparison between conventional aggregates and RCA

Aggregate Type	Cost ton ($)	GWP kg CO_2 eq	ODP kg CFC-11 eq	POCP kg C_2H_4 eq	AP kg SO_2 eq	EP kg PO_4^{-3} eq	ADP kg Sb eq
Limestone aggregate	48	3.14E-2	2.09E-10	1.03E-5	1.75E-4	3.90E-5	1.39E-9
RCA	25	7.44E-3	1.60E-10	2.14E-6	4.05E-5	9.28E-6	2.12E-10
Difference	23	2.39E-2	4.90E-11	8.16E-6	1.34E-4	2.97E-5	1.18E-9
Reduction rate (%)	47.92	76.31	23.45	79.23	76.86	76.21	84.75

(note: GWP -global warming potential; ODP -ozone depletion potential; POCP - photochemical ozone creation potential; AP -acidification potential; EP -eutrophication potential; ADP - abiotic depletion potential)

Table 2.3: Economic and environmental quantitative comparison between conventional aggregates and RCA

Aggregate Type	Cost ton ($)	GWP kg CO_2 eq	ODP kg CFC-11 eq	POCP kg C_2H_4 eq	AP kg SO_2 eq	EP kg PO_4^{-3} eq	ADP kg Sb eq
Granite aggregate	47	2.44E-2	2.43E-10	7.83E-6	1.44E-4	3.18E-5	1.09E-9
RCA	25	7.44E-3	1.60E-10	2.14E-6	4.05E-5	9.28E-6	2.12E-10
Difference	22	1.69E-2	8.30E-11	5.69E-6	1.03E-4	2.25E-5	8.78E-10
Reduction rate (%)	46.81	69.51	34.16	72.67	71.88	70.82	80.55

3. DESIGN AND CONSTRUCTION OF FRENCH DRAIN

3.1. Project Site

The French drain project site was evaluated and selected through the discussion between the researchers, Project Manager (PM), and the University of Central Florida Department of Landscape and Natural Resources. Based on the ease of access and available space, the University of Central Florida Stormwater Academy was chosen as the property to accommodate the experiment. Located at the southwest corner of the Stormwater Academy and adjacent to Ara Drive was a grassed lot that was chosen to contain the experiment. The project site incorporated four French drains with a total of twenty-five groundwater monitoring wells.

3.1.1. Project Site Selection

Having an adequate water supply source was the major concern in selecting the French drain project site, thus two locations were evaluated at the Stormwater Academy. The originally proposed location at the north side of the property had access to a nearby water tank; however, two issues were discovered. The first issue was that trees, underground utilities, a large mound of soil fill, and a retention pond strictly confined the proposed project site, with the concern being that theses boundary conditions would affect the in situ performance of the French drains. The second issue was that the 1,500 gallons water tank may not have enough capacity for testing. In addition, the water tank would supply water with a falling head, which is less desirable over a constant head water supply for this experiment. Therefore, the researchers evaluated an alternate project site located at the southwest corner of the property. The alternate project site was absent of the boundary condition issues identified at the original project site, except for utilities at both ends of the French drain systems. Because the flow at the tips of the French drains were assumed to be negligible, the presence of the utilities was therefore not an issue. A fire hydrant adjacent to the alternate project site provided a water source with a constant head and high flow rate. The alternate project site was selected as the official project site for the experiment and is shown in Figure 3.1, located on the University of Central Florida Stormwater Academy property (GPS coordinates: 28.591607, -81.189902).

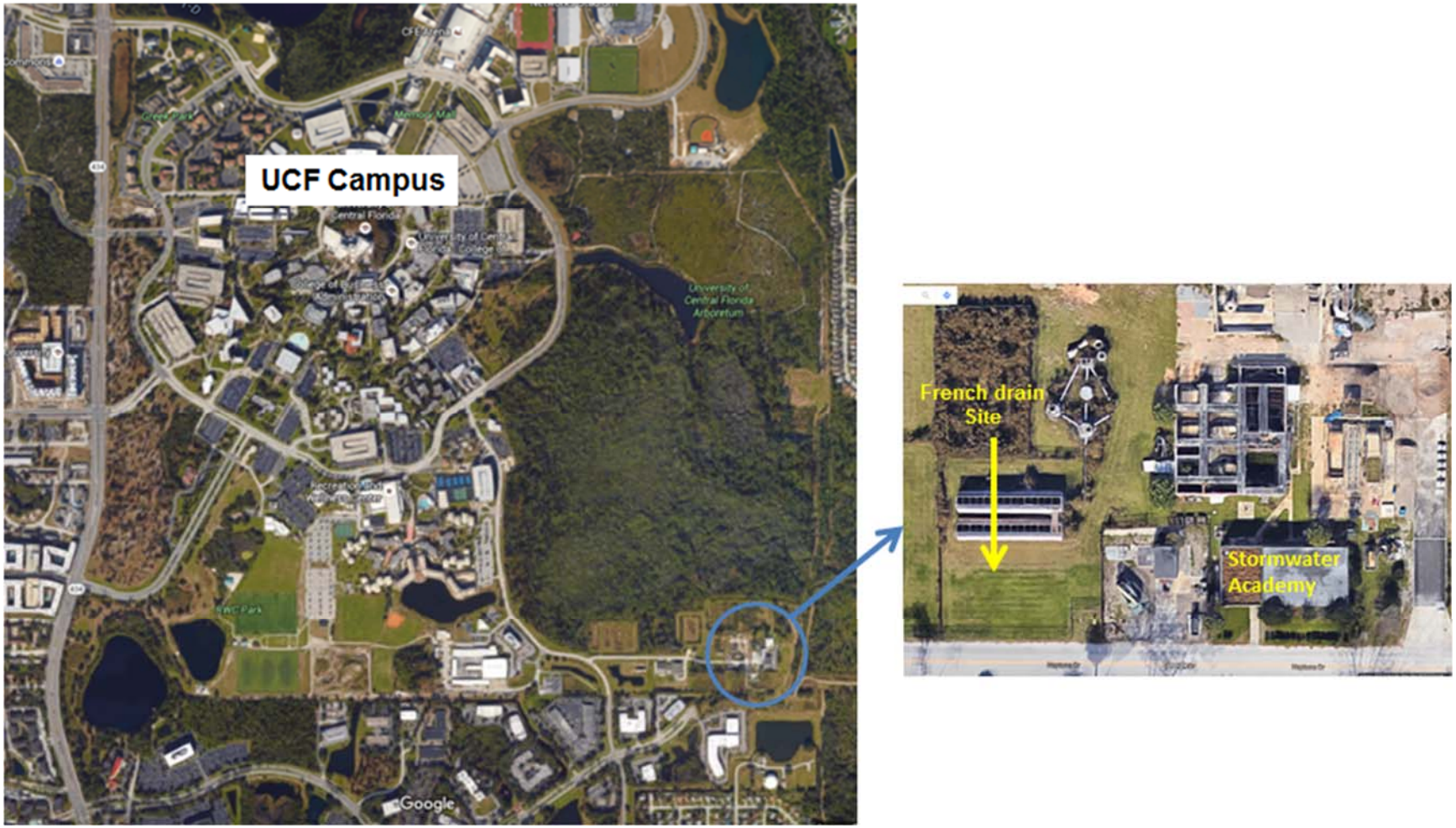

Figure 3.1: Aerial view of UCF campus showing the French drain project site

3.1.2. Project Site Layout

Sunshine 811 performed a subsurface survey (Ticket #: 162606535) to locate existing underground utilities at the site, the results of the survey are shown in Figure 3.2. Information regarding utilities and fence location was then used as design considerations. The dimensions and the separation distances of the French drain systems were dependent upon the available area confined by the unknown utility to the north, electrical utility to the south, and fencing to the east and west. A French drain system length of 23 ft allows for approximately 3 ft of clearance between each end of the system and the electrical and unknown utility lines. A drain width of 4 ft allows the drains to be spaced out 14 ft apart. The plan view with detail spacing information is also shown in Figure 3.2. A finite element analysis was performed in Section 3.2 to check if 14 ft was sufficient spacing between the French drains.

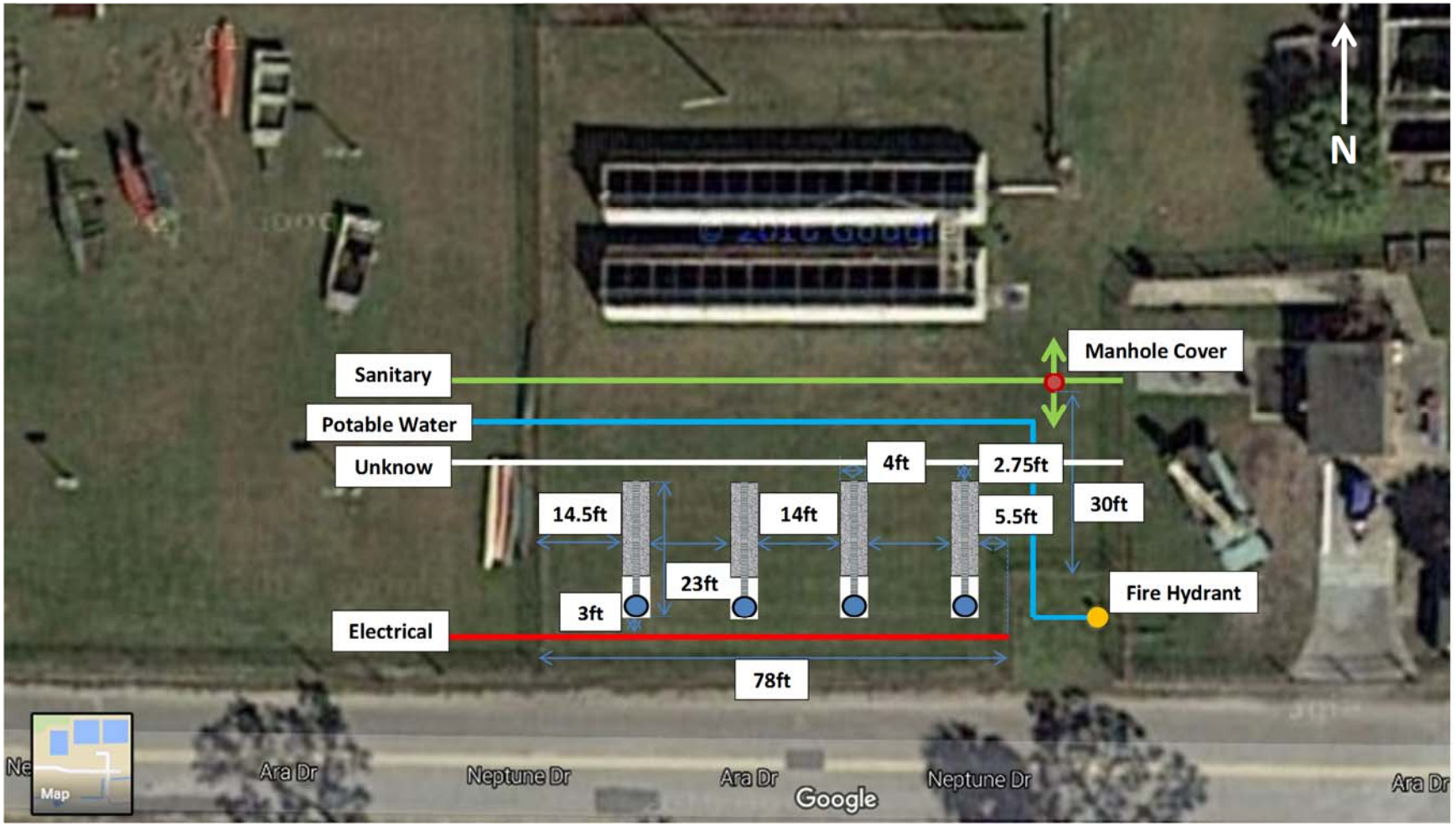

Figure 3.2: Project site location and description

Water supply was a key component of the in situ French drain experiment. The site had access to a fire hydrant which was located to the east of the site on the other side of the fence, see Figure 3.3. Being an orange top fire hydrant, the flow rate was rated between 500-999 gpm. Permission to use the fire hydrant for experimental purposes was requested to and granted by the University of Central Florida Utilities and Energy Services department, who also supplied a flow meter and backflow preventer for the fire hydrant.

Figure 3.3: On site fire hydrant with Badger flow meter and Watts backflow prevent

3.2. Seepage Analysis

Numerical seepage analysis of a single French drain in operation was performed to check if 14 ft between French drains was sufficient spacing to avoid significantly altering the flow behavior of the drain being tested. In addition, an order of magnitude estimation for the steady-state flow rate of the French drain and total water consumption for a single field test was desired. The program chosen to perform the numerical seepage analysis was SEEP/W 2007, a product of GEOSLOPE International Ltd. SEEP/W, which is a finite element method (FEM) program that models the soil-seepage system as whole and continuous.

3.2.1. Numerical Modeling

Geometry: The numerical model for this analysis was composed of three objects. The first object, which makes up most of the model was the in situ soil. The second object was a 4-ft-wide by 3.5-ft-high aggregate box that was 0.25 ft below the ground surface. The last object was a 1-ft diameter pipe located within the aggregate, representing the perforated drainage pipe. The boundaries of the model were located seven times the distance of the respective French drain dimension to avoid boundary interference. The FEM mesh was set to 0.25 ft.

Material Properties: The material properties of the in situ soil were obtained through an open excavation test trench in the field. As mentioned in Section 3.3, the in situ soil profile was found to contain three layers along the depth of the excavation. The weighted average based on layer thickness produced an average hydraulic conductivity of 7.93×10^{-5} ft/sec and an average porosity of 0.46. The No. 4 aggregate was assigned typical values found for gravel, a hydraulic conductivity of 0.328 ft/sec and a porosity of 0.3. The seepage rate of the French drain was more sensitive to changes in the properties of the in situ soil as compared to the No. 4 aggregate because the in situ soil was approximately three to four orders of magnitude more restrictive to flow, thus controlling the equivalent hydraulic conductivity of the French drain system. The pipe was not assigned any material properties because it was considered a boundary condition. The effect of partial saturation on the in situ soil was omitted from the analysis. The hydraulic conductivity of the in situ soil and aggregate was assumed to be isotropic.

Boundary Conditions: Two boundary conditions were used. The first was a total head boundary condition located at the base of the in situ soil layer. This boundary condition could be assigned different total heads to adjust the depth of the water table to any desired elevation. The secondary boundary condition was a total head applied to the perimeter of the 1-ft diameter pipe and the value was kept constant, with a total head equal to the elevation of the top of the French drain aggregate box, which simulates the maximum practical operational water elevation in the sump. The difference between the two boundary conditions was the head difference needed to initiate fluid flow in the numerical model.

3.2.2. Analysis and Results

A total of six cases were analyzed. Cases 1-3 were control cases and model a single French drain in the soil profile. These cases displayed the behavior of a French drain absent the possibility of interference from adjacent French drains. In Figure 3.4, three French drains can be seen. The middle drain was the only drain incorporated into the model, the drains 14 ft away from the center drain are strictly for illustrative purposes and have no effect on the model. Case 1, Case 2, and Case 3 represent the groundwater table having an elevation at the bottom of the pipe invert, base of the French drain, and three feet below the base of the French drain, respectively. Cases 4-6 test for any influence adjacent French drains located in the soil profile may have on the French drain being operated. In Figure 3.8, three French drains can be seen. All French drains illustrated were incorporated into the model, with the center drain being the drain under operation. Case 4, Case 5, and Case 6 represent the groundwater table having an elevation at the bottom of the pipe invert, base of the French drain, and three feet below the base of the French drain, respectively. Units used in the model are feet and seconds. The results of the analysis were for the French drain under steady-state flow. The six cases were summarized in Table 3.1.

Table 3.1: Case scenarios of SEEP/W analysis

Case	Single Drain/ Multiple Drains	ΔH (ft)	In situ Soil Hydraulic Conductivity (ft/sec)	In situ Soil Porosity	Aggregate Hydraulic Conductivity (ft/sec)	Aggregate Porosity
Case 1	single drain	1.5	7.93×10^{-5}	0.46	3.28×10^{-1}	0.3
Case 2	single drain	3.5	7.93×10^{-5}	0.46	3.28×10^{-1}	0.3
Case 3	single drain	6.5	7.93×10^{-5}	0.46	3.28×10^{-1}	0.3
Case 4	multiple drains	1.5	7.93×10^{-5}	0.46	3.28×10^{-1}	0.3
Case 5	multiple drains	3.5	7.93×10^{-5}	0.46	3.28×10^{-1}	0.3
Case 6	multiple drains	6.5	7.93×10^{-5}	0.46	3.28×10^{-1}	0.3

Results of the steady-state analysis are shown in Figure 3.4 through 3.11. The distortion of the groundwater mounding profile can be viewed qualitatively. The flowrates per length of French drain are shown in Table 3.2. Flow through the in situ soil at the tips of the French drains were assumed to be negligible and were not included in the reported flowrates.

Table 3.2: Results of SEEP/W analysis

Case	Single Drain/ Multiple Drains	ΔH (ft)	Flowrate per Length of French drain (ft^2/sec)
Case 1	single drain	1.5	1.50×10^{-4}
Case 2	single drain	3.5	3.50×10^{-4}
Case 3	single drain	6.5	6.50×10^{-4}
Case 4	multiple drains	1.5	1.51×10^{-4}
Case 5	multiple drains	3.5	3.53×10^{-4}
Case 6	multiple drains	6.5	6.56×10^{-4}

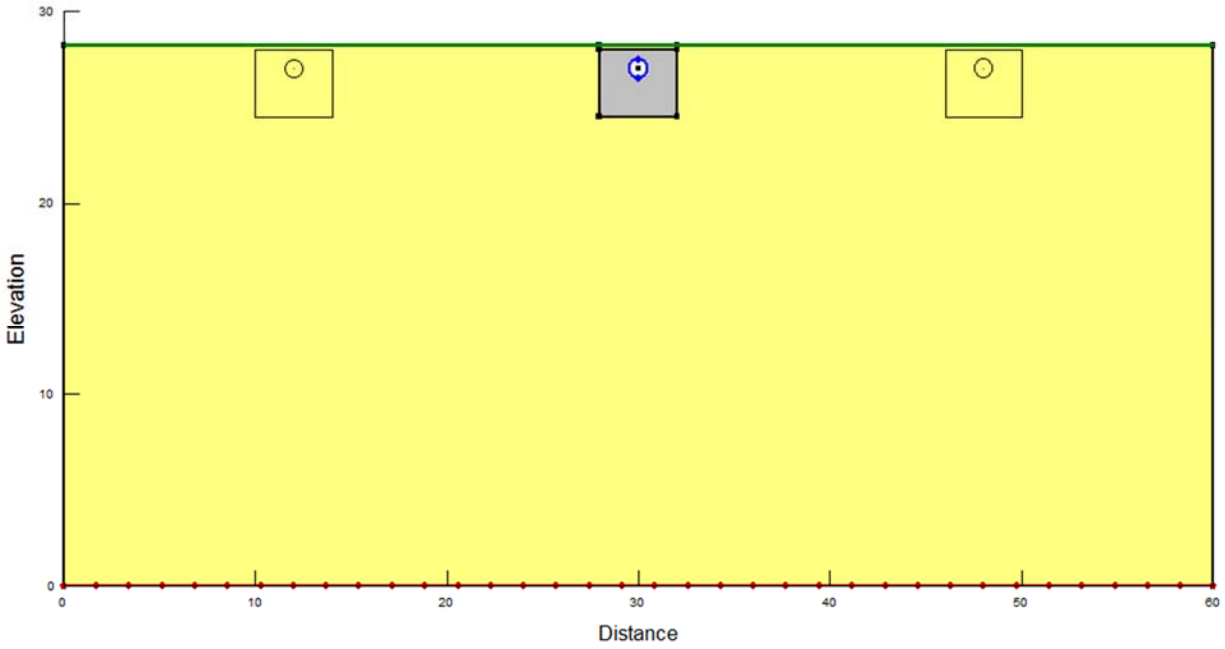

Figure 3.4: Model setup of the seepage analysis for a single drain

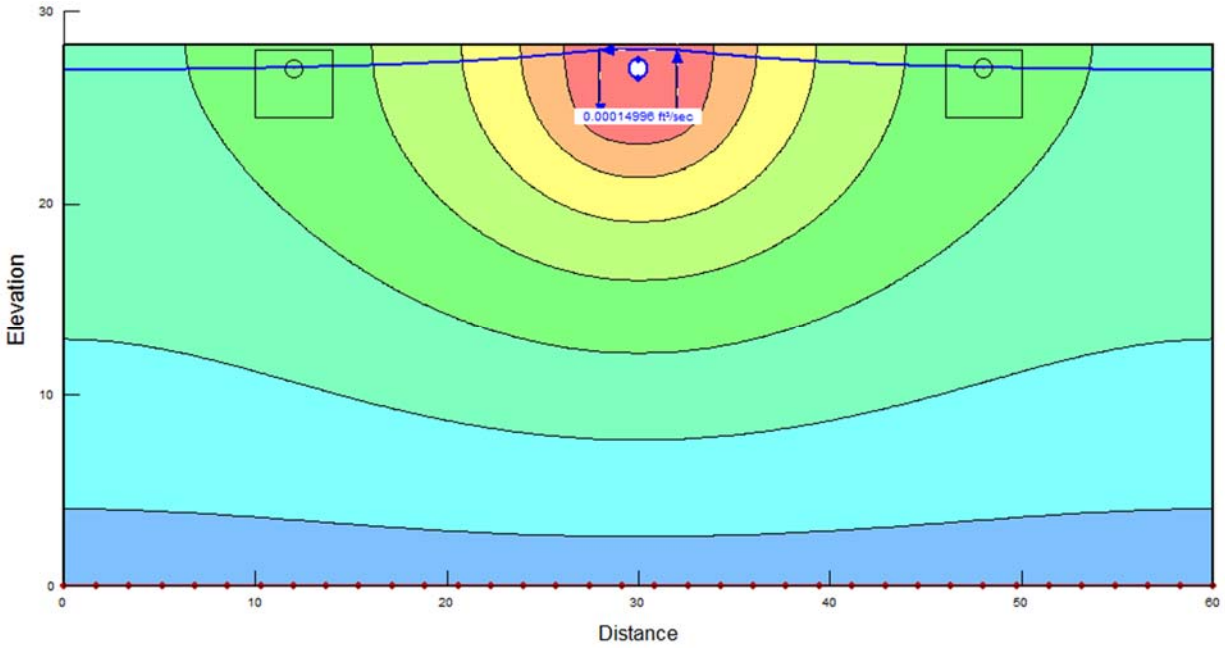

Figure 3.5: SEEP/W result of Case 1
(Head difference 28 ft to 26.5 ft (bottom of invert);
flow rate per foot of drain = 1.4996 x 10^{-4} ft^2/sec/ft)

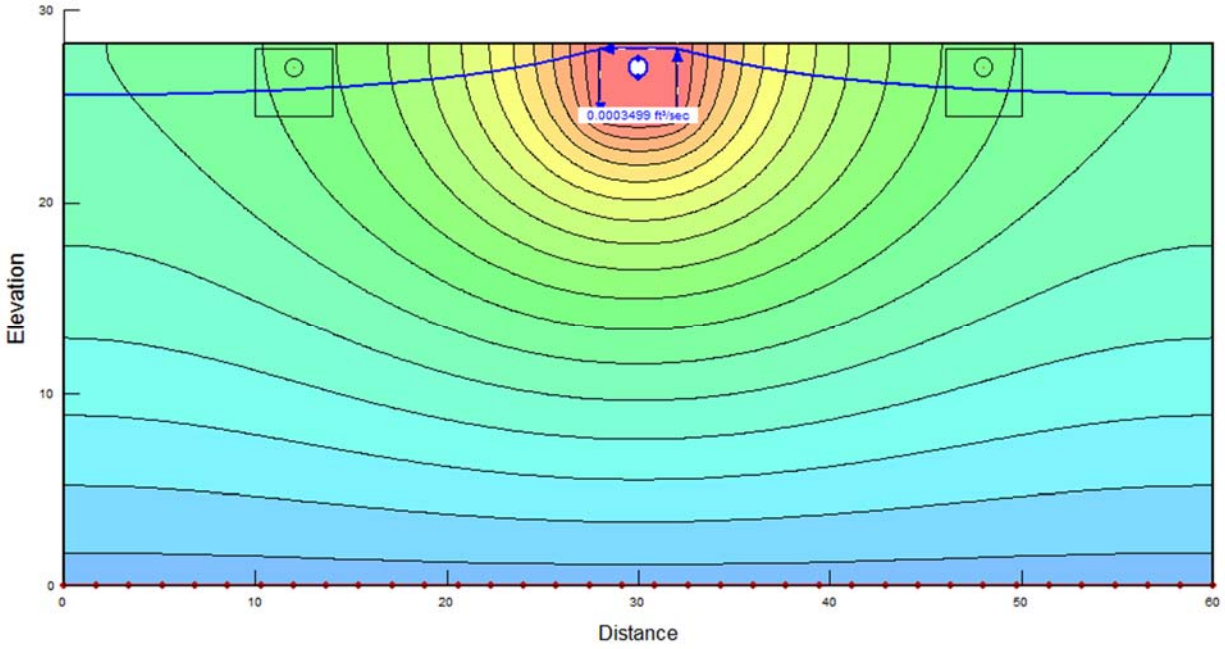

Figure 3.6: SEEP/W result of Case 2
(Head difference 28 ft to 24.5 ft (bottom of trench);
flow rate per foot of drain = 3.499 x 10^{-4} ft^2/sec/ft)

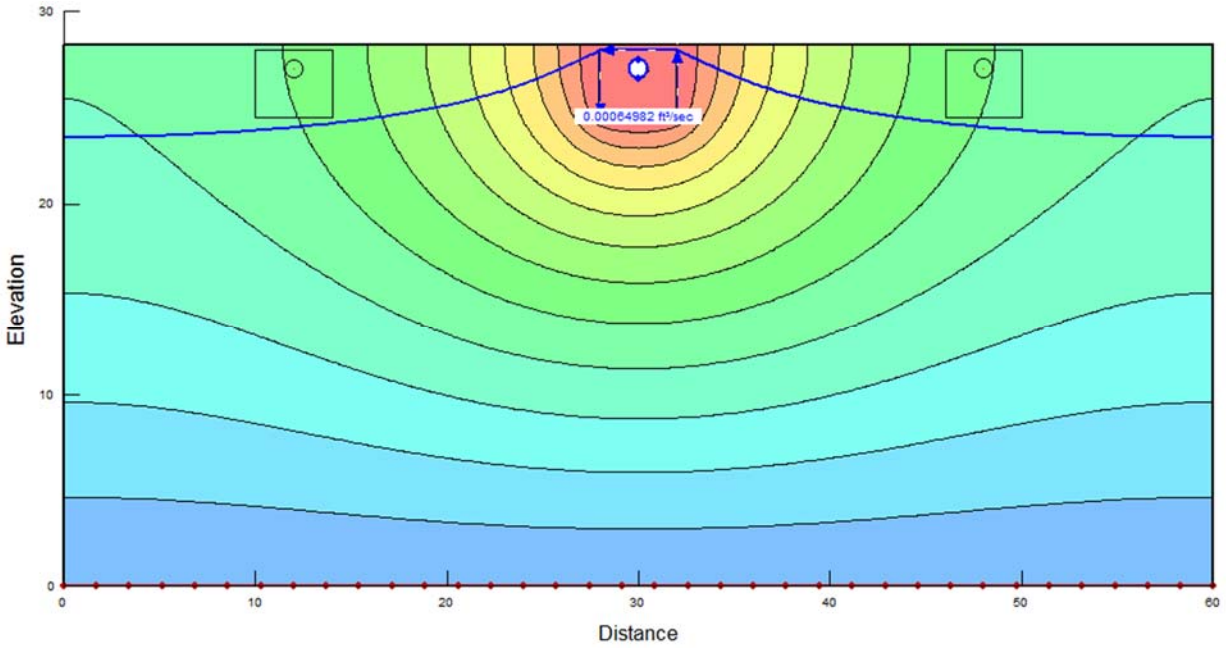

Figure 3.7: SEEP/W result of Case 3
(Head difference 28 ft to 21.5 ft (three feet below trench);
flow rate per foot of drain = 6.4982 x 10^{-4} ft^2/sec/ft)

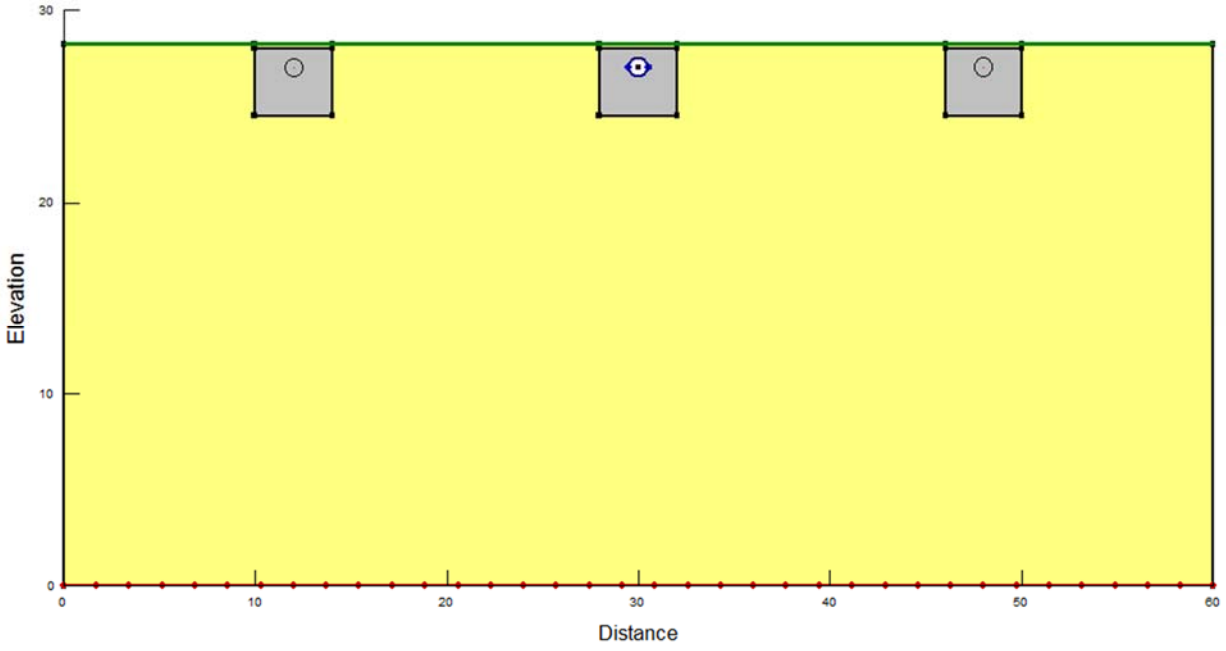

Figure 3.8: Model setup of the seepage analysis for multiple drains

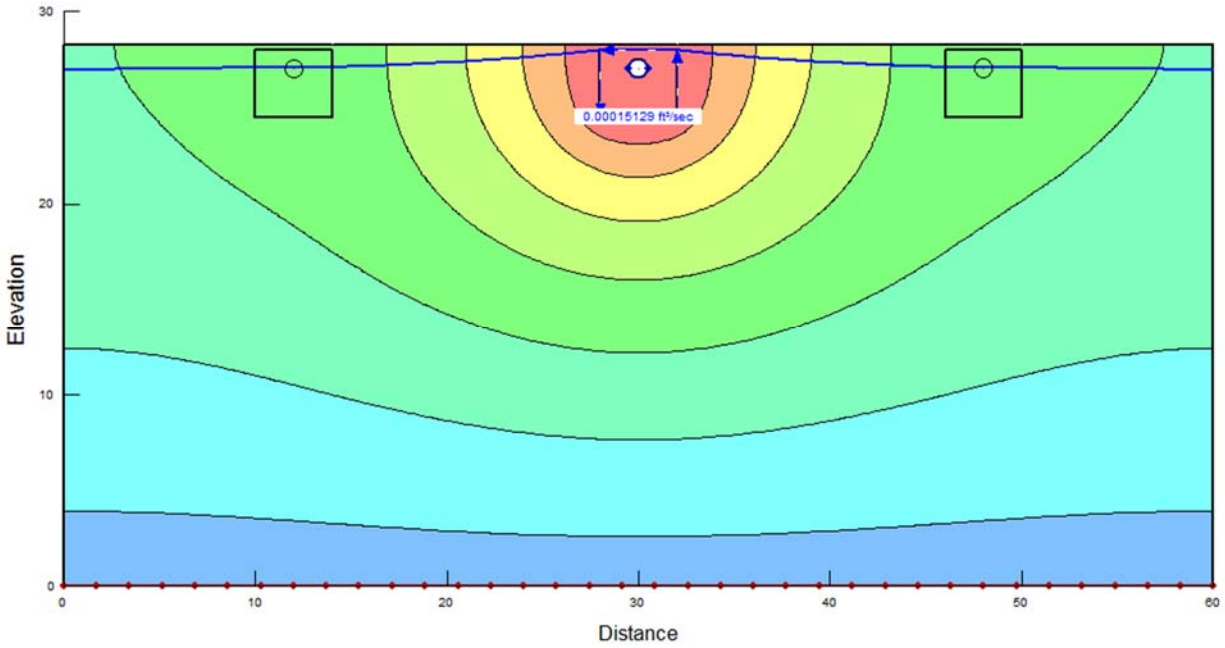

Figure 3.9: SEEP/W result of Case 4
(Head difference 28 ft to 26.5 ft (bottom of invert);
flow rate per foot of drain = 1.5129 x 10^{-4} ft^2/sec/ft)

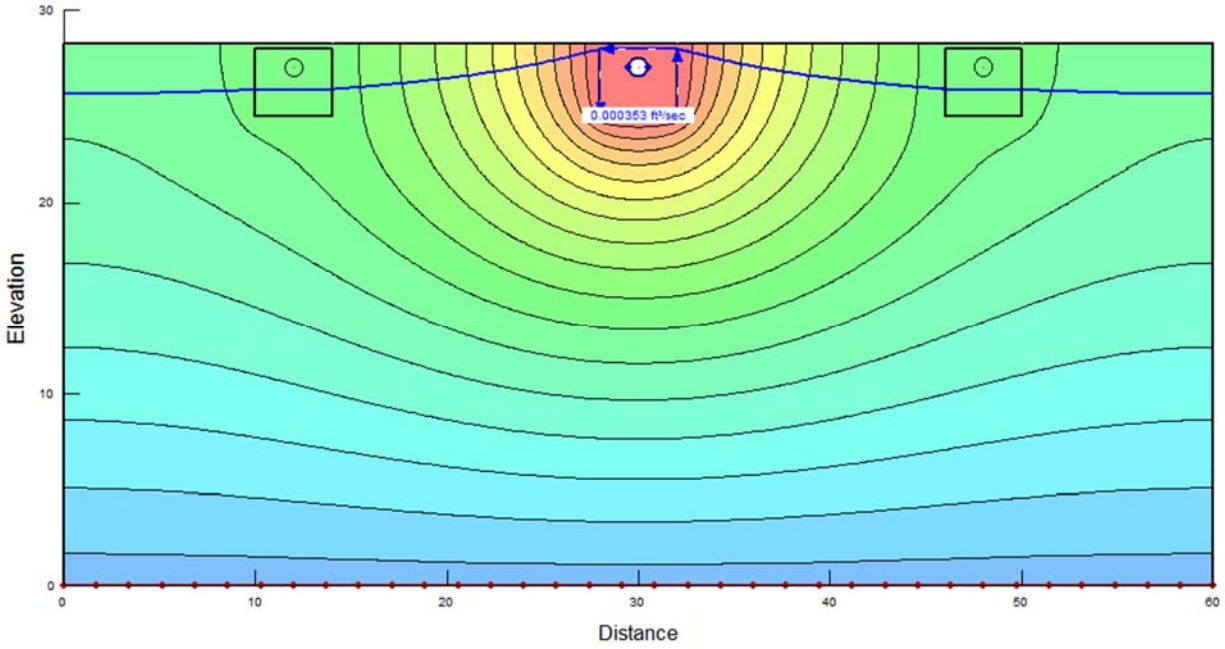

Figure 3.10: SEEP/W result of Case 5
(Head difference 28 ft to 24.5 ft (bottom of trench);
flow rate per foot of drain = 3.530 x 10^{-4} ft^2/sec/ft)

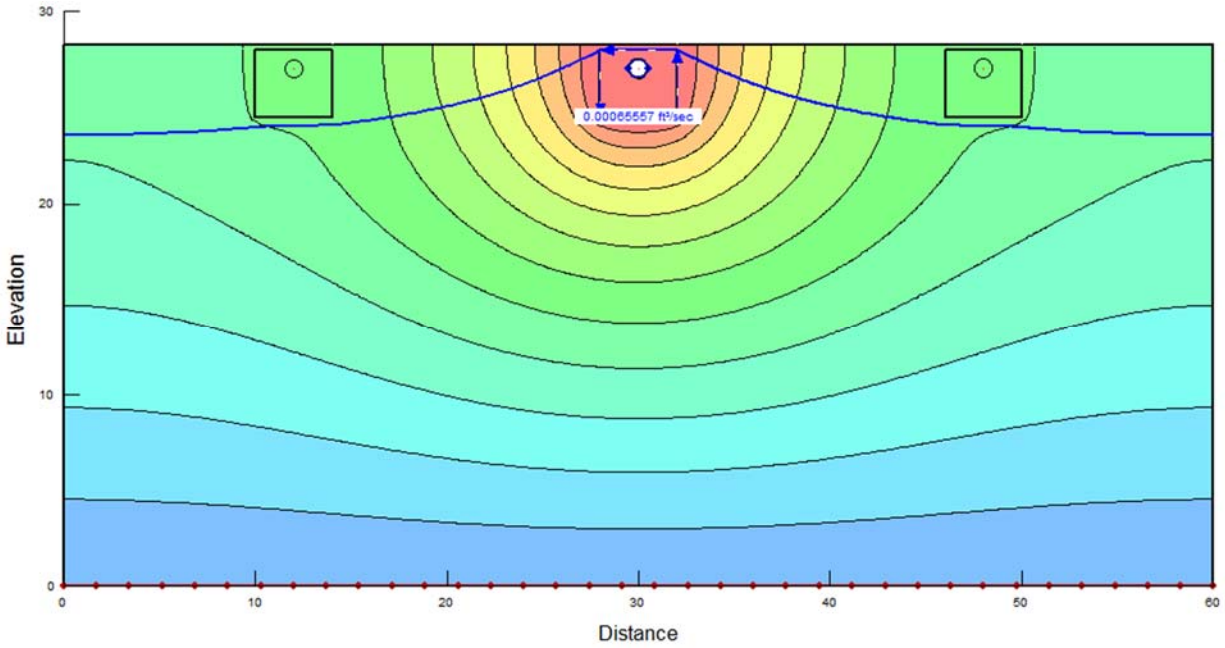

Figure 3.11: SEEP/W result of Case 6
(Head difference 28 ft to 21.5 ft (three feet below trench);
flow rate per foot of drain = 6.5557 x 10^{-4} ft^2/sec/ft)

3.2.3. Flow Rate and Water Consumption Estimation

An order of magnitude estimation for the steady-state flowrate and total water consumption during a field test was desired. Results in the previous section showed that the flowrate and head difference were directly proportional. Dividing the flowrate per length of French drain by head difference then multiplying the result by 15 ft (length of the French drain) and converting to gallons resulted in a normalized flowrate of 1.51×10^{-3} ft^3/sec/ft (1.13×10^{-2} gal/sec/ft). The water consumption for a field test will roughly be equal to the amount of water initially needed to saturate the French drain system plus the product between the steady-state exfiltration rate (normalized flowrate), testing time, and head difference. The amount of water needed to initial fill the French drain system is:

Volume of water between No. 4 aggregate

Dimensions of the aggregate box are $4ft \times 3.5ft \times 15ft$

$$Volume\ of\ box - Volume\ of\ pipe\ section\ in\ box = Volume\ of\ aggregate$$

$$(4ft)(3.5ft)(15ft) - \frac{\pi}{4}(1ft)^2(15ft) = 198ft^3$$

Assume a porosity for the gravel of $n = 0.30$

$$(Volume\ of\ gravel)(porosity) = Volume\ of\ water\ between\ aggregate$$

$$(198ft^3)(0.30) = 59.5ft^3 = 445gallons$$

Volume of water within pipe and sump

Assume pipe is 19 ft long, sump has an inner diameter of 3 ft and has a head of water of 2 ft

$$Volume\ of\ pipe\ + Volume\ of\ wetted\ part\ of\ sump = Volume\ of\ water\ in\ supply\ system$$

$$\frac{\pi}{4}(1ft)^2(19ft) + \frac{\pi}{4}(3ft)^2(2ft) = 29.1ft^3 = 217gallons$$

Total volume of water needed to initial fill French drain system

$$Volume\ of\ water\ between\ aggregate + Volume\ of\ water\ in\ supply\ system = Volume\ of\ water\ needed\ to\ initially\ fill\ system$$

$$59.5ft^3 + 29.1ft^3 = 88.6\ ft^3 = 663\ gallons$$

Thus, 88.6 ft^3 (663 gallons) of water are needed to initially fill the French drain system. The water consumption per hour of French drain operation is calculated in Table 3.3.

Table 3.3: The water consumption per hour of French drain operation

Normalized Flowrate (ft^3/sec/ft)	ΔH (ft)	Time (1hr) (sec/hr)	Flowrate (ft^3/hr) / (gal/hr)
1.51×10^{-3}	1.5	3600	8.17 / 61.1
1.51×10^{-3}	3.5	3600	19.1 / 143
1.51×10^{-3}	6.5	3600	35.4 / 265

3.2.4. Conclusions and Recommendations

Based on the numerical seepage analysis, the researchers have drawn the following conclusions:

- The groundwater mounding profile was parabolic. The original groundwater table elevation served as an asymptote to the groundwater mounding profile.

- A slight distortion of the groundwater mounding profile occurred when passing through or under an adjacent French drain. Due to the distance between the French drains the distortion occurred along a relatively shallow slope portion of the groundwater mounding profile, thus not significantly altering the profile. In addition, the results showed that the flowrates were negligibly affected by the presence of the adjacent French drains. A separation distance of 14 ft between French drains was shown to be acceptable.

- Flowrate through the French drain system and head difference had a proportional relationship, with an order of magnitude estimation for the flowrate during steady-state being 1.51×10^{-3} ft^3/sec/ft (1.13×10^{-2} gal/sec/ft). The order of magnitude estimation for water consumption was around 700 - 1,000 gal for tests running an hour.

- Based upon the observed rate of dissipation of the groundwater mound in the field it was necessary to wait 24 to 48 hours between testing of an adjacent French drain to allow the water table to return to normal.

3.3. Material Properties

Excluding the perforated drainage pipe, the French drain system had three material components that restricted the flow of water, which were the aggregate (limestone or RCA in this experiment), geotextile, and in situ soil. The performance of the drainage system from a materials perspective, was most sensitive to the properties of the in situ soil as compared to the aggregate or geotextile because the in situ soil was by far the most restrictive element, thus controlling the equivalent hydraulic conductivity of the French drain system.

3.3.1. Laboratory Testing for Materials

Material properties of limestone

The limestone was tested, and its material properties are presented in this section. Figure 3.12 shows a photo of the limestone as received. Sieve analysis (AASHTO T 27/T 11/M 145) on the limestone (used in the control trench) was conducted, and the results are presented in Table 3.4 and Figure 3.13. The limestone met the specification requirements for an FDOT No. 4 aggregate.

Figure 3.12: Limestone aggregate (1-ft ruler used for scale)

Table 3.4: Sieve analysis of fine and coarse aggregates (AASHTO T 27/T 11/M 145)

Limestone				
Percent Finer (%)	Diameter (in)	Classification	Cu	Cc
D60	1.190			
D30	0.988	A-1-a	1.51	1.04
D10	0.790			

where,

D60 = diameter corresponding to 60% finer
D30 = diameter corresponding to 30% finer
D10 = diameter corresponding to 10% finer
Cu = uniformity coefficient
Cc = coefficient of gradation

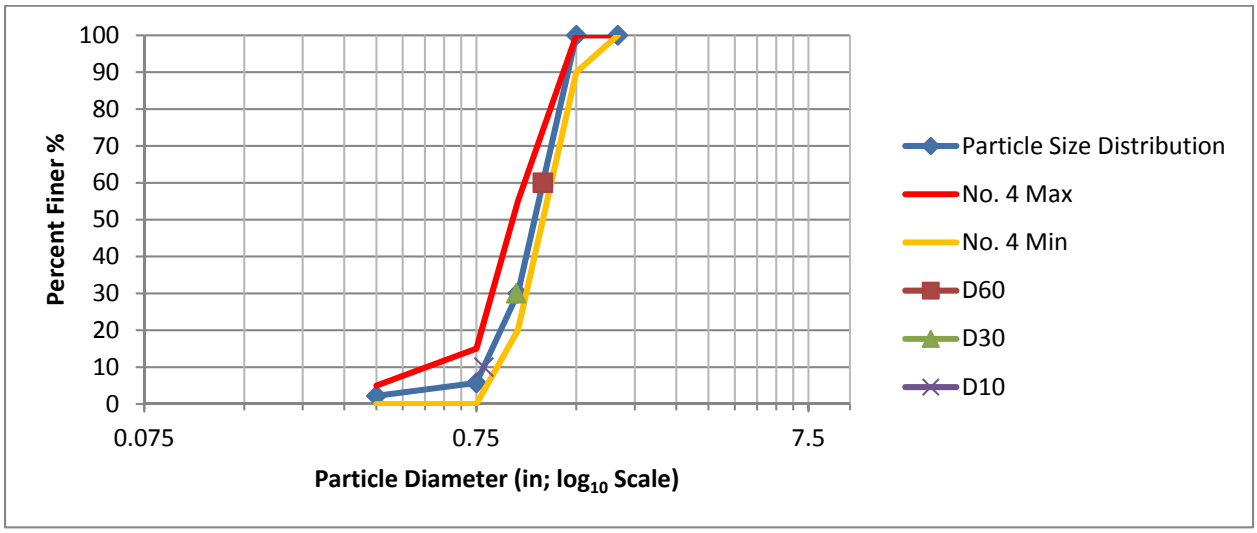

Figure 3.13: Particle size distribution of limestone

In addition, L.A. abrasion (ASTM C535) and specific gravity (AASHTO T 85) tests were conducted on the limestone. The L.A. abrasion of 28.9% was measured and the specific gravities are presented in Table 3.5. The bulk density and voids in limestone aggregate were measured according to AASHTO T 19 and the results are shown in Table 3.6.

Table 3.5: Specific gravity and absorption of coarse aggregate (AASHTO T 85)

Specific Gravity Type and Absorption	Specific Gravity @ 68°F
Bulk Dry Sp. Gr.	2.31
Bulk SSD Sp. Gr.	2.39
Apparent Sp. Gr.	2.51
Absorption (Oven Dried before Saturation, %)	3.5

Table 3.6: Bulk density and voids in limestone (AASHTO T 19)

Bulk Dry Density (lb/ft^3)	Void Content (%)
80.5	44.1

Material properties of RCA

The RCA was tested and its material properties are presented in this section. Figure 3.14 shows the photo of RCA as received. Sieve analysis (AASHTO T 27/T 11/M 145) on the RCA was conducted and the results are presented in Table 3.7 and Figure 3.15. The RCA met the specification requirements for an FDOT No. 4 aggregate.

Figure 3.14: RCA aggregate (1-ft ruler used for scale)

Table 3.7: Sieve analysis of fine and coarse aggregates (AASHTO T 27/T 11/M 145)

Percent Finer (%)	Diameter (in)	Classification	Cu	Cc
D60	1.190			
D30	0.970	A-1-a	1.49	0.988
D10	0.800			

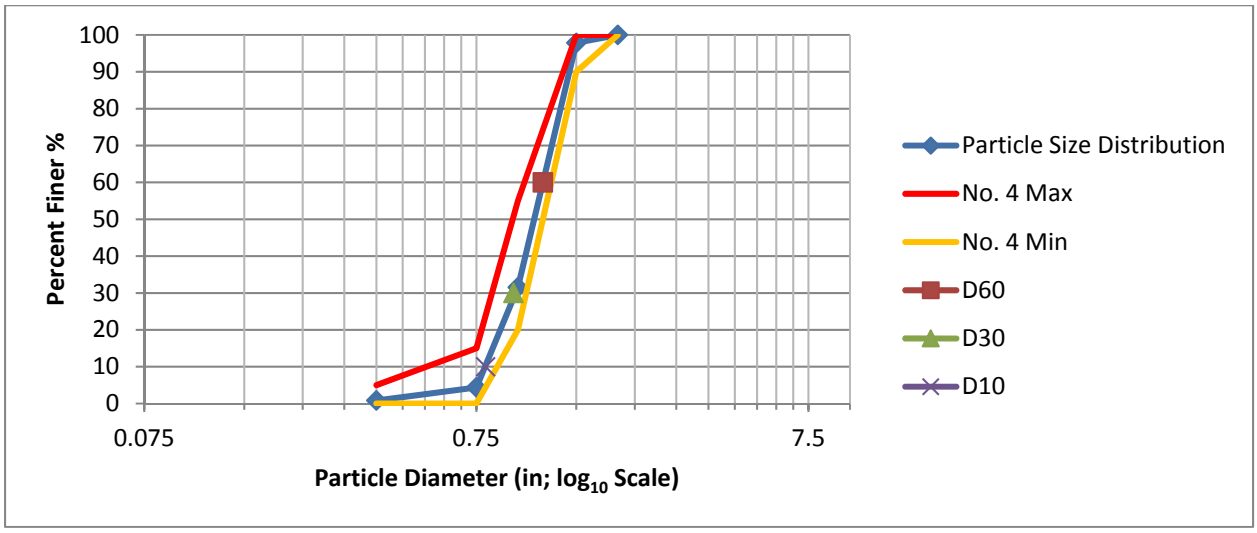

Figure 3.15: Particle size distribution of RCA aggregate

In addition, LA abrasion (ASTM C535) and specific gravity (AASHTO T 85) tests were conducted on the RCA aggregate. The LA abrasion of 43.7% was measured and the specific gravities are presented in Table 3.8. The bulk density and voids in RCA aggregate were measured according to AASHTO T 19 and the results are shown in Table 3.9.

Table 3.8: Specific gravity and absorption of coarse aggregate (AASHTO T 85)

Specific Gravity Type and Absorption	Specific Gravity @ 68°F
Bulk Dry Sp. Gr.	2.02
Bulk SSD Sp. Gr.	2.21
Apparent Sp. Gr.	2.50
Absorption (Oven Dried before Saturation, %)	9.6

Table 3.9: Bulk density and voids in aggregate (AASHTO T 19)

Bulk Dry Density (lb/ft^3)	Void Content (%)
70.8	43.7

Material properties of in situ soils

Materials properties of the in situ soils were tested. The testing methods included sieve analysis (AASHTO T 27/T 11/M 145), specific gravity (D854 Method B), and permeability (ASTM D2434). The in situ soil profile was composed of three layers as shown in Figure 3.16. Table 3.10 shows the results of sieve analysis for soils in Layers 1, 2, and 3. The particle size distributions of soils in Layers 1, 2, and 3 are shown in Figures 3.17 a, b, and c, respectively. The specific gravity and permeability of those soils are presented in Tables 3.11 and 3.12, respectively.

Figure 3.16: Photo showing the three layers of soil at the project site

Table 3.10: Sieve analysis of fine and coarse aggregates for Layers 1, 2, and 3 (AASHTO T 27/T 11/M 145)

Layer 1				
Percent Finer (%)	Diameter (mm)	Classification	Cu	Cc
D60	0.200			
D30	0.149	A-3	1.89	1.05
D10	0.106			
Layer 2				
Percent Finer (%)	Diameter (mm)	Classification	Cu	Cc
D60	0.198			
D30	0.145	A-3	1.85	0.99
D10	0.107			
Layer 3				
Percent Finer (%)	Diameter (mm)	Classification	Cu	Cc
D60	0.197			
D30	0.145	A-3	1.82	1.00
D10	0.108			

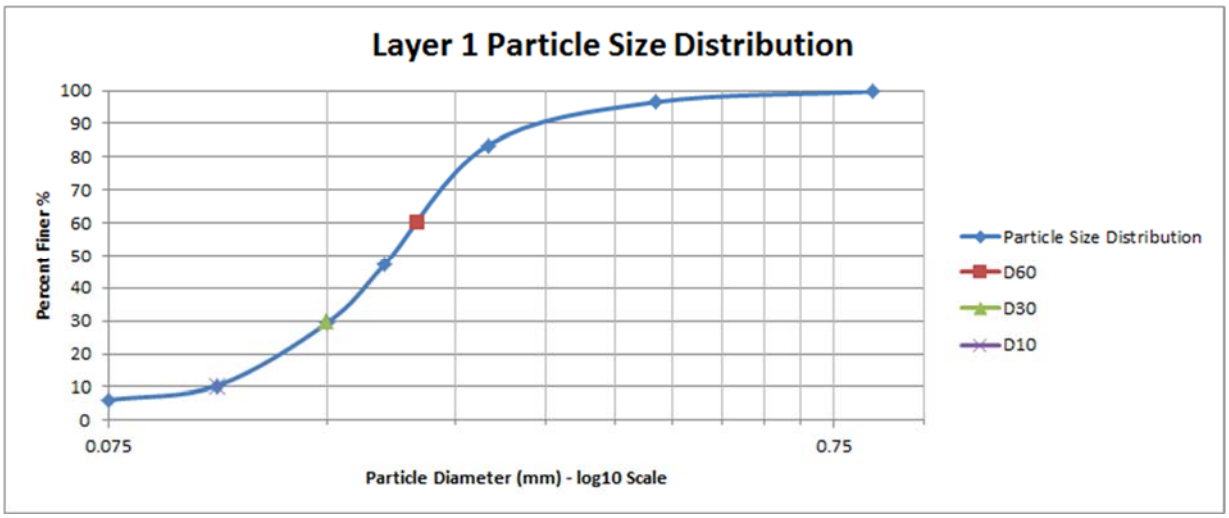

(a) Layer 1

Figure 3.17: Particle size distributions of soils (Note: (a) layer 1; (b) layer 2; and (c) layer 3)

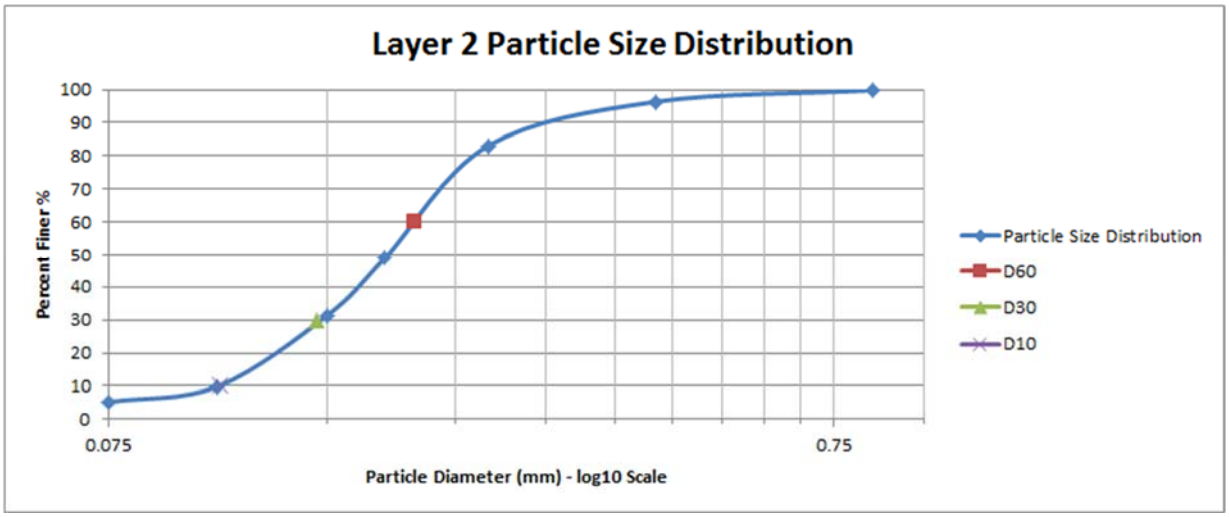

(b) Layer 2

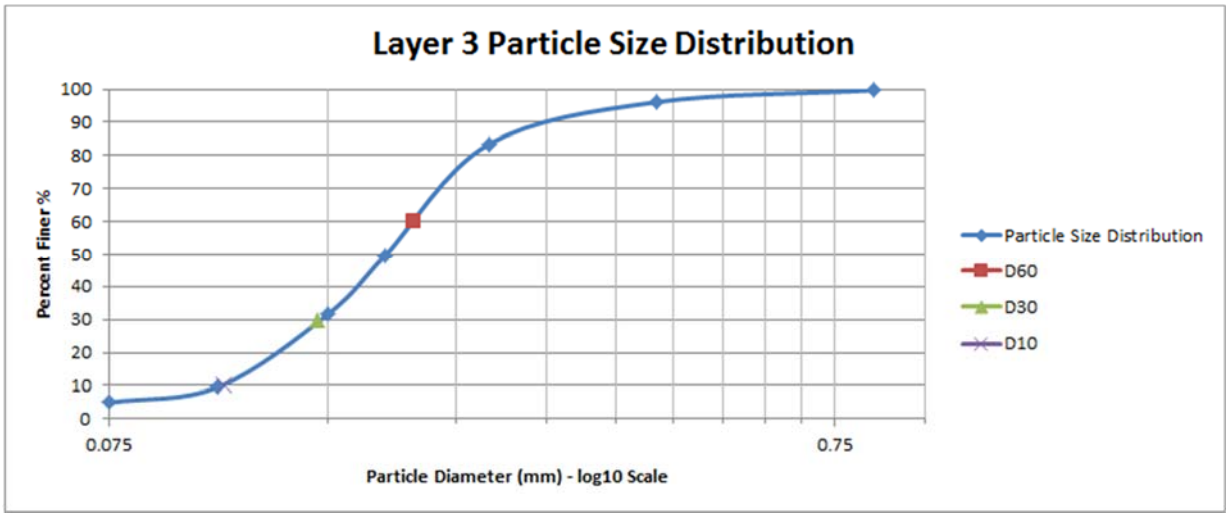

(c) Layer 3

Figure 3.17: Particle size distributions of soils
(Note: (a) layer 1; (b) layer 2; and (c) layer 3, (continued))

Table 3.11: Specific gravity of soils in Layers 1, 2, and 3 (D854 Method B)

Layer	Trial 1 @ 68°F	Trial 2 @ 68°F	Average @ 68°F
Layer 1	2.63	2.65	2.64
Layer 2	2.61	2.61	2.61
Layer 3	2.63	2.64	2.63

Table 3.12: Permeability of soils from Layers 1, 2, and 3 (ASTM D2434)

Layer	Constant Head (ft/s) @ 68°F	Falling Head (ft/s) @ 68°F	Average (ft/s) @ 68°F	Moist Unit Weight (lb/ft^3)	Dry Unit Weight (lb/ft^3)	Void Ratio
Layer 1	1.48×10^{-4}	1.23×10^{-4}	1.35×10^{-4}	92.2	84.5	0.95
Layer 2	1.49×10^{-4}	1.33×10^{-4}	1.41×10^{-4}	105.1	93.4	0.74
Layer 3	1.96×10^{-5}	2.16×10^{-5}	2.06×10^{-5}	107.6	89.0	0.84

Material properties of geotextile

Geotextile (polypropylene nonwoven fabric) was obtained from ACF Environmental Inc. and the material specs are summarized in Table 2. The geotextile permittivity from the manufacturer showed a minimum average roll value of 1.6 sec^{-1}. Drainage geotextiles, as required by 2016 FDOT Standard Specifications for Road and Bridge Construction, Section 985-2.2, are required to have a minimum permittivity of 0.5 sec^{-1} (D-3a) for the least restrictive D-3 geotextile listed. Product certification, in accordance with 2016 FDOT Standard Specifications for Road and Bridge Construction, Section 985-3.2, was conducted by the FDOT State Materials Office and it was concluded that the samples of the geotextile provided met all the requirements for type D-3 French drain filter fabric application.

Table 3.13: Technical data sheet N060 nonwoven geotextile

Property	**Min. Avg. Roll Value**	**Test Method**
Grab tensile strength	160 lbs	ASTM D4632
Grab tensile elongation	50%	ASTM D4632
CBR Puncture	410 lbs	ASTM D6241
Trapezoid tear strength	60 lbs	ASTM D4533
UV Resistant @ 500 hrs	70%	ASTM D4355
Apparent opening size (AOS)	70 US Sieve	ASTM D4751
Permittivity (sec^{-1})	1.6 (sec^{-1})	ASTM D4491
Flow rate	110 gpm/ft^2	ASTM D4491

3.4. Fines Migration Test

Two fine migration tests were conducted to observe how fines migrate under two different dispersal conditions within the aggregate: 1) homogenous dispersal and 2) heterogeneous dispersal. The homogenous dispersal involved the fines adhering to the surface of the aggregate, thus the fine concentration was distributed/homogenous throughout the whole aggregate mass. The heterogeneous dispersal involved the fines being applied to the top of clean 6" lifts of aggregate, thus the fines were concentrated/heterogeneous within thin layers in the whole aggregate mass. Fines are defined as soil passing the No. #60 sieve because production and collection of soil passing the #200 sieve was not feasible for this scale of a project. It was observed that the heterogeneous dispersal resulted in an accelerated reduction in the flow performance of the geotextile.

3.4.1. Experiment Procedure

General

1. From the RCA stockpile obtain a 5-gallon bucket sample of aggregate
2. Sieve the aggregate sample taken from the RCA stockpile to obtain a supply of each of the following sizes of aggregate (1-1/2", 1", 3/4", 3/8")
3. Wash the different sized aggregates
4. Place all the different sized aggregates in the oven for at least 24 hr. at or above 110°C
5. Determine the relative batch size that can fit in the permeameter
6. Construct an aggregate batch with a No. 4 gradation and record the oven dry weights of each sized aggregate portion
7. Submerge the batch for at least 24 hr.
8. Obtain an RCA rock powder sample from the fine generation method utilizing a cement mixer, the rock powder is collected by passing the aggregate over a No. 4 screen
9. Place the soil in the oven for at least 24 hr. at or above 110°C
10. Dry sieve the rock powder and save the soil passing the No. #60 sieve, these are considered the fines
11. Wet sieve a portion of the fines to determine the gradation

Homogenous Test

1. Cut a piece of geotextile to line the bottom of the permeameter and record the weight
2. Place the geotextile in the permeameter
3. Take the batch and record the weight in the SSD condition
4. Roll the batch in the oven dried fines
5. Place the aggregate covered in fines in the permeameter, then record the weight
6. Calculate the percentage of fines that stuck to the surface of the aggregate
7. Place the constant head system at a 3.5-ft head differential
8. With the permeameter outlet closed and the stop cock opened, allow the water to percolate through the aggregate until the permeameter is saturated (top-down saturation)

9. Close the stop cock, open the permeameter outlet and flow water from top down for the desired length of time and record visual observations and flowrate values
10. After the experiment record the thickness of the fine layer on the geotextile
11. Record the weight of an empty evaporation dish
12. Remove the geotextile with the embedded fines and aggregate from the permeameter then place it in the evaporation dish
13. Fill the evaporation dish with water and remove aggregate pieces, only leaving fines
14. Place the evaporation dish with the geotextile in the oven for at least 24 hr. at or above 110°C, then record the dry weight afterwards
15. Calculate the fine mass retained on the geotextile
16. Wash and saturate the aggregate for the Heterogeneous test

Heterogeneous Test

1. Cut a piece of geotextile to line the bottom of the permeameter and record the weight
2. Place the geotextile in the permeameter
3. Place a 6" lift of clean aggregate in the permeameter
4. From the percentage/amounts of fines calculated in the Homogenous batch add half that amount to the top of the first lift
5. Place an additional 6" lift of aggregate on top of the fine layer in the permeameter
6. From the percentage/amounts of fines calculated in the Homogenous batch add the other half of that amount to the top of the second lift
7. Place the constant head system at a 3.5-ft head differential
8. With the permeameter outlet closed and the stop cock opened, allow the water to percolate through the aggregate until the permeameter is saturated (top-down saturation)
9. Close the stop cock, open the permeameter outlet and flow water from top down for the desired length of time and record visual observations and flowrate values
10. After the experiment record the thickness of the fine layer on the geotextile
11. Record the weight of an empty evaporation dish
12. Remove the geotextile with the embedded fines and aggregate from the permeameter then place it in the evaporation dish
13. Fill the evaporation dish with water and remove aggregate pieces, only leaving fines
14. Place the evaporation dish with the geotextile in the oven for at least 24 hr. at or above 110°C, then record the dry weight afterwards
15. Calculate the fine mass retained on the geotextile

(a) No. 4 gradation construction

(b) SSD determination

(c) Weighing geotextile

(d) Geotextile in permeameter

(e) Coating aggregate in fines

(f) Homogeneous 5.1% fines test

(g) Heterogeneous 5.1% fines test 6”

(h) Heterogeneous 5.1% fines test 12”

Figure 3.18: Experiment procedures of fine migration test

(i) Homogeneous 2% fines test

(j) Heterogeneous 2% fines test 6”

(k) Heterogeneous 2% fines test 12”

(l) Constant head setup

(m) Fines deposits

Figure 3.18: Experiment procedures of fine migration test, (continued)

3.4.2. Laboratory Soil Testing

RCA Batch gradation

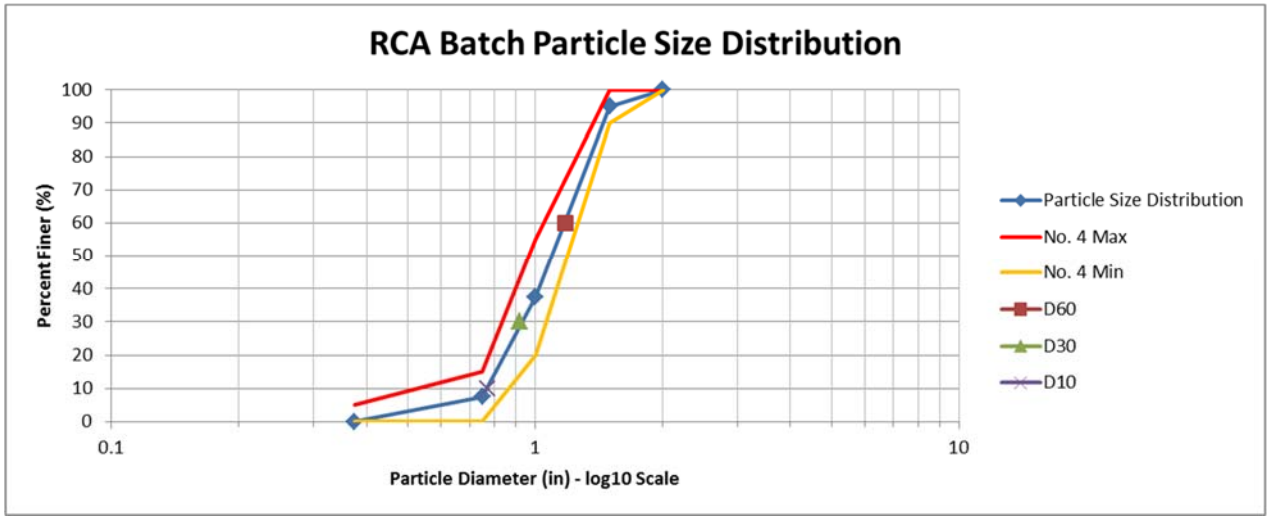

Figure 3.19: RCA batch particle size distribution

where,
D60 = diameter corresponding to 60% finer
D30 = diameter corresponding to 30% finer
D10 = diameter corresponding to 10% finer
Cu = uniformity coefficient
Cc = coefficient of gradation

Table 3.14: RCA batch particle size distribution

Sieve Number	Opening (in)	Soil Retained (lb)	Cumulative Retained (lb)	Percent Finer (%)	Percent Finer Max (%)	Percent Finer Min (%)
2"	2	0	0	100	100	100
1 1/2"	1.5	1.354	1.354	95.040838	100	90
1"	1	15.706	17.06	37.51602388	55	20
3/4"	0.75	8.195	25.255	7.501007215	15	0
3/8"	0.375	2.048	27.303	0	5	0
Wet Sieve	-	0	27.303	-		

Percent Finer (%)	Diameter (in)	Cu	Cc
60	1.18	1.532467532	0.931543033
30	0.92		
10	0.77		

Fine Generation Rate

Approximately four 5-gallon buckets (200 lb.) of RCA were placed into the cement mixer. Once agitated for the desired time period the aggregate was poured onto a No. 4 screen located on top of a collection tub. Everything passing the No. 4 screen was considered "rock powder". Then the rock powered passed through the No. 60 sieve (0.250 mm) and everything passing was considered "fines". Of the fines (passing the No. 60 sieve) the "true fine content" was approximately 65% (passing the No. 200 sieve).

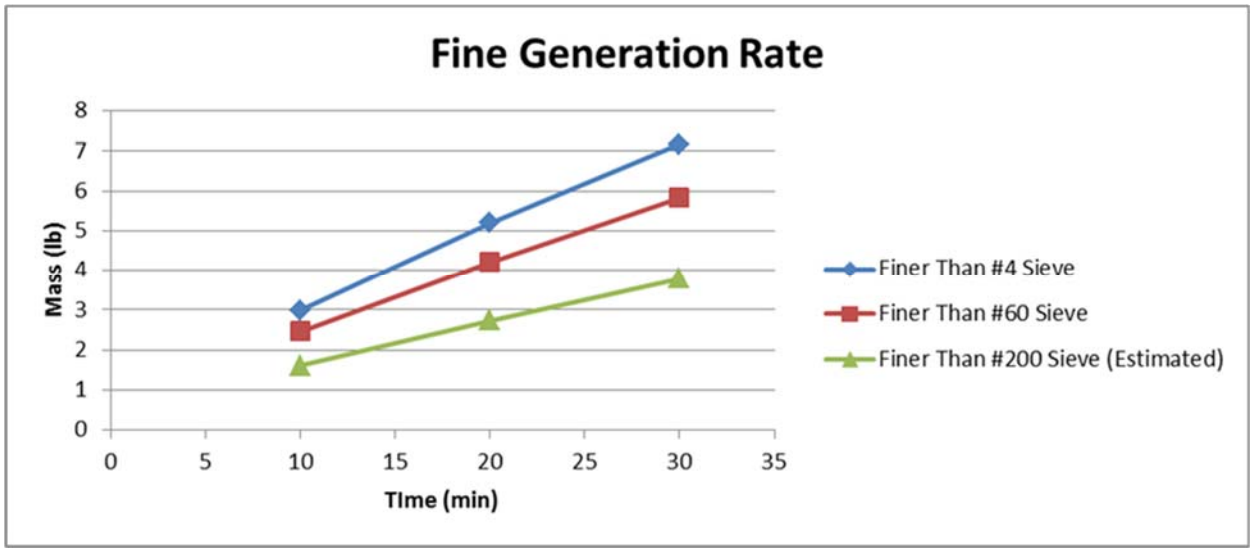

Figure 3.20: Fines generated over time

3.4.3. Experiment Results

The 5.1% fine content was produced by rolling the SSD RCA aggregate in the fine powder (passing the No. #60 sieve) and leaving only the particles which attached to the surface of the aggregate, this served to determine the maximum surface adhesion capacity. This test is referred to as the Homogeneous 5.1% Fines Test. In the Heterogeneous 5.1% Fines Test, the proportion of fines needed to achieve a 5.1% fine content were added into the aggregate in two layers. The Homogeneous 2% Fines Test involved taking 2% fines by weight and hand mixing them with the aggregate. The Heterogeneous 2% Fines Test was prepared in a similar manner as the 5.1% test.

Flow rate change

The 5.1% Fines Migration Tests have a smoother trend because the mass of water collected was over a 1 minute-period, whereas in the 2% Fines Migration Tests mass of water was only collected for a 15 second period because the beaker filled up quickly. The error from placing and pulling out the beaker not exactly at the right time was more influential on shorter sampling periods.

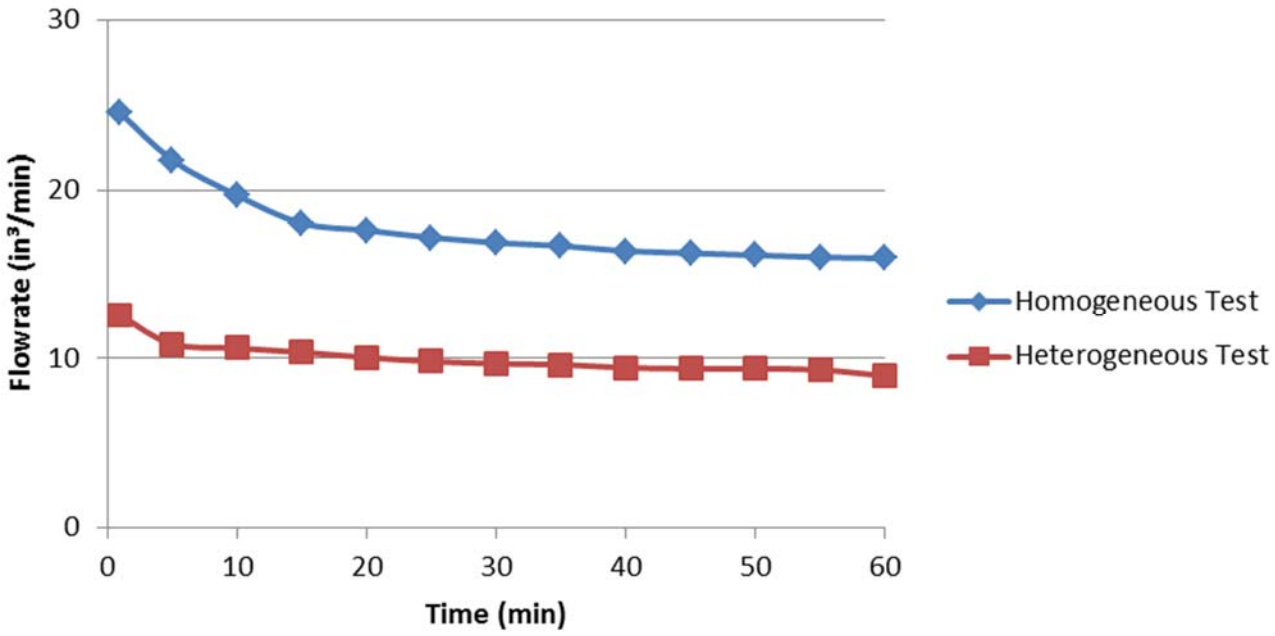

Figure 3.21: 5.1% fines migration tests

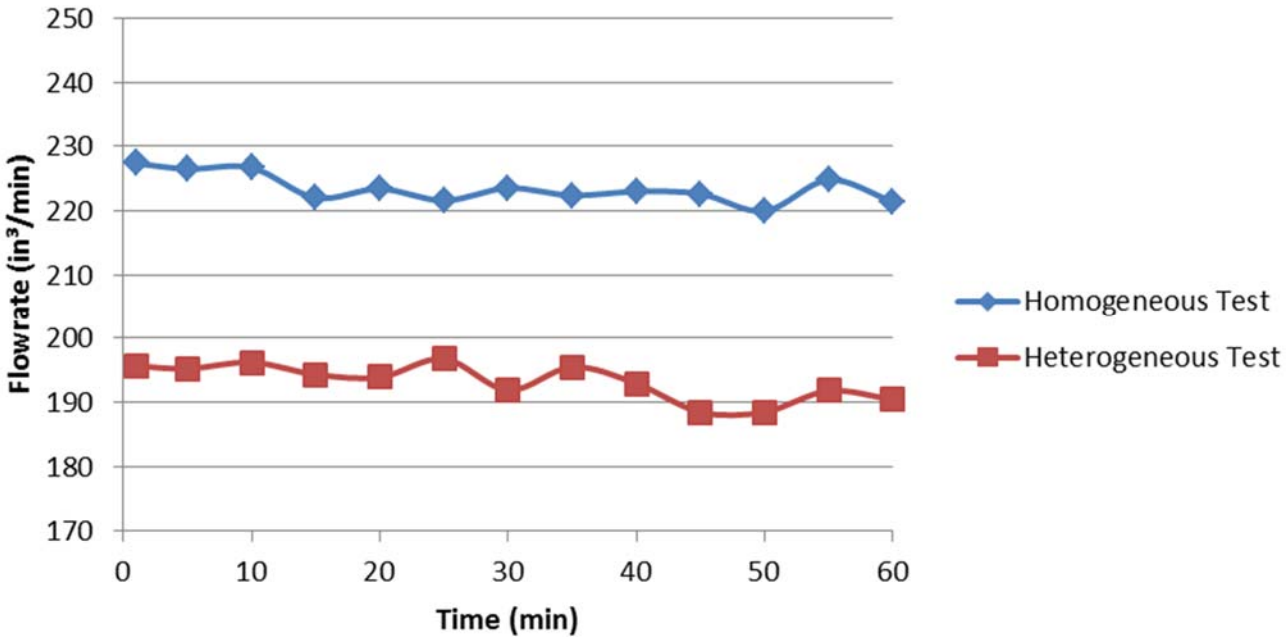

Figure 3.22: 2% fines migration tests

Fines deposited on geotextile

Table 3.15 Geotextile fine layer properties

Measurement	Homogeneous 5.1% fines	Heterogeneous 5.1% fines	Homogeneous 2% fines	Heterogeneous 2% fines
Weight of Dry Fines Deposited (oz)	13.7	13.9	1.5	3.1
Thickness of Layer (in)	0.75	0.5	≈0	≈0

(a) Deposits (Homogeneous; 5.1% fines)

(b) Deposits (Heterogeneous; 5.1% fines)

(c) Deposits (Homogeneous; 2% fines)

(d) Deposits (Heterogeneous; 2% fines)

Figure 3.23: Fines deposited on geotextile

Visual Migration

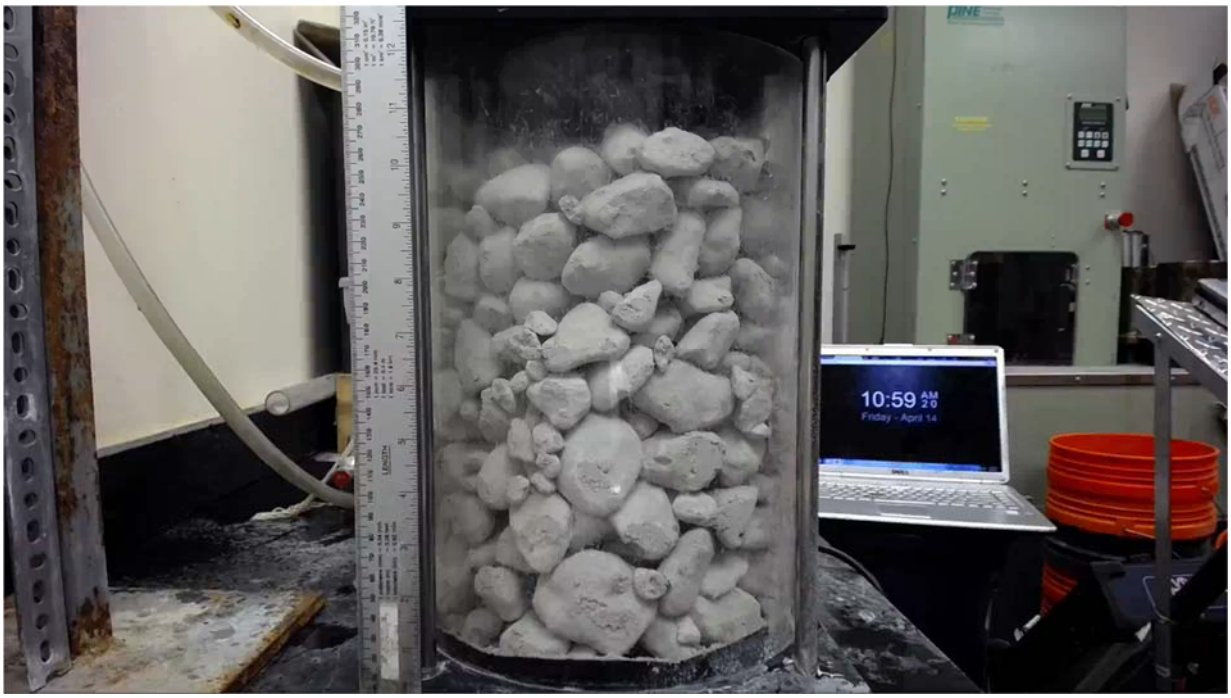

(a) Before experiment starts

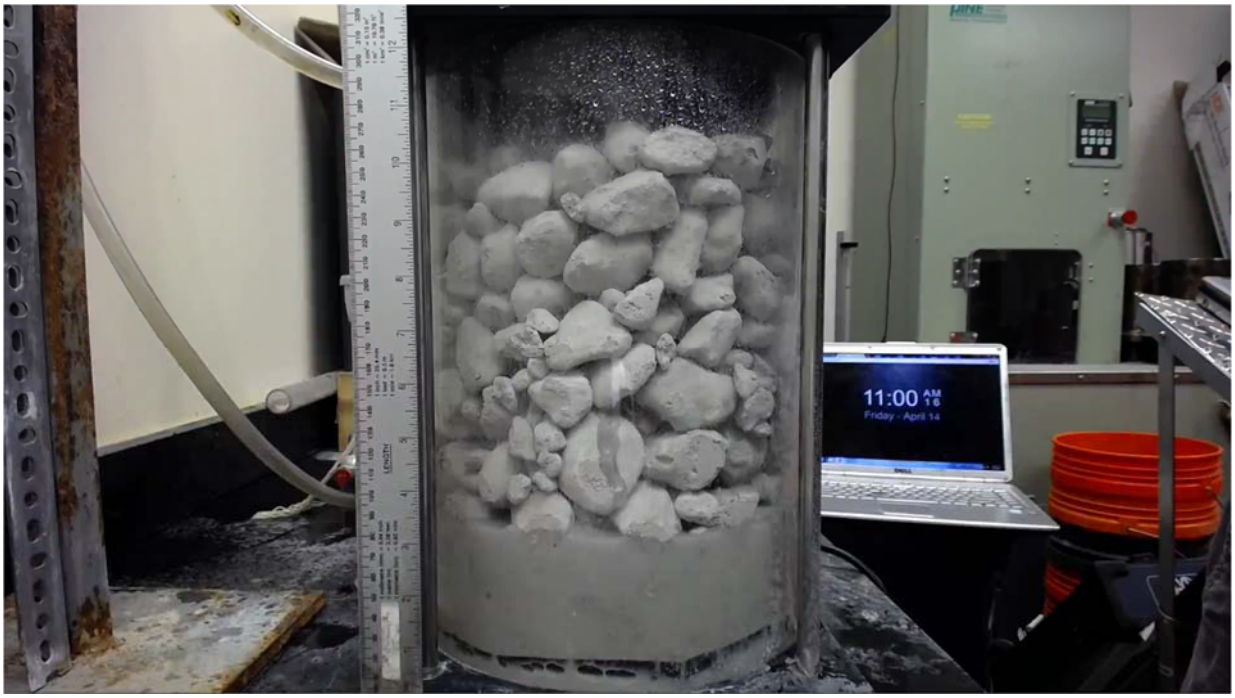

(b) Water percolation

Figure 3.24: Percolation test: homogeneous dispersal; 5.1% fines

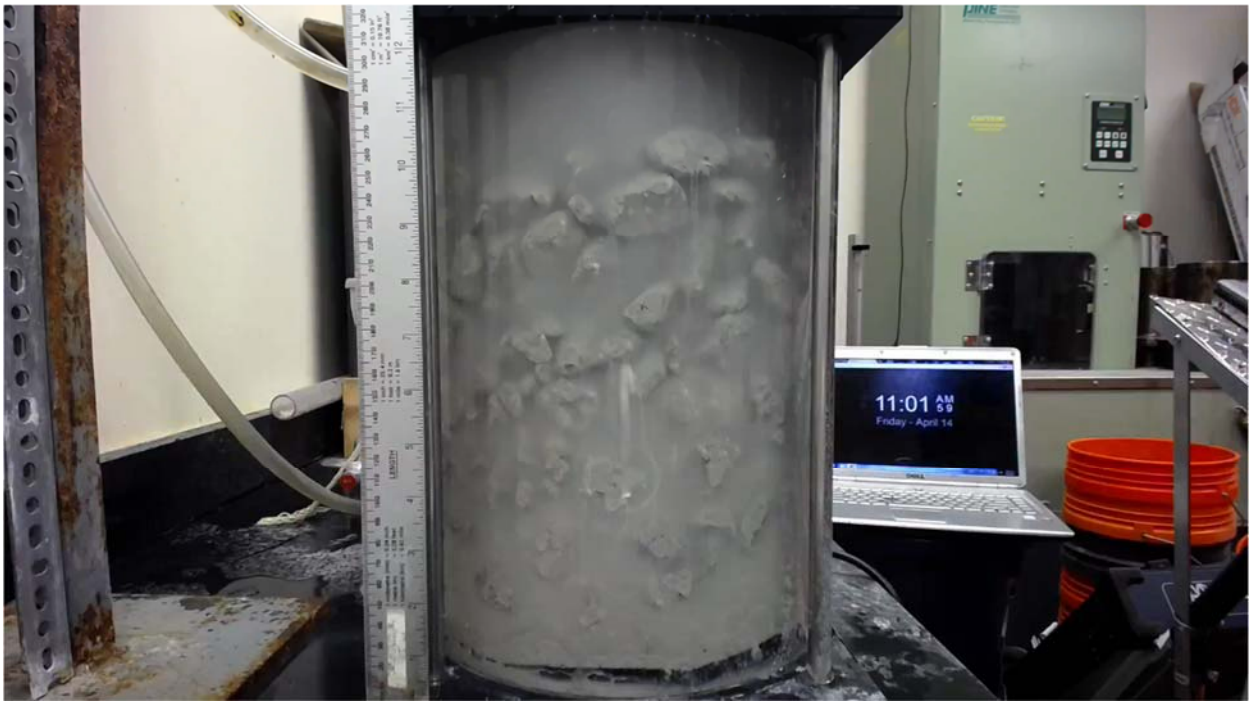

(c) 1 minute into experiment

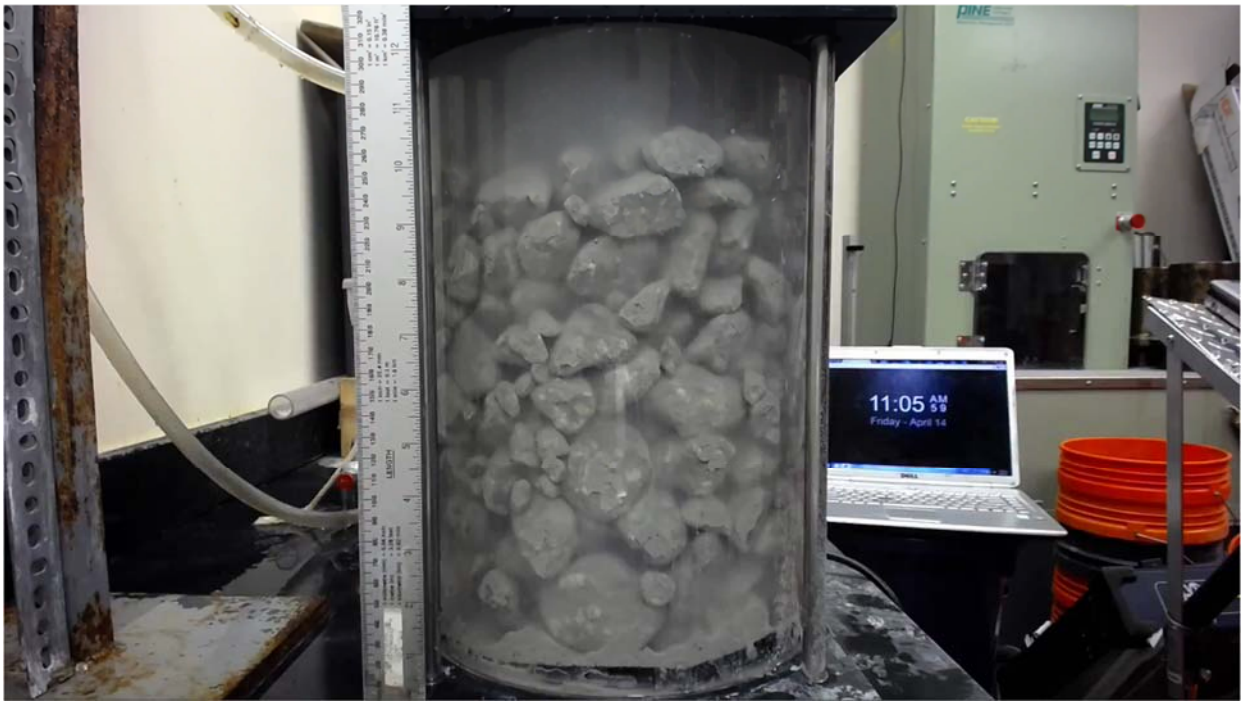

(d) 5 minutes into experiment

Figure 3.24: Percolation test: homogeneous dispersal; 5.1% fines (continued)

(e) 30 minutes into experiment

(f) 60 minutes into experiment

Figure 3.24: Percolation test: homogeneous dispersal; 5.1% fines (continued)

(a) Before experiment starts

(b) Water percolation

Figure 3.25: Percolation test: heterogeneous dispersal; 5.1% fines

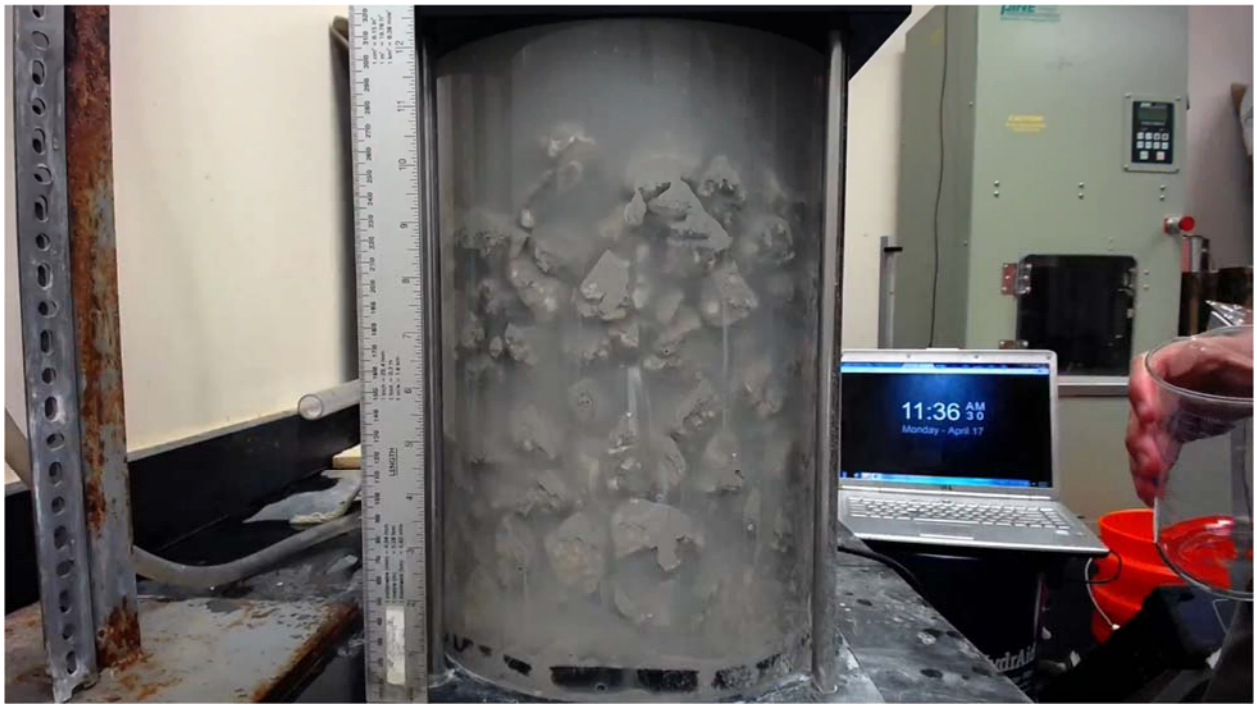

(c) 1 minute into experiment

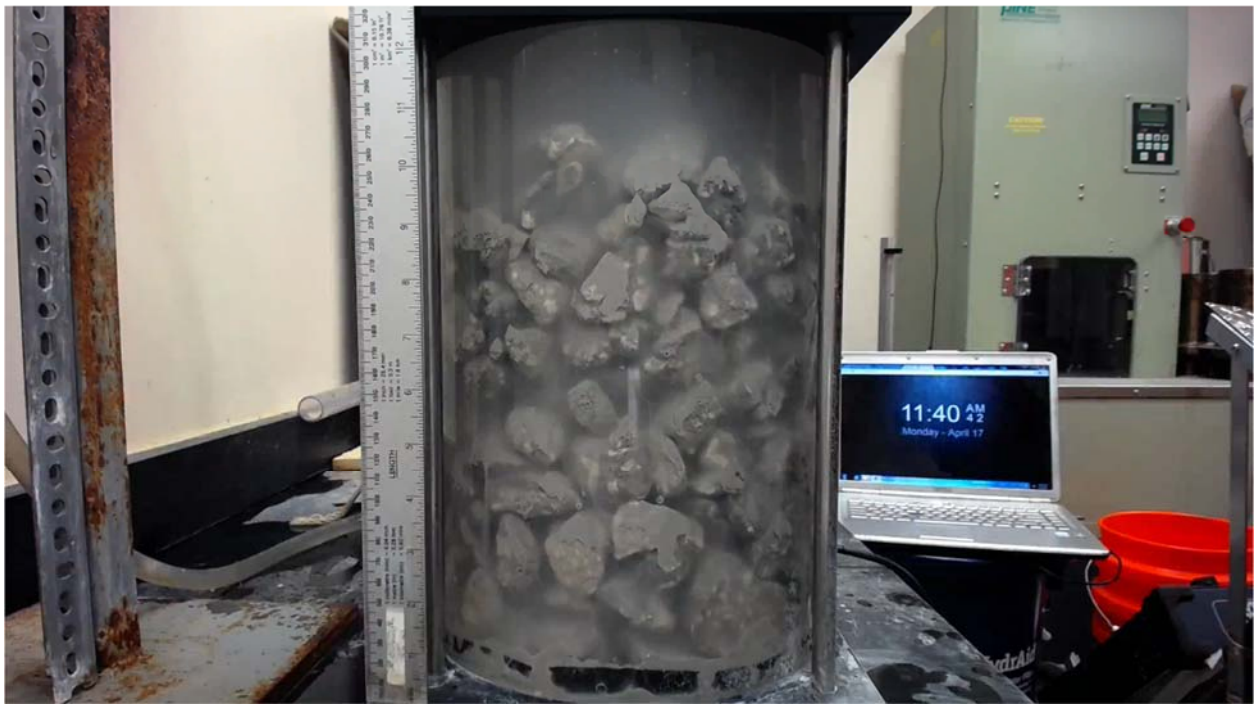

(d) 5 minutes into experiment

Figure 3.25: Percolation test: heterogeneous dispersal; 5.1% fines (continued)

(e) 30 minutes into experiment

(f) 60 minutes into experiment

Figure 3.25: Percolation test: heterogeneous dispersal; 5.1% fines (continued)

(a) Before experiment starts

(b) Water percolation

Figure 3.26: Percolation test: homogeneous dispersal; 2% fines

(c) 1 minute into experiment

(d) 5 minutes into experiment

Figure 3.26: Percolation test: homogeneous dispersal; 2% fines (continued)

(e) 30 minutes into experiment

(f) 60 minutes into experiment

Figure 3.26: Percolation test: homogeneous dispersal; 2% fines (continued)

(a) Before experiment starts

(b) Water percolation

Figure 3.27: Percolation test: heterogeneous dispersal; 2% fines

(c) 1 minute into experiment

(d) 5 minutes into experiment

Figure 3.27: Percolation test: heterogeneous dispersal; 2% fines (continued)

(e) 30 minutes into experiment

(f) 60 minutes into experiment

Figure 3.27: Percolation test: heterogeneous dispersal; 2% fines (continued)

3.4.4. Discussion and Conclusions

Top-down saturation (percolation) was chosen as the means of saturation because it closely resembles operating conditions in the field, versus bottom-up saturation which does not occur within the French drain unless excessive groundwater table rise occurs. Because the aggregate was large and a stop cock was present on top of the permeameter, trapped air within the aggregate was not a concern under top-down saturation. A head differential of 3.5 ft was used because this was the maximum depth of the aggregate within the French drain.

An extreme amount of aggregate disturbance was required to generate an appreciable amount of rock powder. Even then, the rock powder was not wholly composed of fines. The processed rock powder passing the No. 60 sieve (0.250 mm) contained only 65% fines. The No. 60 sieve was chosen as the size to redefine fines because (1) a large amount of rock powder could be processed quickly without easily clogging the sieves, (2) particle sizes smaller than 0.250 mm were classified as being the size of fine sands, silts and clays, and (3) the apparent opening size of the geotextile was slightly smaller at an equivalent No. 70 sieve (0.210 mm), thus nearly all the particles within the rock powder posed a risk of clogging the geotextile.

At a relatively high fines content, it was observed that the heterogeneous dispersal method, when compared to the homogeneous dispersal method, showed signs of an accelerated reduction in the flow performance of the geotextile. The initial flow rate of the heterogeneous dispersal was half of the homogeneous dispersal. Performance of the homogeneous sample geotextile was decreased by 38% over an hour period versus 25% for the heterogenous sample, but at the end of the testing period, the homogenous samples still maintained a higher flow rate over the heterogenous sample.

3.5. As-built Plans of the Field Drainage System

The French drains were increased in width from the originally planned 3 ft to 4 ft. This increase in width allowed for at least 1 ft of aggregate to be on both sides of the drains as required in FDOT Design Standard 285. After the preliminary field drainage system design was submitted to FDOT the actual outer diameter of the drains was discovered to be 14.5 inch and not the previously assumed nominal 12 in, which caused the non-compliance with FDOT Design Standard 285 that had to be fixed by widening the trenches. The French drains and sumps were constructed from (ADS N-12 ST IB) 12 inch and 36-inch nominal sized HDPE pipes, respectively. A non-woven D-3 geotextile was approved by FDOT and used as the filter fabric. The sumps were sealed with a 40 mil PVC linear and a bituminous sealant. Backfill used was a mixture of the excavated in situ soils. The design of the in situ French drain system is shown in Figure 3.28. The construction procedures of a French drain are shown as photos in Figures 3.39 through 3.47. More photos showing the construction of a French drain are presented in Appendix.

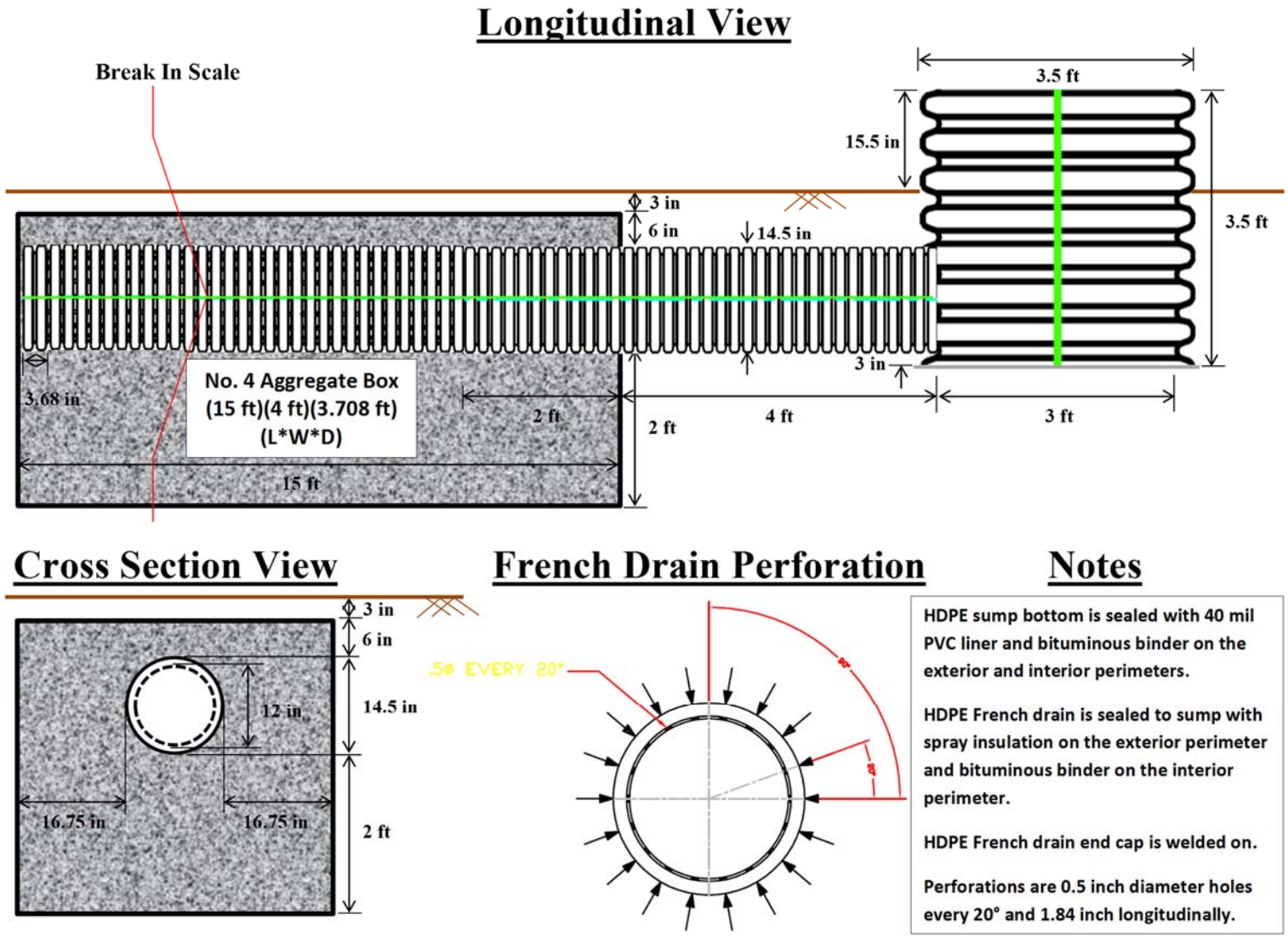

Figure 3.28: Design of the in situ French drain system

System Construction

Construction of the French drain experiment started in fall 2016 and was completed in summer 2017. The research team manually performed the experimental site work. A total of four French drain systems and twenty-five monitoring wells were constructed at the project site. Each French drain contained a different aggregate composition. From east to west, the four French drains were composed of washed RCA "as is", RCA with 2% fines, RCA with 4% fines, and virgin limestone as the control. The French drains were constructed in the east to west order, with the monitoring wells constructed subsequently.

Trench Excavation

All French drain trenches were excavated using shovels, with the spoil being placed adjacent to the trenches. Three distinct volumes were excavated within a French drain trench: (1) the volume removed for the drainage aggregate, approximately 15 ft × 4 ft × 4 ft; (2) the volume removed for the pipe segment between the sump and drainage aggregate, approximately 4 ft × 2 ft × 2 ft; and (3) the volume removed for the sump, approximately 5 ft × 5 ft × 2 ft. The different volumes of excavation are shown in Figure 3.39. As the washed RCA French drain trench was being excavated it also served as a test trench to collect in situ soil samples. Three soil layers were identified along the depth of the trench and soil samples were obtained by pushing the acrylic tube portion of permeameter cells into the side of the trench by means of a mechanical jack. The acrylic tubes were then taken to the lab and reinstalled into the respective permeameters. Laboratory testing of the in situ soil samples is outlined in the Section 3.3 Material Properties.

3.5.1. Material Procurement

HDPE Pipes

The HDPE pipes were purchased from Advanced Drainage Systems (ADS), Inc., see Figure 3.29. The perforation design for each 12-inch diameter pipe (FDOT Standard Specifications for Road and Bridge Construction, Section 443-2.1(5)) was adjusted from 3/8-inch diameter holes to ½-inch diameter holes with an equivalent perforated area. The ADS engineer recommended this change because the 3/8-inch diameter perforation required more holes and risked the structural integrity of the 12-inch diameter pipe. Four sumps were constructed from the one 36-inch diameter pipe. Each French drain consists of a 12-inch diameter pipe with a welded end cap and a 36-inch diameter sump. The product information is shown in Table 3.16.

Table 3.16: Materials for sumps and French drains

Description	Model Number	Quantity
12".N12 HWY.STIB.PERF.20'	12810020IB	4
36".N12 HWY.STIB.SOLID.20'	36850020IB	1
12".END CAP.(4/BG)	1267AA	4

Figure 3.29: Pipes for sumps and French drains

Geotextile

Non-woven D-3 geotextile was purchased from ACF Environmental, see Figure 3.30. The samples and mill certification were shipped to the FDOT State Materials Office (SMO) as required by Standard Specifications for Road and Bridge Construction, Section 985-3. The sample testing was conducted by Mr. Timothy Blanton and it was concluded that the samples met all the Section 985 requirements for type D-3 drainage geotextiles.

Table 3.17: Non-woven D-3 geotextile (ACF Environmental)

Description	Model Number	Quantity
N060 NONWOVEN GEOTEX	N06012360	12.5' × 360' = 500 SY/RL

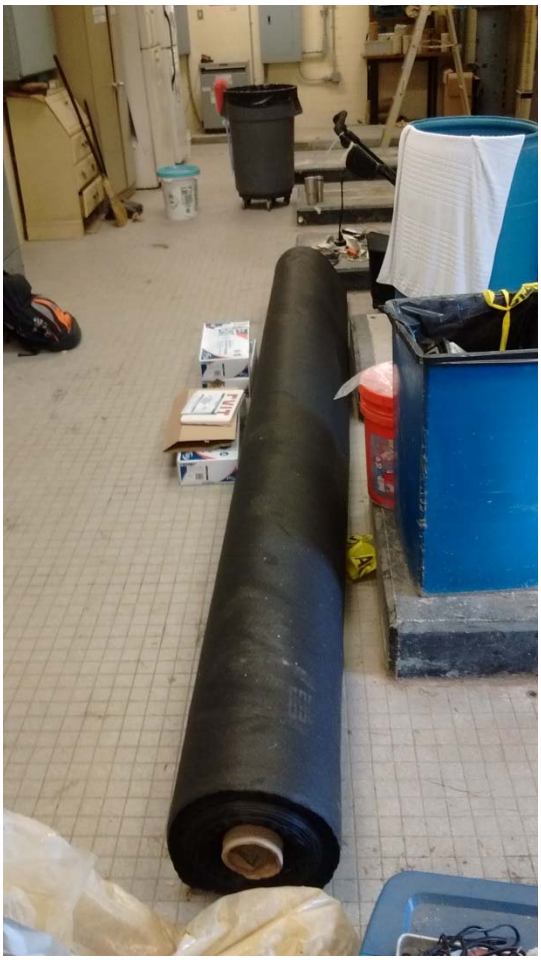

Figure 3.30: Geotextile used in French drains

Aggregates

Four French drains were constructed, consisting of one with virgin limestone and three with RCA. RCA French drains contained varied fine contents at as received, 2% and 4%. The drain with No. 4 limestone was used as a control system for comparison purposes. The Researchers purchased 8 tons of No. 4 virgin limestone (2.2% fines as is) from Vulcan Materials Company and were donated 24 tons of No. 4 RCA (0.8% fines as is) from Independence Recycling of Florida, Inc. The aggregate wet sieving was complied with the FM 1-T 011 method. Figure 3.31 shows the aggregates stored at the UCF site. For RCA with varied fine contents, the researchers mechanically conditioned the No. 4 RCA. A concrete mixer was used for the fine generation, Figure 3.32.

Table 3.18: Limestone and RCA (as received) and related materials

Description	Model Number	Quantity
Virgin limestone	No. 4 Gradation	18 tons
RCA	No. 4 Gradation	24 tons
Grizzly 47 Gallon Heavy-Duty Cement Mixer	H8172	1
Coleman Cable Extension Cord, 100-Feet	02309	2

Figure 3.31: No. 4 virgin limestone and No. 4 RCA aggregates

Figure 3.32: Concrete mixer for fines generation prior to the placement of aggregates

Sump Supplies

The bottoms of the sumps were sealed with a 40 mil PVC linear and a bituminous sealant applied to all joints, Figure 3.33. Because the exterior corrugation on the sump had to be cut an expansion foam was used where the French drain pipe mounted to the sump, Figure 3.34.

Table 3.19: Materials for waterproofing sump

Description	Model Number	Quantity
Henry Wet Patch 1 Gallon	208	5
Oatey 5-ft Wide Gray PVC Shower Pan Liner	41597	15 ft
Great Stuff, Gaps & Cracks Insulating Foam Sealant	99053937	5

(a) (b)

Figure 3.33: Materials for waterproofing sump

Figure 3.34: Sump-French drain interface

In situ Water Level System and Sensors

The in situ water level system for an individual French drain consisted of seven 8-ft-long 4-in-inner diameter perforated HDPE monitoring wells, each containing a data logging piezometer suspended by a wire connected to the well cap, with an additional eighth piezometer exposed to the atmosphere to record the barometric pressure. Figure 3.35 shows the piezometer sensor and the schematic diagram of the piezometer sensor installation in the HDPE well. The piezometers were easily installed and removed, and were only placed into the French drain well system.

Table 3.20: Materials for in situ water-level system

Description	Model Number	Quantity
HOBO Water Level (13 ft) - U20L Series	U20L-04	8
HOBOware PRO v.3. × for PC & Mac	BHW-PRO-CD	1
HOBO Waterproof Shuttle	U-DTW-1	1
10’ long 4” ID perforated HDPE Pipe	0453-0010	25
Well Caps	40154	25
4-in Standard Auger Head	S-11012	1

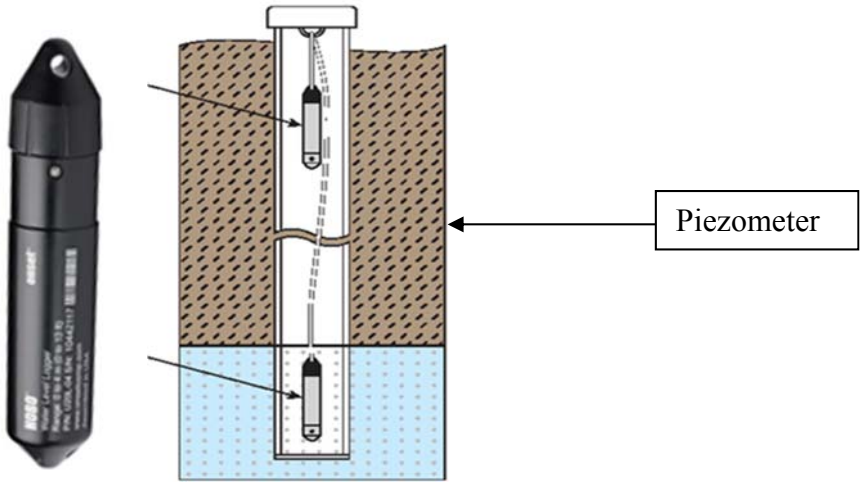

Figure 3.35: Water level sensor: (a) piezometer sensor and (b) sensor installation

Water Delivery System

The fire hydrant on site (Figures 3.36 and 3.37) was rated orange (500 – 999 gpm) and served as the water supply when running the French drain experiment. The University's Utilities & Energy Services department performed the flow meter and backflow preventer installation. The fire hose connected to the flow meter and supplied water to the individual French drain under testing.

Table 3.21: Materials for water delivery system

Description	Model Number	Quantity
*Badger Meter Model 450 Fire Hydrant Meter, 3"	RTS-DS-00546-EN-02	1
*Zurn Wilkins Backflow Preventer	975XL2	1
Heavy-Duty Adjustable Fire Hydrant Wrench	FHWHD	1
2.5" x 100' Double Jacket Fire Hose	25D8100	1

*Was borrowed from the University's Utilities & Energy Services department

Figure 3.36: On-site fire hydrant

Figure 3.37. Badger meter and Watts backflow preventer installed on the fire hydrant

Camera Investigation Equipment

A Logitech webcam with 1080p HD capability was used to inspect the inside of the French drains.

Table 3.22: Camera investigation equipment

Description	Model Number	Quantity
Logitech Webcam	C930e	1

Figure 3.38: Camera to inspect inside pipe

3.6. French Drain System Construction

3.6.1. French Drain Construction

Once a trench was excavated, a sump was then prepared by cutting a segment off the 20-ft-long 36-inch inner diameter HDPE pipe. Once segmented, a hole was then cut into the sump to allow the perforated 12-in inner diameter pipe to be inserted (see Figure 3.40). Before placing the sump into the trench, a tailored section of the PVC pipe was first placed between the in situ soil and sump bottom. The sump was then placed on top of the PVC pipe, then sealed with a bituminous sealant (see Figure 3.42). Next, the drainage portion of the trench was lined with geotextile, and aggregate was poured to an elevation that would be level with the bottom of the horizontal 12-inch inner diameter perforated pipe, once it was installed (see Figure 3.44). For the washed RCA and limestone trenches, the aggregate was placed directly into the trench, but for the RCA with 2% fines and RCA with 4% fines trenches, the fines had to be added to the aggregate before placement into the trench because the only source of RCA was washed RCA, which has a negligible fines content. Fines were generated by taking a sacrificial portion of the RCA stockpile and grinding it in a Los Angeles (LA) abrasion machine. The generated fines and washed RCA were both placed into a concrete mixer located at the edge of the trench, with specific proportions of each to obtain the desired fines content for a specific French drain. Water was also added to the aggregate to prevent the fines from producing a hazardous vapor during mixing. After approximately a minute of mixing to obtain a near homogenous dispersion of the fines, the contents of the cement mixer were then poured into the trench (see Figure 3.43). Once the aggregate was poured to an elevation that would be level with the bottom of the horizontal 12-inch inner diameter perforated pipe, the pipe was then installed through the hole in the sump and placed on top of the bed of aggregate (see Figure 3.45). The 12-inch inner diameter pipe was then sealed to the sump with expansion foam on the exterior and bituminous sealant on the interior. Any excess of the 12 in inner diameter pipe extending more than 6 in into the sump was removed. After the geotextile was secured around the unperforated portion of the 12-inch inner diameter pipe, the aggregate was further poured until it was within three inches of the ground surface. Lastly, the geotextile was folded over to cover the top of the aggregate (see Figure 3.46) and backfill was then placed and compacted (see Figure 3.47).

Figure 3.39: Construction of trench

Figure 3.40**:** French drain plumbing

Figure 3.41: The sump placed in the trench

Figure 3.42: Sealing the sump

Figure 3.43: Mixing fines and aggregate

Figure 3.44: Placement of aggregate in trench

Figure 3.45: Placement of HDPE pipe in trench

Figure 3.46: Geotextile covering aggregate

Figure 3.47: Completion of French drain 1 (RCA ”as is”) construction

3.6.2. In Situ Water Level System Construction

The in situ groundwater monitoring system for an individual French drain consisted of seven HDPE monitoring wells which collected data on the groundwater mounding profile. Each well contained a data logging piezometer suspended by a wire connected to the well cap. These monitoring wells were placed along the lateral and axial centerline of the aggregate box. The wells were constructed out of 4-inch inner diameter perforated pipe and placed into the ground 7-ft deep. Figure 3.35 shows the piezometer sensor and the schematic diagram of the piezometer sensor installation in a monitoring well. The piezometers were easily installed and removed, and were only placed into the French drain well system. The wells placed at 7 ft laterally between French drains marked the halfway point between drains; these wells were used by adjacent French drains when subsequently tested. In addition to variation in flow rates, changes in the groundwater mounding profiles were used to quantify the performance of the French drains.

The site plan view showing the locations of four French drains and the fire hydrant is presented in Figure 3.48. The schematic diagrams showing the water level measuring system design are presented in Figures 3.49 and 3.50 (top and cross-sectional views, respectively). Three monitoring wells were at a distance of 1 ft from the edge of the French drain to the centerline of the well, with one being at the tip of the drain and the other two being along the lateral center line of the drain, with one well on each side of the drain. Four additional wells were placed along the lateral center line of the drain at 3 ft increasing increments away from the 1-ft well, with two of these additional wells being on each side of the drain. If the outermost lateral well (7 ft from the French drain) was the half way point between two drains, then this well was shared between the well systems of both drains. The data logging piezometers were manufactured by Onset Computer Cooperation and were the (HOBO U20L-04) model, a single data extracting device known as the HOBO Waterproof Shuttle model (U-DTW-1) was also purchased, as well as the data analysis software labeled HOBOware PRO v.3.x for PC & Mac item number (BHW-PRO-CD).

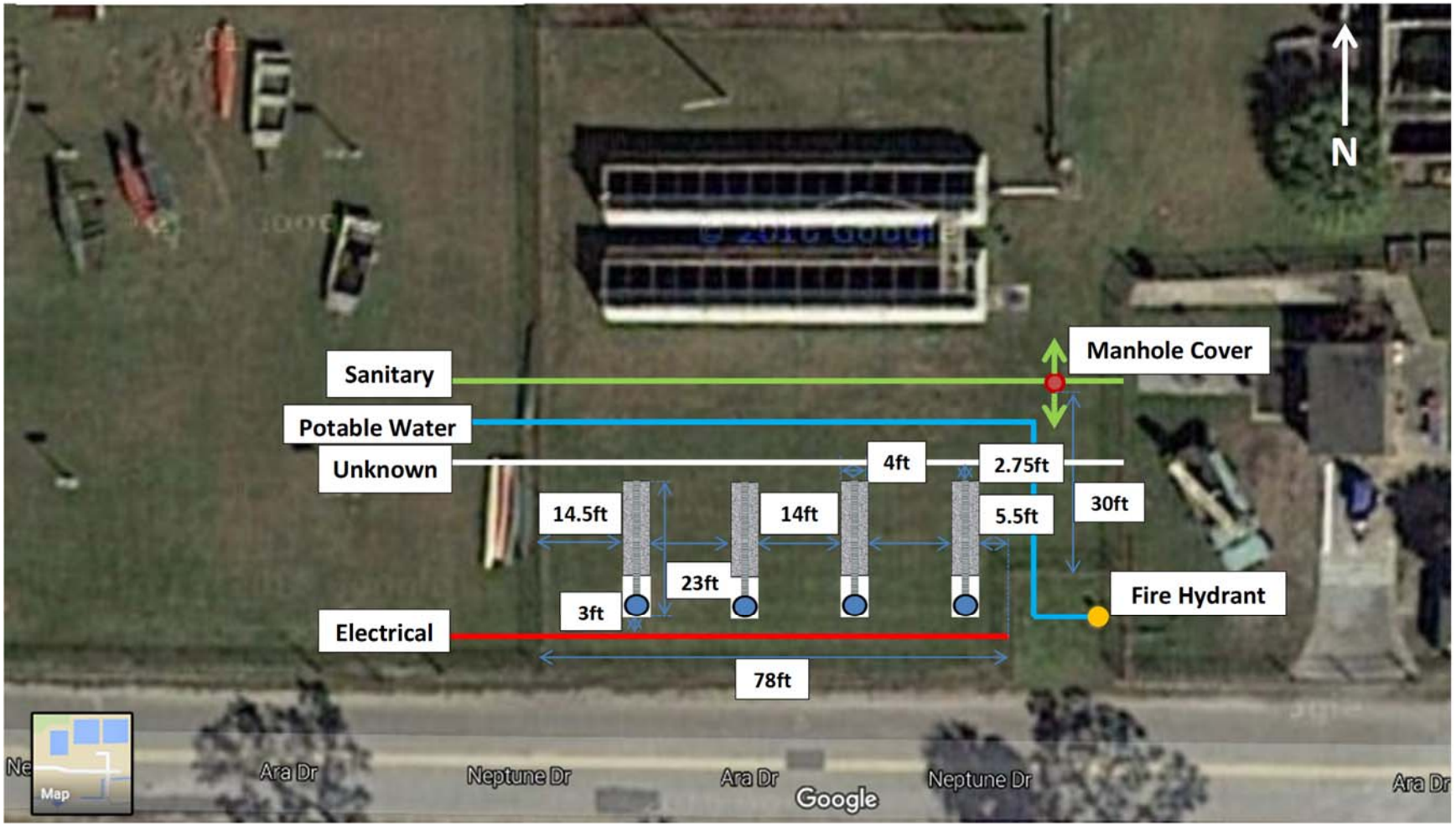

Figure 3.48: French drain site plan view

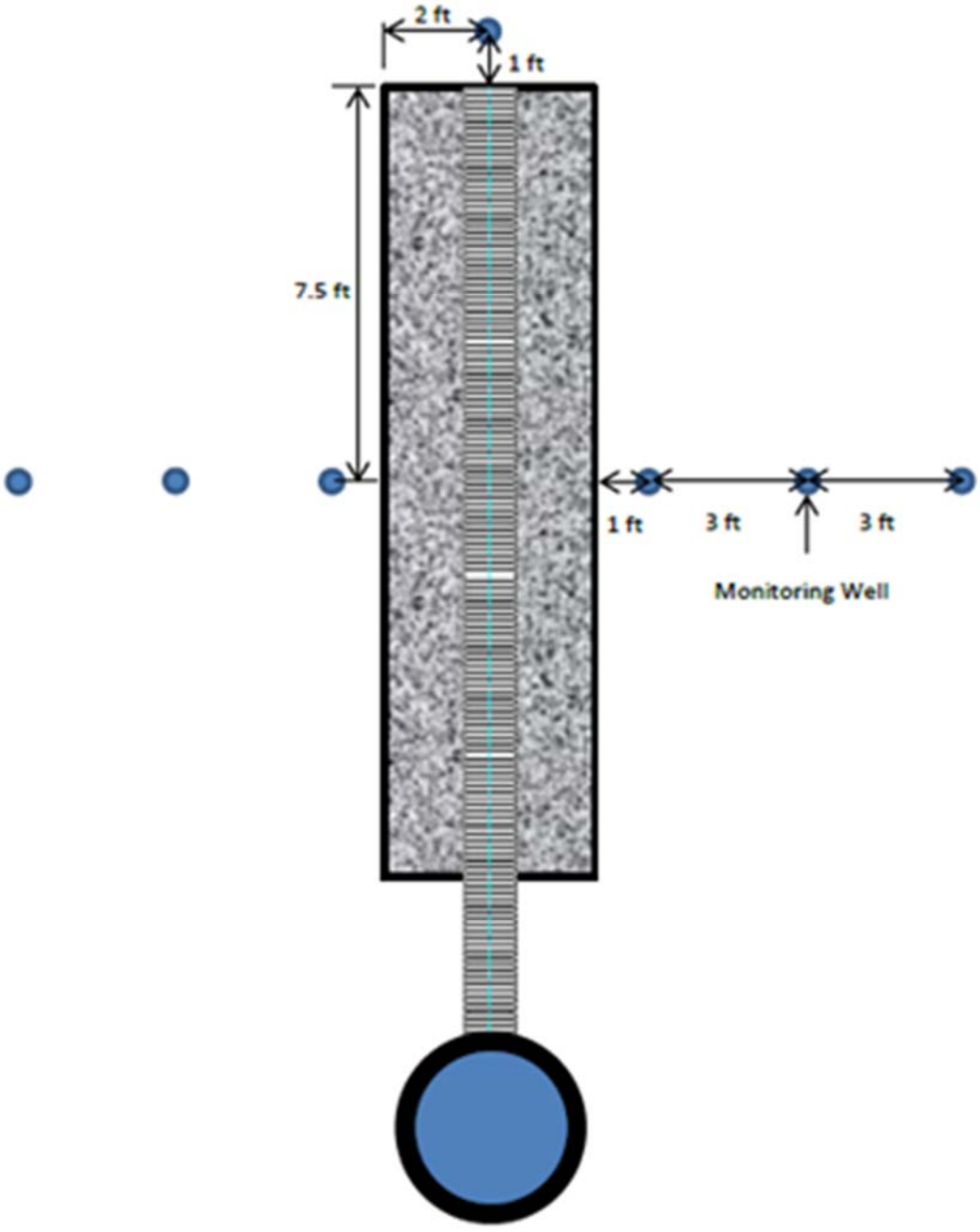

Figure 3.49: Field water level system plan view

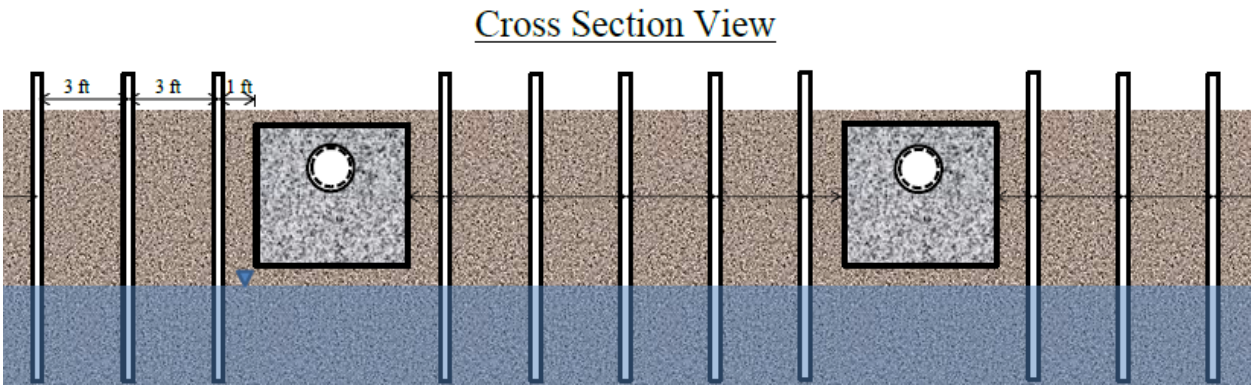

(a) Two adjacent French drains

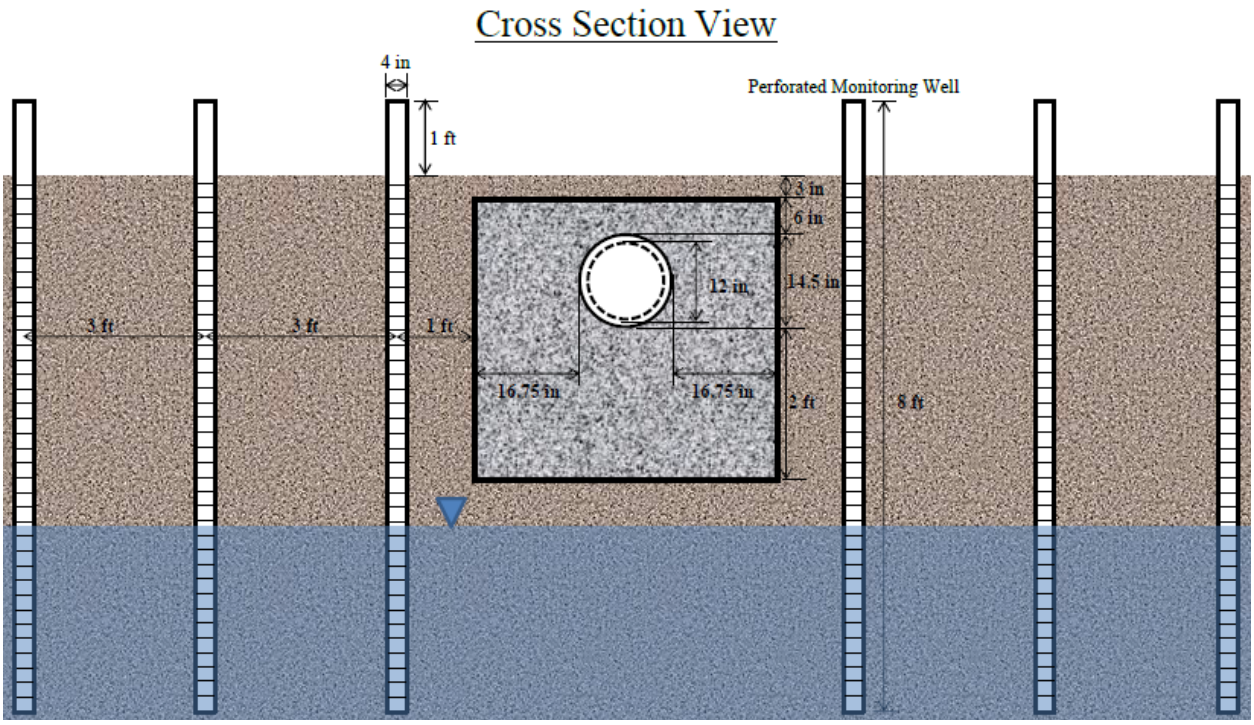

(b) Expanded view

Figure 3.50: Design of in situ water level measuring system: (a) cross-sectional view of two adjacent French drains and (b) expanded view with dimensional information

Construction of the groundwater monitoring system started with first prepping the 4-inch inner diameter HDPE monitoring wells. This process involved drilling additional perforations along the length of the well (because the pipes were only perforated along 120° of pipe circumference), then an adhesive was sprayed along the bottom 12-inch length of the well and wrapping the portion of the well that would be placed into the soil in the same geotextile used within the French drains. The purpose of the spray adhesive was to prevent the geotextile from sliding off the smooth surface of the well during driving. Prepared and unprepared wells can be seen in Figure 3.48.

Well installation followed well preparation. Each well point was bored to a depth of at least 7 ft with a hand auger. The hole diameter created by the hand auger nearly matched the outer diameter of the monitoring wells wrapped in geotextile, which prevented the wells from simply being placed into the boreholes. To install the wells required dynamic driving, which was accomplished by hammering the top of the well until the desired depth was reached. Depth of well installation was verified by ensuring the portion of the 10-ft well exposed at the ground surface was less than 3 ft (see Figure 3.52). Once all wells were installed into the ground, then the exposed portion was cut down to approximately 1 ft and capped. Screw eyes were installed on the inside of the well, caps to allow piezometers to be suspended by braided fishing line, and swivels. The completed system is shown in Figure 3.53.

Figure 3.51: Prepared and unprepared wells

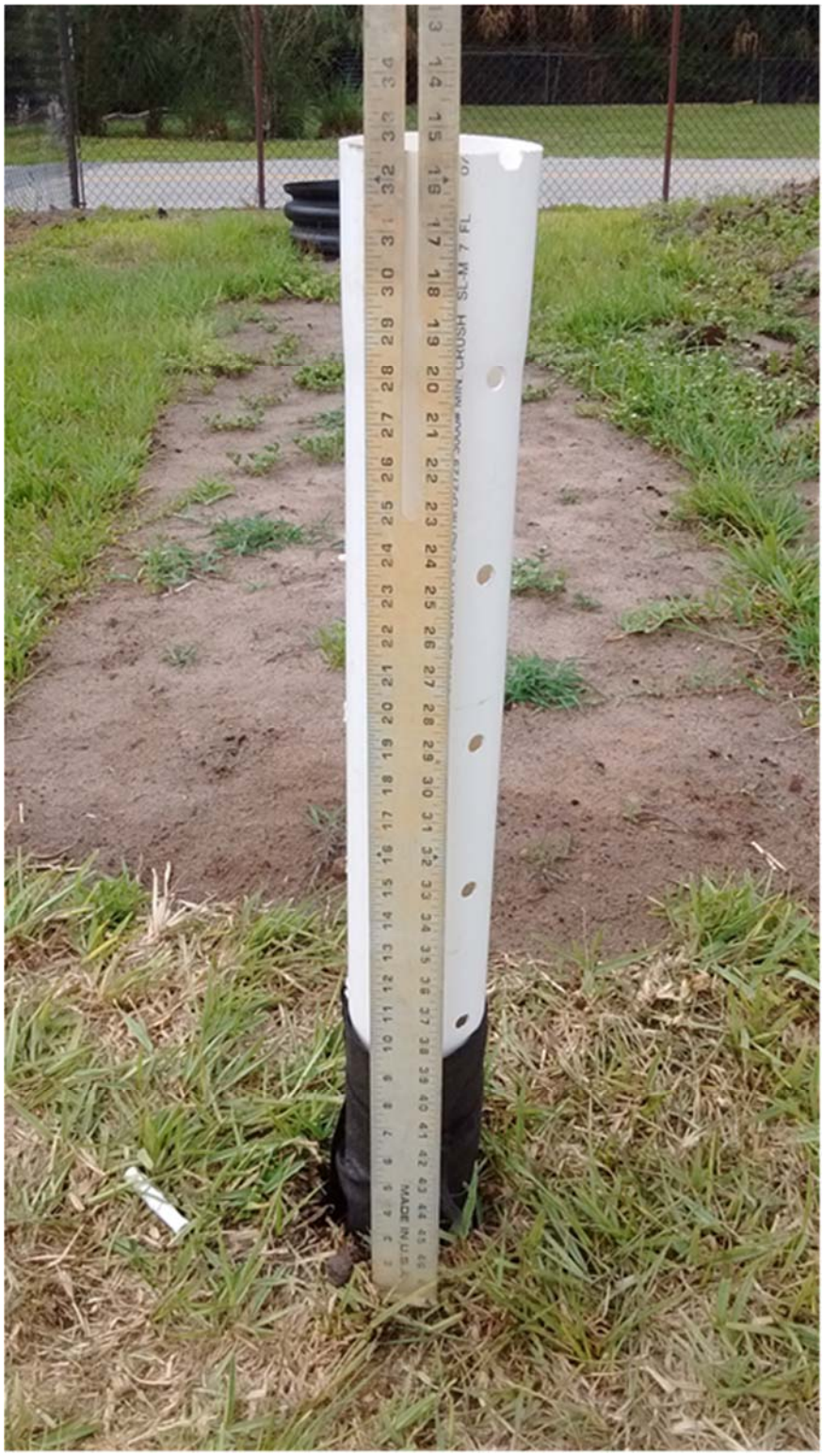

Figure 3.52: Verification of well placement depth

Figure 3.53: Completed system

3.6.3. Instrumentation

Multiple forms of instrumentation were used to assess the performance of the French drain systems both quantitatively and qualitatively. Quantitative means of assessing the performance of the drainage systems included monitoring the behavior of groundwater mounding profiles, measuring flow rates at steady state and under a constant head, and measuring the difference between the initial (new samples) and final (exhumed samples) geotextile permittivity values. Both the behavior of the groundwater mounding profile and flow rate measurement depended on the initial groundwater table depth. This depth was determined by using a water level meter on the wells located around a specific French drain prior to placing the piezometers in the monitoring wells and supplying the water for testing. Qualitative means of assessing the performance of the drainage systems involved performing camera investigations of the interior of each French drain every three months.

Water Delivery System

The fire hydrant on site was rated orange (500 – 999 gpm) and served as the water supply when running the French drain experiment. The University's Utilities & Energy Services department performed the flow meter and backflow preventer installation, Figure 3.37. Table 3.21 shows the description of the flow meter and backflow preventer. The fire hose connected to the flow meter and supplied water to the individual French drains.

Groundwater Mounding Instrumentation

Before supplying water to the French drain system under investigation, the HOBO water level sensors (piezometers which also serve as data loggers) were programmed in the HOBOware Pro software. Programming included selecting when a sensor starts recording data and the sampling frequency. Uploading the program into the water level sensor was performed by using the HOBO waterproof shuttle as a docking station for the sensor, which in return was connected to a computer with HOBOware Pro software installed. Inside the software interface there was an icon labeled "launch device", this option was chosen to upload the program into the piezometer. Programming the sensors for a delayed start versus an immediate start allowed all sensors to have the same sampling cycle, Figure 3.54. Also, the delayed start allowed the first data point to be taken after the sensors had been placed within the monitoring wells of the respective French drain.

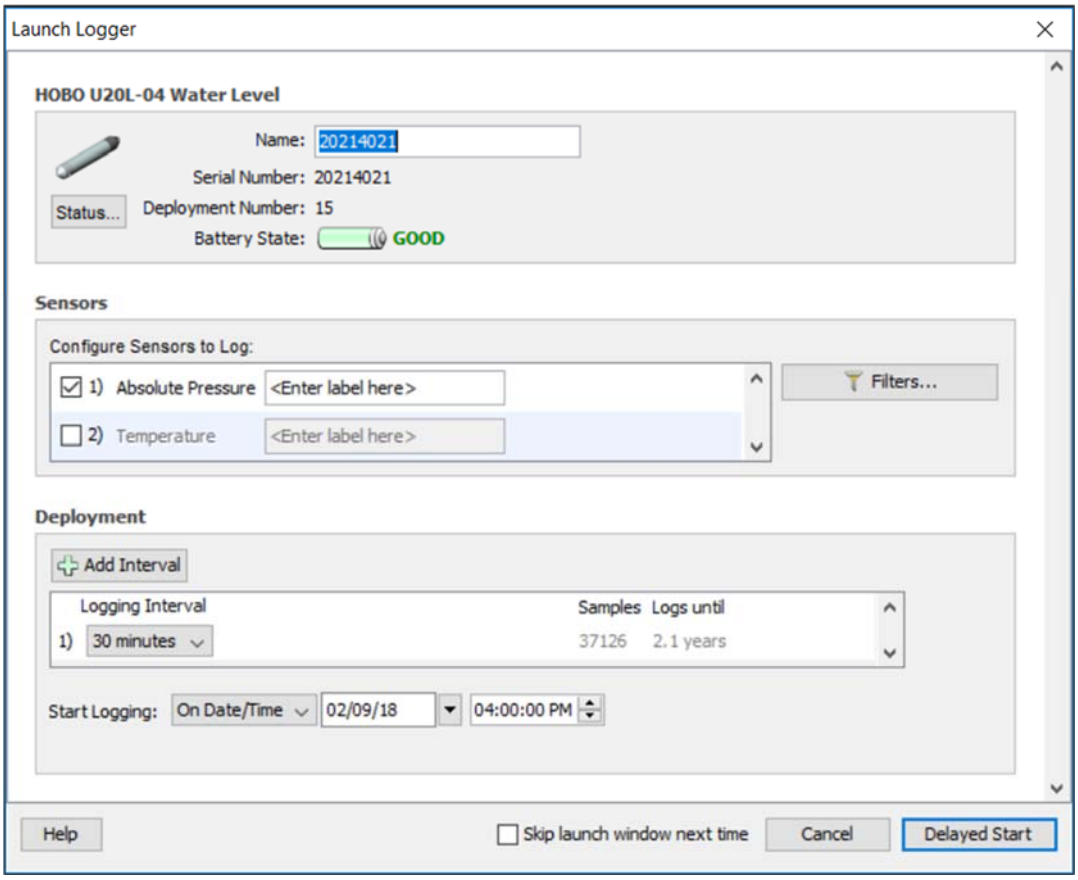

Figure 3.54: Sensor programming

After the sensors were launched, they were attached to their monitoring well cap lanyard and were submerged under the initial groundwater table. These lanyards have been constructed from braided fishing line and swivels, Figure 3.55. Once the sensors were suspended within the wells and before the water was turned on to the French drain, the first data point was taken at the designated delayed start time. The first data point when used in combination with the water level meter reading for that monitoring well was used to determine the position of the piezometer with respect to the ground surface.

Figure 3.55: Sensor attachment to well cap

Once the first data point was collected, then the water supply to the French drain was turned on and the change in the groundwater mounding profile was recorded. From the first few trials it was determined that the groundwater mounding profile approached peak elevation and remained relatively constant after approximately an hour and a half, also the flow rate through the system remained relatively constant, both indicating steady-state had been achieved and that a constant head was being applied. After steady-state was reached and flow rate measurements were obtained, the water supply to the system was then turned off. With the piezometers still left in the monitoring wells, the discharging behavior of the French drain system was measured through the change in the groundwater mounding profile over a 72-hr period. A 72-hr monitoring period of the discharging behavior of the French drain was chosen because initial testing data indicated that this period was more than enough to allow full dissipation of the groundwater mounding profile.

Multiple piezometer sampling frequencies where experimented with during the first few tests, ranging from as much as every 30 sec to as little as every 30 min. The initial data collected showed that a sampling frequency of 30 min maintained a similar trend when compared with a 30-sec sampling frequency. Finding the optimal sampling frequency preserved the factory replaceable battery inside the piezometer and reduced the overaccumulation of data.

After the 72-hr monitoring period the piezometers were removed from the monitoring wells and then placed back into the HOBO waterproof shuttle. Data was uploaded to the computer by selecting the “readout device” option in the HOBOware Pro software. Readings from the sensor allowed the user to save the data on the computer, plot the data in the software, and provided the option to export the data as a comma-separated values (CSV) file. Figure 3.56 showed the typical readout of an individual sensor.

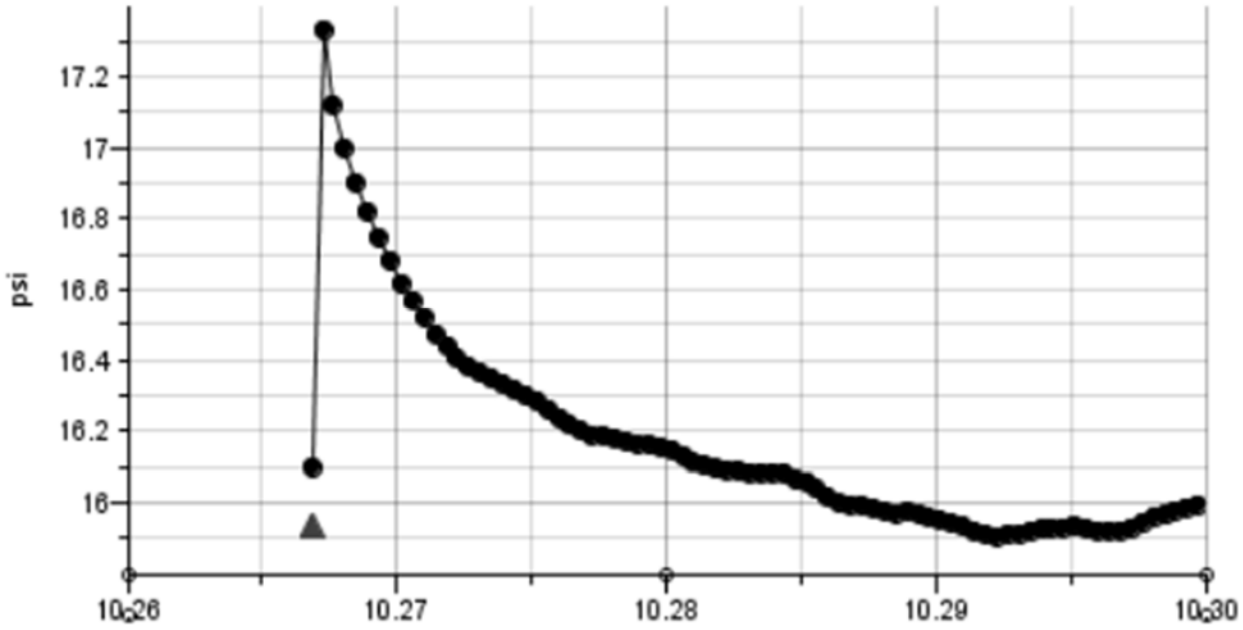

Figure 3.56: Typical sensor readout of absolute pressure versus time

Flow Rate Instrumentation

The flow rate measurements were taken once a steady-state had been reached and a constant head was being applied throughout the system. Through initial testing it had been determined that typical flow rate values for the French drain systems had been found to be on the order of 5 gal/min. Because the Badger flow meter had an operable flow rate lower limit of 4 gal/min, Figure 3.57 (a), a second method for determining the flow rate was also employed to ensure the accuracy of the Badger flow meter reading, which was determined as the time it takes for the dial to display a 5-gallon flow through the meter, Figure 3.57 (b). The second method involved timing how long it took for the water supply hose to fill up a 5-gal bucket (filled to the rim the volume was 5.45 gal), Figure 3.58. The water collection method directly measured the amount of water per unit time, which made it inherently more reliable than the Badger flow meter, which indirectly measures the flow rate by the spinning of an impeller. Both flow rates were recorded, but emphasis was given to the water collection method.

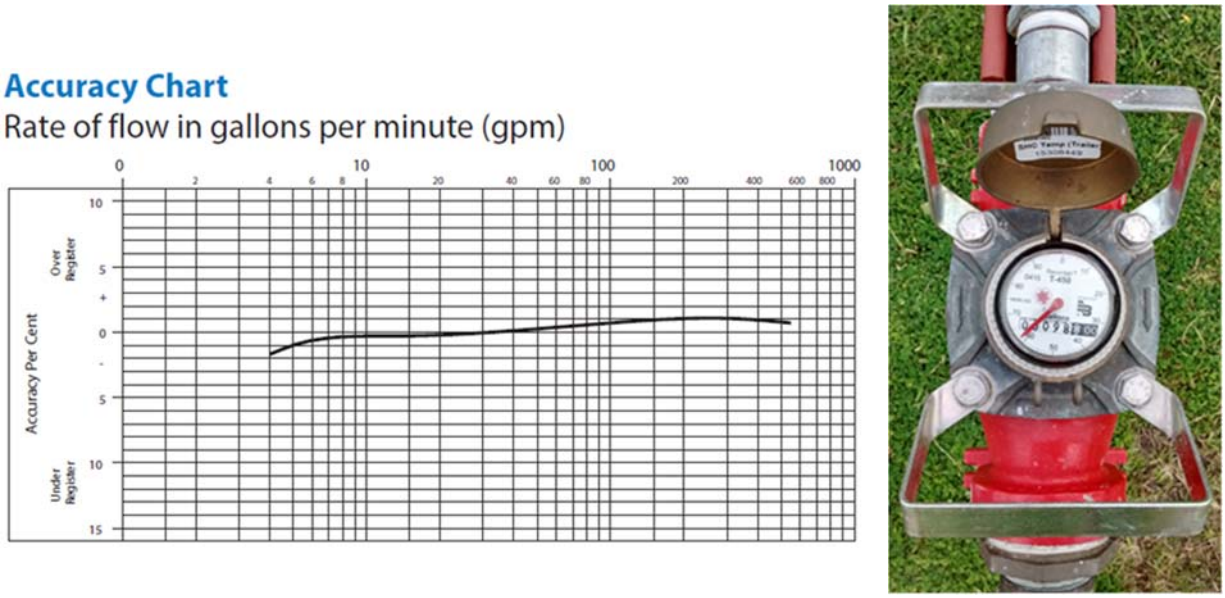

(a) Accuracy chart (b) badger flowmeter

Figure 3.57: (a) Accuracy chart and (b) Badger flowmeter

Figure 3.58: Water collection method

Experiment Procedure

1. Travel to the test site
2. With the water level meter, calculate the depth of the initial groundwater table in each monitoring well relative to the ground surface before testing
3. Remove the piezometers from the French drain that was tested days prior
4. Upload the data from the previously tested French drain and re-launch the piezometers with a 30-min sampling rate for the French drain which is about to be tested
5. Place the piezometers in the monitoring wells of the French drain under testing and insure they are fully submerged under the initial groundwater table
6. Allow the piezometers to take one measurement before testing so the positions of the piezometers relative to the initial groundwater table can be back calculated through the increase in absolute pressure above atmospheric pressure (14.7 psi).
7. Install the hose to the flowmeter and place the other end into the sump
8. Turn on the water
9. Obtain a head of water in the sump equal to the elevation of the ground surface (head difference across the French drain system is then equal to the difference between the initial groundwater table and ground surface) within the first 10 min and maintain a constant head at that level for 80 min
10. After the 80 min (90 min total) collect flow rate data from the flowmeter and by the water collection method
11. Turn off the water supply
12. Allow the piezometers to measure the behavior of the groundwater mounding dissipation over a minimum of 72 hr, collect data later on before testing of the next French drain
13. Put away hose and water level meter
14. Leave test site

4. DRAINAGE PERFORMANCE OF FRENCH DRAIN

4.1. Groundwater Table Depth (GWT)

Groundwater table (GWT) depth (distance from the ground surface) was measured in the field over the duration of the experiment. The measured data is presented in Figure 4.1. Florida, for the most part, is classified as a temperate climate (Cfa), with some southernmost coastal areas being classified as tropical (Af, Am, and Aw) under the Köppen climate classification system. The rainy season is generally accepted as being from June through September. Testing of the French drain systems commenced 10 days after Hurricane Irma hit central Florida. This extreme rainfall event, in combination with the near conclusion of the wet season, was the main reason why the depth to initial GWT was nearly 2 ft from the ground surface at the beginning of the experiment, as seen in Figure 4.1. The depth to GWT over the "dry season" (the "f" in the Cfa classification of the Köppen climate classification system technically states this zone is "without dry season") increased in a parabolic manner until it reached the maximum depth just before the beginning of the rainy season (around June). It took nearly 8 months for the GWT depth to drop from 2 ft to 7 ft, but only took approximately 2 months for the water table to rise back to its original level. During French drain testing, it was noticed that rainfall events during the wet season (from June through August) highly affected soil moisture conditions and groundwater recharge rates, which in return influenced the flow rates and groundwater mounding discharge behaviors of the French drains. In addition, as the GWT lowered below the bottom of the French drains, capillary forces on the unsaturated soils increased, as well as the head difference between the GWT and water surface in the French drains. Both phenomena resulted in an increase in flow. Therefore, the relationship between both flow rate and groundwater mounding discharge rate versus GWT depth were investigated in the following sections.

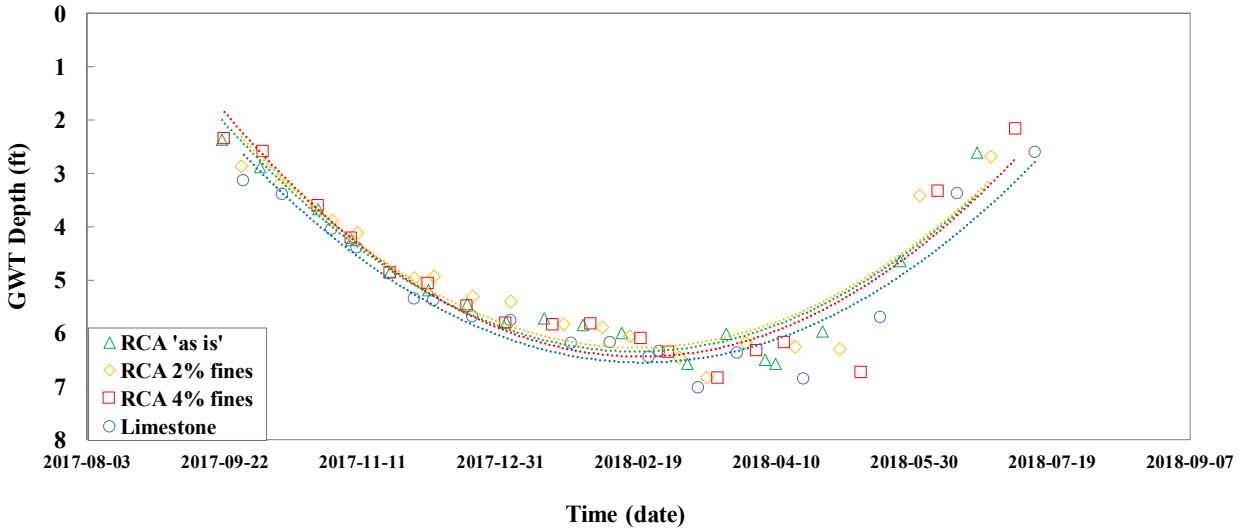

Figure 4.1: Groundwater table (GWT) depth with time

4.2. French Drain Flow Rate

During flow rate testing, the flow rate was measured once a constant flow rate and sump water level were reached (i.e. system equilibrium); which took approximately 1.5 hours after the water supply to the French drain system was turned on. Flow rate testing occurred over a 10-month period, as shown in Figure 4.2. The data showed high variability because of several factors such as surrounding soil moisture conditions before testing, direction of regional groundwater flow, and the time in between tests. The soil moisture conditions before testing were affected by preceding rainfall events and/or prior flow tests in the adjacent French drain systems. In Figure 4.2, the red box after May 30, 2018 indicated the beginning of the wet season. The wet season data set was not included in further analyses because the data showed significant variation and deviation.

Upon initial observation, the monitored flow rates from the French drains showed a clear trend. The flow rate did not decrease with elapsed time, suggesting no significant clogging in the drain systems occurred over the monitoring period. It is important to note that other factors relating to in situ site conditions were more impactful on flow rate. Figure 4.3 shows the aerial view layout of the four French drains. Trench 2 (RCA with 2% fines) and Trench 3 (RCA with 4% fines) were interior drains and Trench 1 (RCA 'as is') and Trench 4 (limestone) were exterior drains.

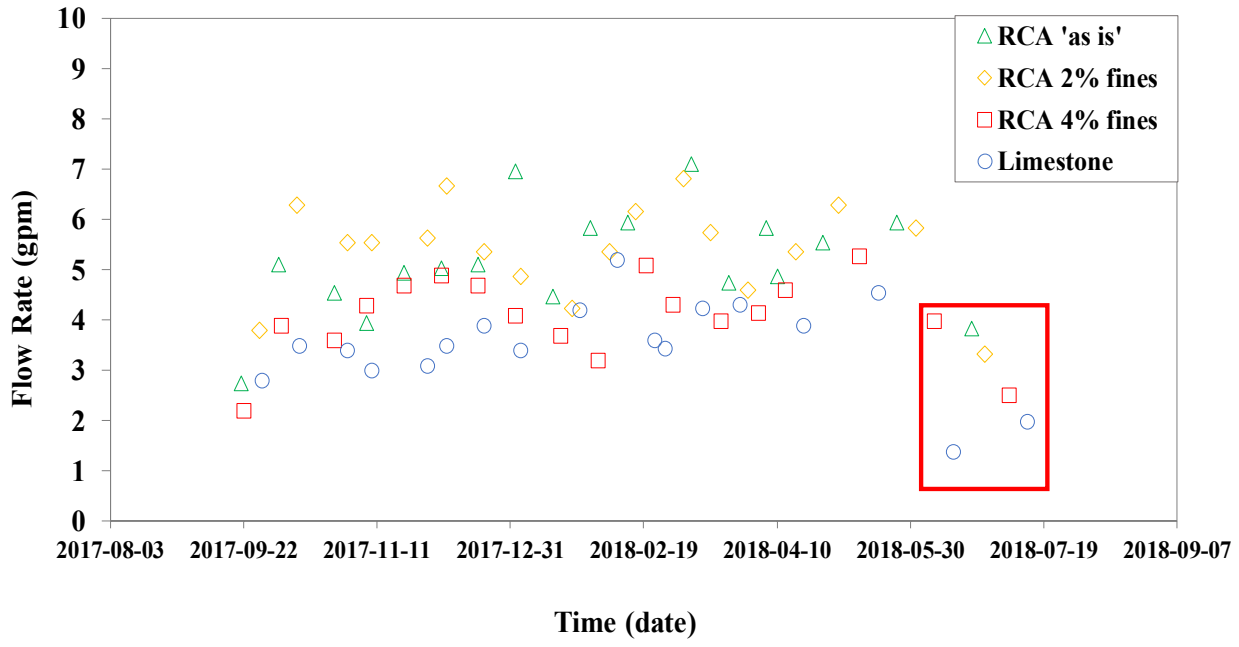

Figure 4.2: Flow rate measurement with time

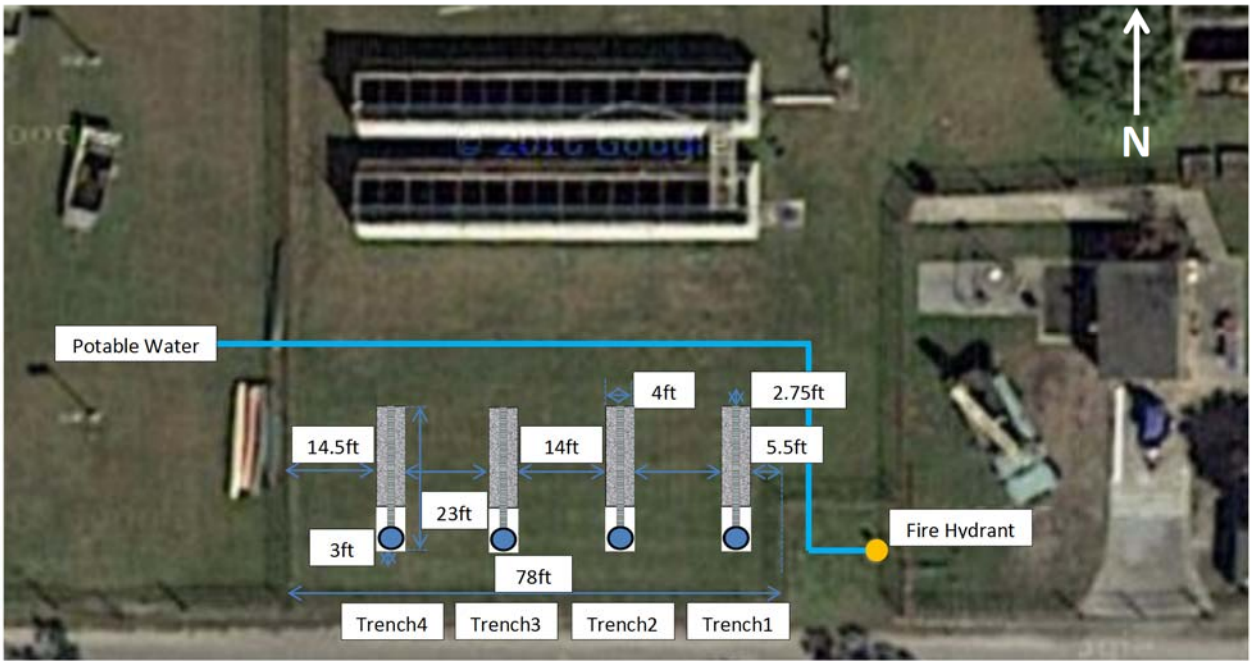

Figure 4.3: Site view showing the layout of French drains.
(note: Trench 1=RCA "as is", Trench 2=RCA with 2% fines, Trench 3=RCA with 4% fi nes, and Trench 4=limestone)

The coarse aggregate used in French drains allowed much higher drainage (discharge) than existing in situ soils (e.g. fine sand, A-3). As a result, the interior drains had "double-sided" drainage paths because of adjacent French drains. The exfiltration flows from the two exterior drains were to some extent limited by the in situ soils, which had much lower permeability than the coarse aggregate. In order to compare the drainage performance of French drains under similar site conditions, the interior and exterior drains were separately analyzed. Figures 4.4a and 4.4b show the measured flow rates of the interior and exterior drains, respectively. It was clearly observed that a greater quantity of fines resulted in a lower flow rate. RCA 'as is' contained 0.8% fines, whereas limestone had 2.2% fines.

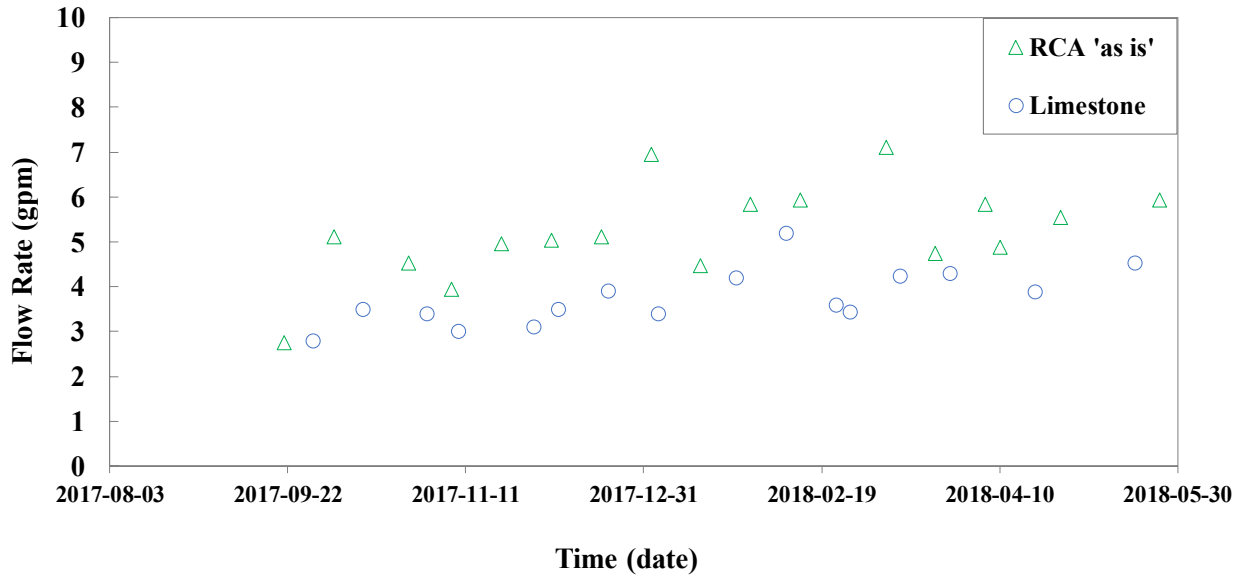

(a) Exterior drains

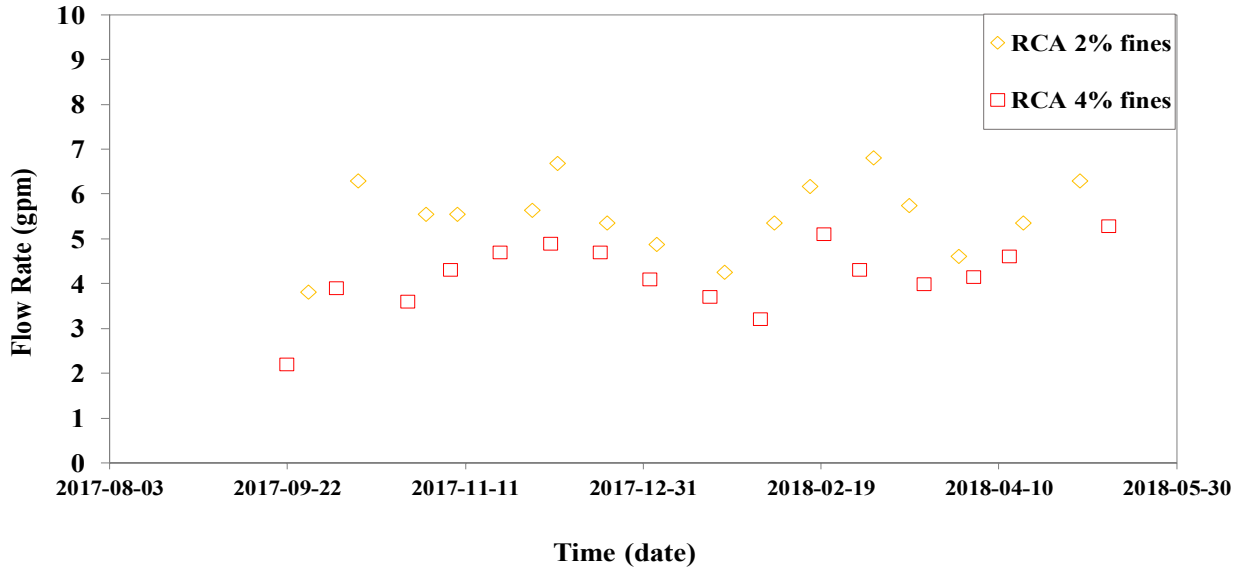

(b) Interior drains

Figure 4.4: Flow rate measurements with different drainage conditions

The flow rate versus time trendlines for the French drains had a positive slope over the period of experimental testing. This gradual increase in flow rate was due to the seasonal change in the GWT depth, Figure 4.1. As the GWT dropped further beneath the bottom of the French drains, it caused capillary forces on the unsaturated soils to increase. In addition, the head difference between the GWT and water surface in the French drain increased, both resulting in an increase in flow. The flow rate was plotted versus GWT depth in Figure 4.5.

The relationship between flow rate versus GWT depth was plotted because GWT depth controls the head difference within the system and was the most significant affecting factor in driving fluid flow. Figure 4.5 shows the flow rate measurement for the exterior and interior drains. Separating the plots into exterior and interior drains allowed for the comparison of French drains under similar drainage circumstances. Within the range of GWT depth tested, the interior drains seemed less sensitive to changes in head difference. Regardless of a French drain being exterior or interior, it can be seen by both comparisons that a higher fines content caused a reduction in flow rate.

Additional analysis was performed on the flow rate data. Trendlines were added on the data so that correlations between flow rate and GWT depth were defined. The curves intersected the origin because no flow occurred when the GWT depth was zero (no head difference in the system). In addition, there would be a maximum flow rate corresponding to a "terminal GWT depth". The terminal GWT depth can be defined as the depth at which an increase in depth no longer corresponds to an increase in flow. In other words, the GWT was deep enough not to influence the flow rate. Mathematically, the maximum flow rate would be represented as a horizontal asymptote on the plot of flow rate versus GWT depth.

The flow rate can be estimated by the following equation:

$$Q = Q_{avg\_max}(1 - EXP(-\alpha \times \Delta h)) \quad (1)$$

where, Q = flow rate, Q_{avg_max} = average maximum flow rate (i.e. horizontal asymptote), α = shape parameter that indicated how fast the flow rate reached the average maximum value, and Δh = head difference (i.e. groundwater table depth).

The parameters for each French drain are shown in Table 4.1. Q_{avg_max} values are the average maximum flow rate values, based on initial soil moisture conditions the value has a variation in each direction of approximately 0.9 gpm, as can be seen by the data for each French drain.

Table 4.1: Q_{avg_max} and α values of French drains

French drain	Q_{avg_max} (gpm)	α
RCA 'as is'	6.68	0.31
Limestone	5.38	0.22
RCA with 2% fines	5.90	0.55
RCA with 4% fines	4.85	0.41

Figures 4.5 (a) and (b) show the exterior and interior French drains paired together. Both pairs of drains exhibited similar trends. The interior drains seem to flow better at a lower GWT depth when compared to the exterior drains, but the interior drains were quicker to decay in flow rate and flatten out with an increasing GWT depth. The vertical offset between the drains of similar drainage conditions can be attributed to fines content, whereas the general shape of the curve when

comparing between exterior and interior drainage groups can be attributed to the drainage conditions.

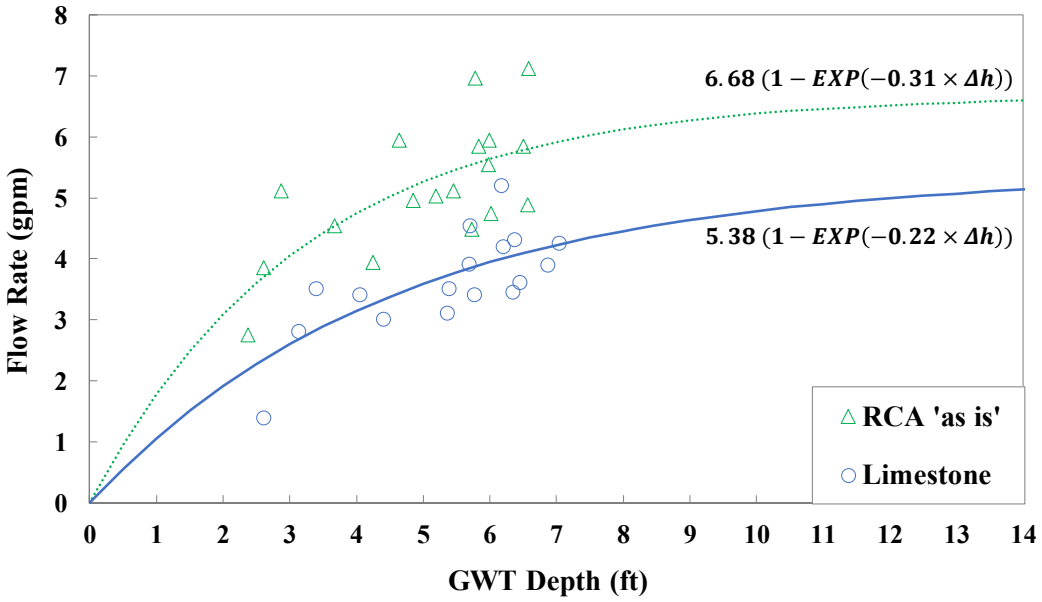

(a) Exterior drains

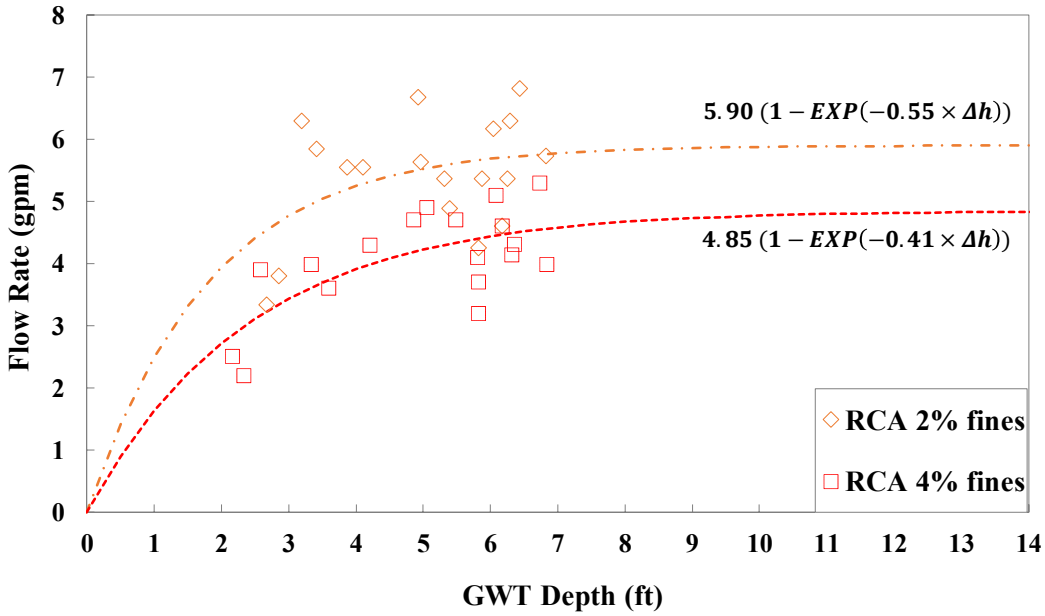

(b) Interior drains

Figure 4.5: Flow rate versus GWT depth relationship with different drainage conditions

4.3. French Drain Discharge Behavior

4.3.1. Secant Slope Analysis

The storage discharge behavior of each French drain was evaluated by analyzing the data of monitoring wells. Figure 4.6 shows the cross-section view of French drains along with the monitoring wells. In each monitoring well, an in situ water level sensor was installed to monitor the water level over at least 72 hours. Wells 3 and 5 were chosen for the discharge behavior analysis because they are closest to the trench, which better represents the water level within the French drain system.

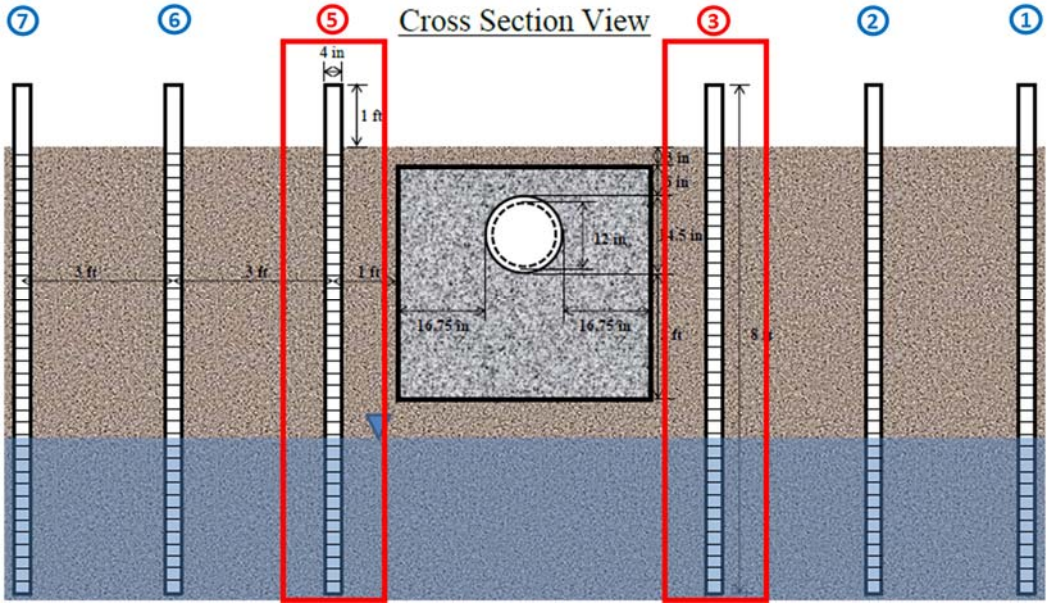

Figure 4.6: Locations of wells 3 and 5 (Design of in situ water level measuring system)

The rate of drop in the monitoring wells, as representing the discharge of the storage within the French drain, was calculated by measuring the head drop in both wells over a specific time interval and averaging the values together. Two time intervals were chosen for the measurement: from 2 hr to 3 hr and from 4 hr to 5 hr after the flow test began. The first interval (2 hr to 3 hr), designated as Stage 1, was selected as this corresponded to the exfiltration behavior 30 minutes after the water supply to the trench was turned off. This 30-minute waiting period allowed the full storage volume to shift to a stable discharge. The second interval (4 hr to 5 hr), designated as Stage 2, was selected as this provided information about how the trends changed as the water level within the trench lowered. In addition, the two stages covered the measurements when the water level in the drain was at both an upper level (Stage 1) and lower level (Stage 2) relative to the French drain bottom.

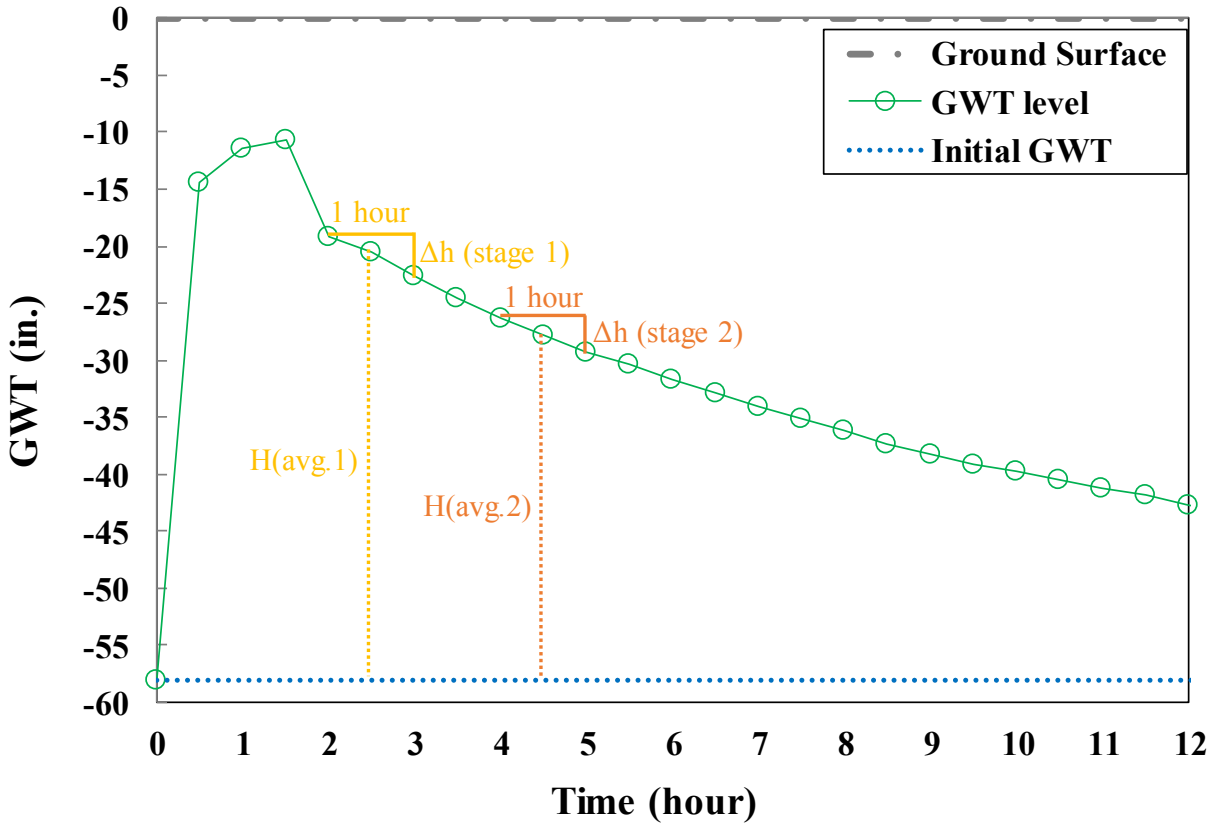

Figure 4.7: Methodology for secant slope analysis

The discharge performance is expressed as the slope of the relationship of GWT versus time, which indicates the discharge rate. The concept behind the secant slope is that the more a French drain became clogged, then the slower the storage level drop was, thus a flatter slope in the relationship between GWT level and time. Figures 4.8 and 4.9 show the change in slope for Stages 1 and 2, respectively. The interior and exterior drains were separately plotted. As seen in the figure, the slope increased with time, which was due to the increase in GWT depth shown in Figure 4.1. The drain with limestone aggregate showed lower discharge rates than RCA 'as is' over the monitoring period because of the greater amount of fines within the drain. In the same way, the drain with RCA 4% fines had lower slope values than RCA with 2% fines.

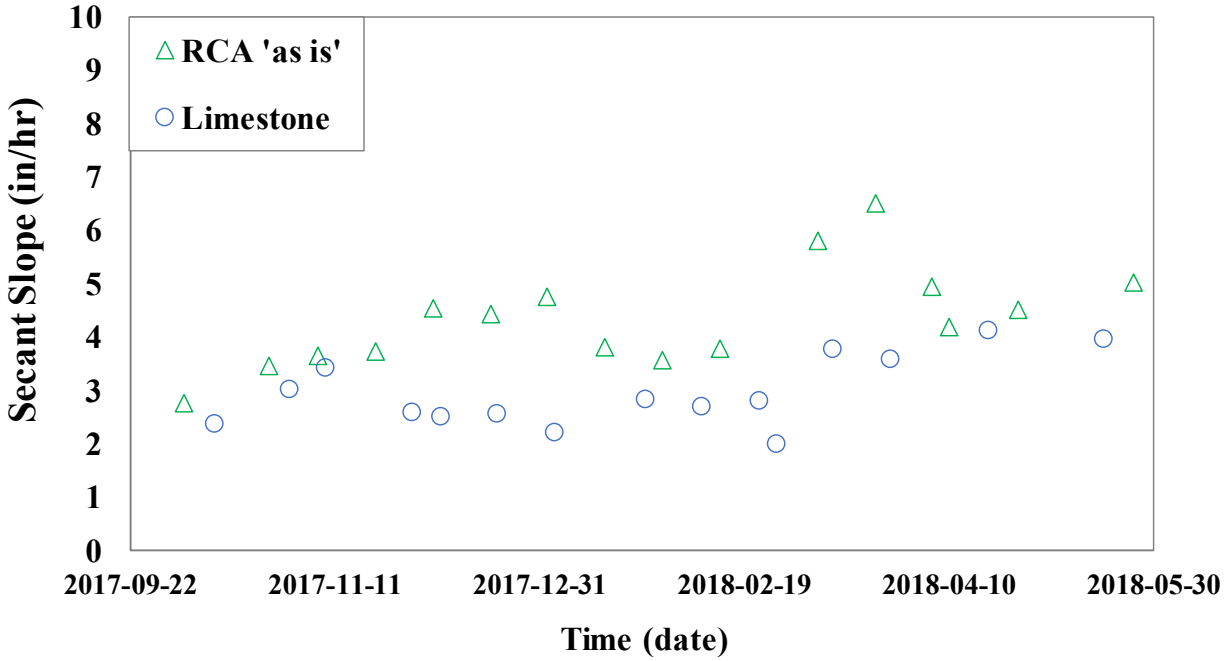

(a) Exterior drains

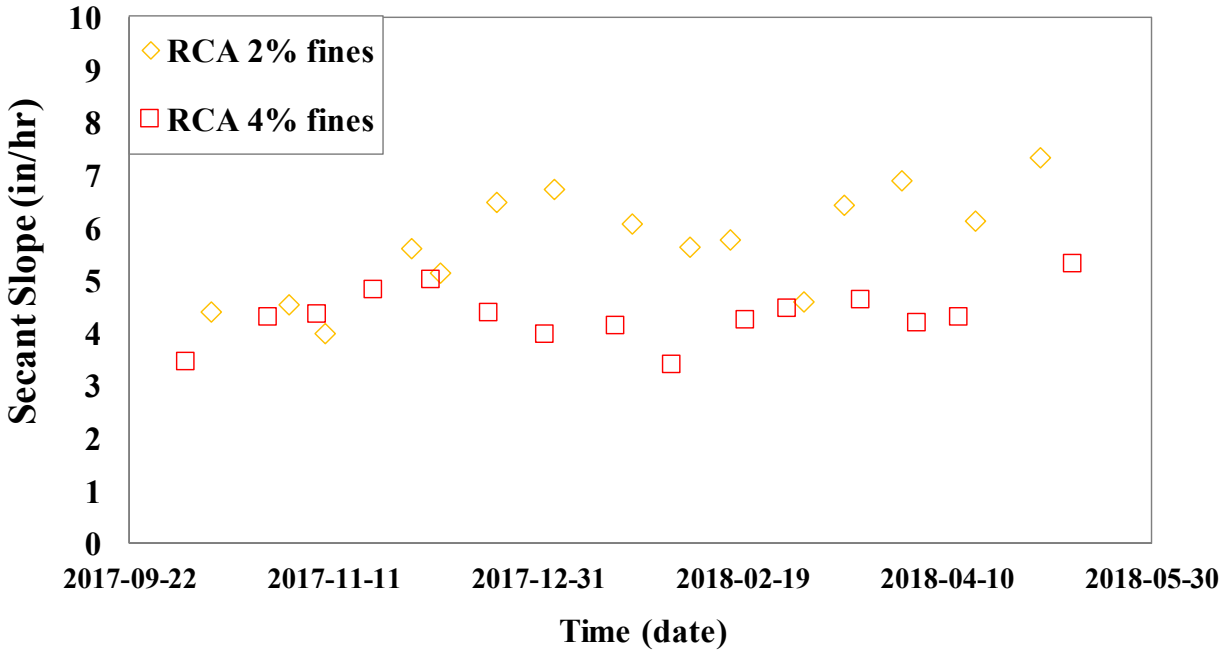

(b) Interior drains

Figure 4.8: Discharge behavior (secant slope) with different drainage conditions (Stage 1)

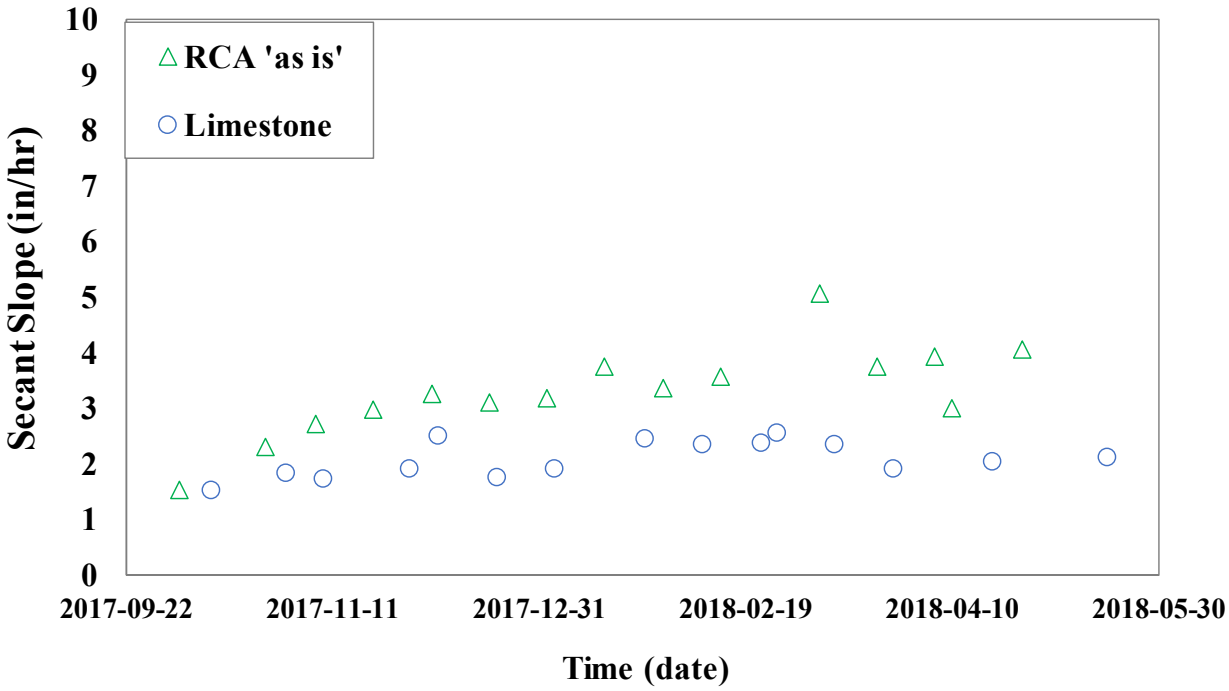

(a) Exterior drains

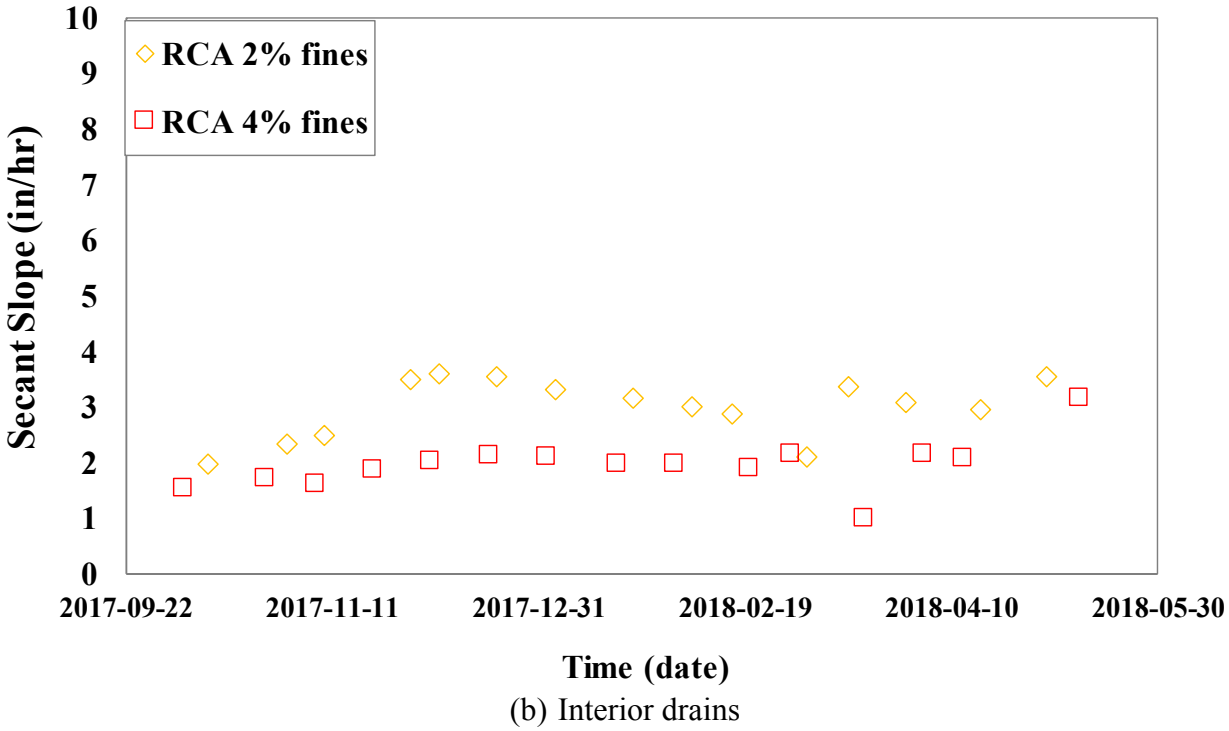

(b) Interior drains

Figure 4.9: Discharge behavior (secant slope) with different drainage conditions (Stage 2)

4.3.2. Secant Slope versus Initial GWT Depth

In Figures 4.10 and 4.11, the secant slope is plotted against initial GWT depth. The resulting trends were very similar to those in Figures 4.8 and 4.9, which indicated that as time advanced throughout the experimental period the GWT depth increased, making time and initial GWT depth strongly correlated. Once again, the interior drains had better discharge performance near full storage than the exterior drains, and as the water level decreased the discharge rates of the interior drains deteriorated faster than the exterior drains. As the water level decreased (Figure 4.11), the Stage 2 trends with the steepest slopes in decreasing order were, RCA 'as is', RCA with 2% fines, limestone, and RCA with 4% fines. This was also the order of increasing fines content, reinforcing that more fines caused a decrease in average drain permittivity, thus reducing the drain's slope (i.e. response to a change in head) in the relationship secant slope versus initial GWT depth. The secant slope versus initial GWT depth relationship was similar to the relationship between discharge velocity *(v)* versus hydraulic gradient *(i)*, where the slope of the relationship (determined by resistance in the system) was the hydraulic conductivity *(k)*. The secant modulus (discharge rate) versus initial GWT depth (protentional energy) at a given storage water level was used to give an indication of the average permittivity value (system resistance) for the drainage system at that water level.

The discharge rate also was estimated by the following equation below. Mathematically, the maximum discharge rate is represented as a horizontal asymptote on the plot of discharge rate versus GWT depth,

$$S = S_{avg\_max}(1 - EXP(-\alpha \times \Delta h)) \quad (2)$$

where, S = discharge rate, S_{avg_max} = average maximum discharge rate (i.e. horizontal asymptote), α = shape parameter that indicates how fast the discharge rate reached the average maximum value, and Δh = head difference (i.e. groundwater table depth).

The parameters for each French drain are shown in Table 4.2. S_{avg_max} values are the average maximum discharge rate values, based on initial soil moisture conditions the value has a variation in each direction of approximately 1 in./hr, as can be seen by the data for each French drain.

Table 4.2: $S_{avg\text{-}max}$ and α values of French drains

Stage	French drain	$S_{avg\text{-}max}$ (in/hr)	α
1	RCA 'as is'	5.44	0.32
	Limestone	3.05	0.75
	RCA with 2% fines	7.89	0.25
	RCA with 4% fines	4.39	0.81
2	RCA 'as is'	4.81	0.32
	Limestone	2.91	0.74
	RCA with 2% fines	4.39	0.21
	RCA with 4% fines	2.46	0.31

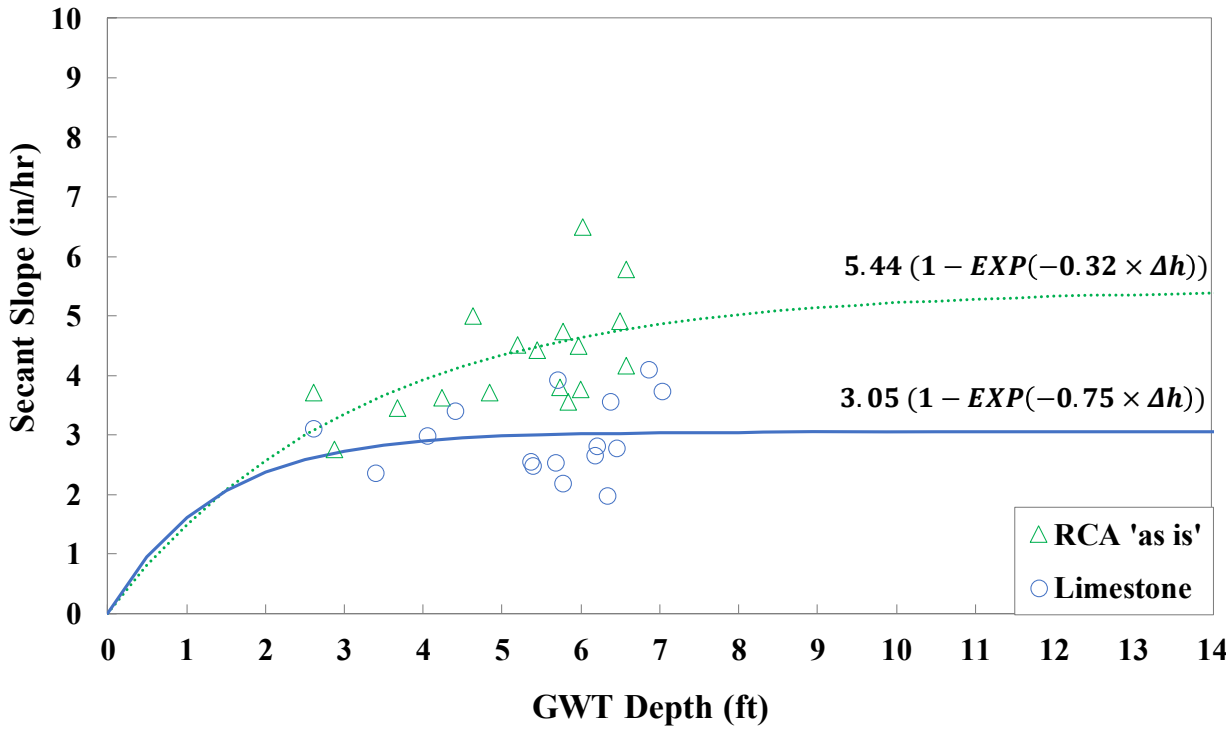

(a) Exterior drains

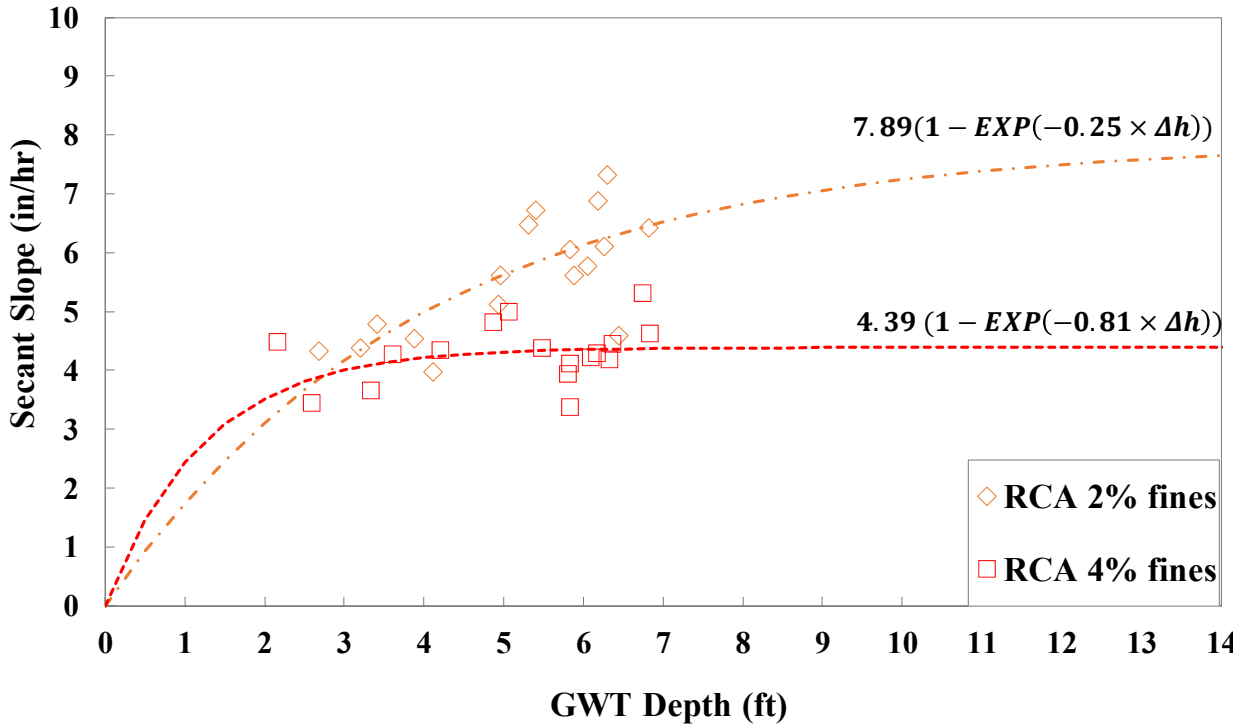

(b) Interior drains

Figure 4.10: Secant slope versus GWT depth (Stage 1)

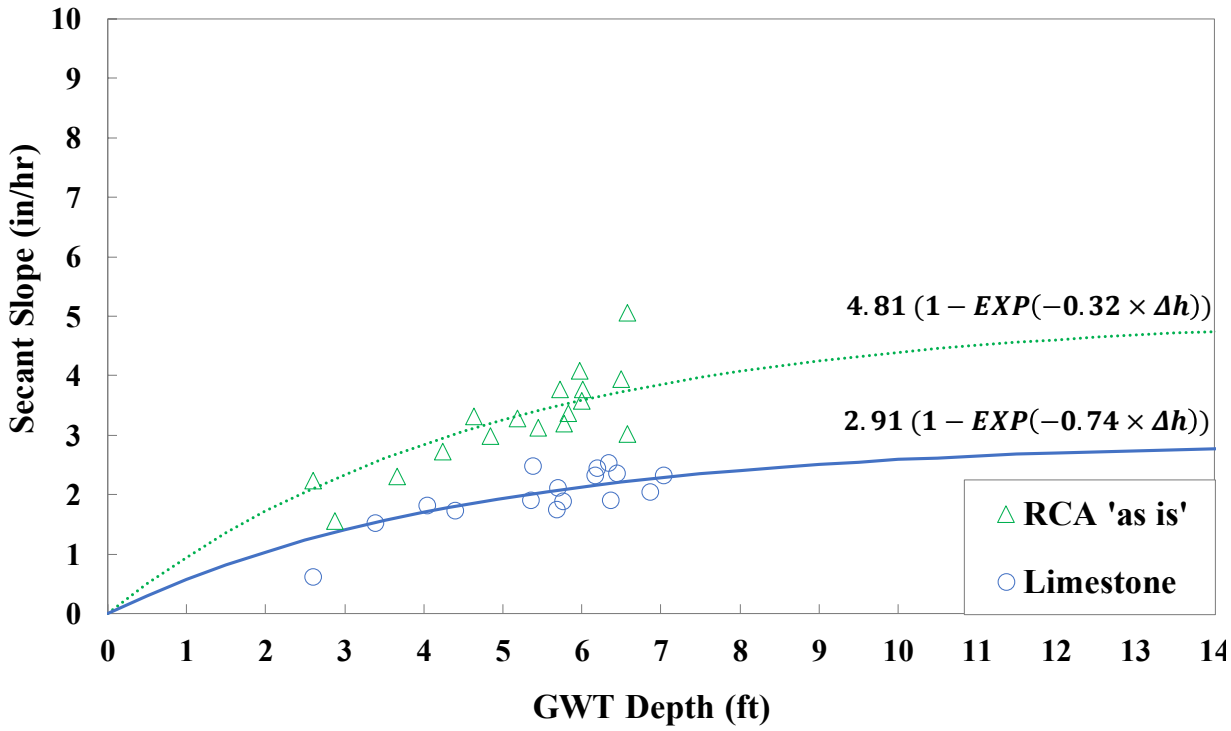

(a) Exterior drains

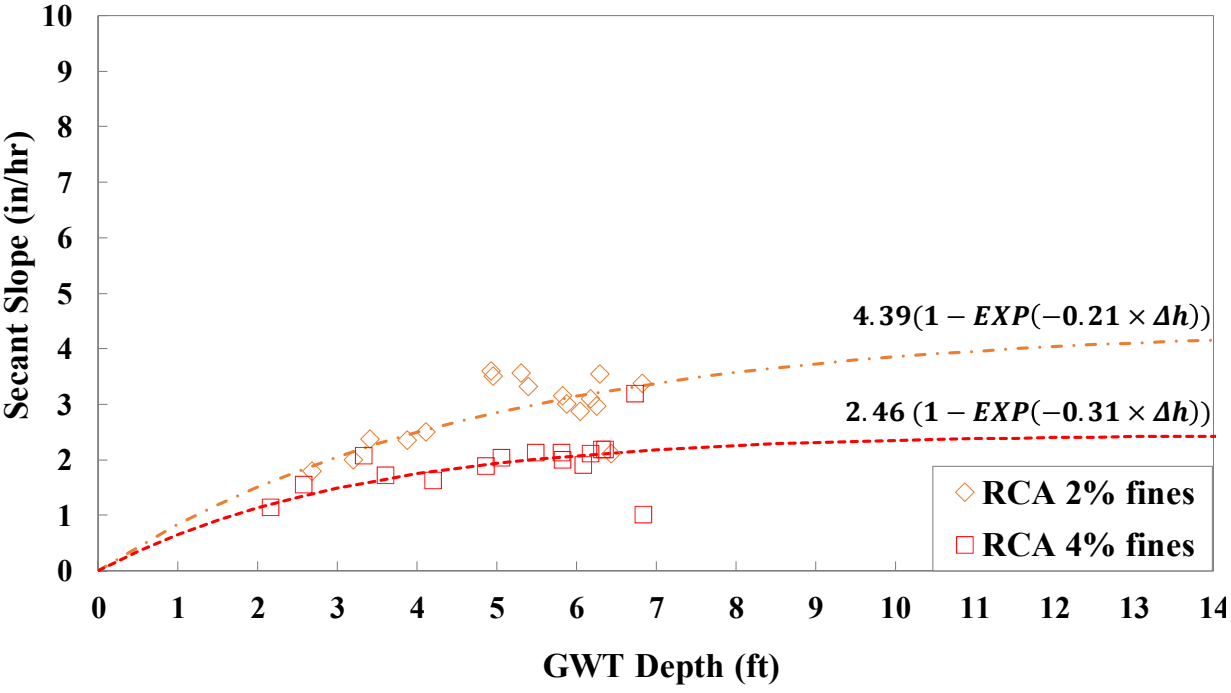

(b) Interior drains

Figure 4.11: Secant slope versus GWT depth (Stage 2)

4.4. Groundwater Mounding Analysis

The groundwater mounding analysis provides information on the length of time for the GWT to go back to equilibrium after water has stopped entering the French drain. A recovery time of 72 hours is generally used if a specific time period is not provided by the permitting agencies where the project is located. Based on the groundwater mounding profiles in Figures 4.12 and 4.13, all four French drains within this experiment completely discharged their storage volume within 72 hours if the GWT was below the bottom of the trench (i.e. 48 in. deep). Figure 4.12 pairs the exterior drains together, whereas Figure 4.13 pairs the interior drains together.

The RCA 'as is' French drain maintained the most symmetric groundwater mounding profile out of the four drains throughout the experiment, even though well 5 seemed to have an interval of rapid discharge. Because the GWT monitoring wells penetrated multiple soil strata, this rapid discharge may be the result of an individual well draining into a more permeable layer which did exist or was not as pronounced around the other wells. In Figure 4.12 (e) it can be seen that wells 2, 3, and 6 also had an interval of rapid drawdown, but not as extreme as in well 5. In all there seemed to be minimum distortion in the RCA 'as is' French drain groundwater mounding profile and a strong response to head change (change in the initial groundwater table depth).

When observing the French drain containing limestone a distorted groundwater mounding profile is shown. Wells 5 through 7 seemed to take longer to discharge, causing a residual groundwater mounding effect that lasted beyond 72 hours. Wells 1 through 3 seemed to discharge more quickly, which may be attributed to the presence of the RCA 4% fines French drain 14 ft away. In test 16 even though the initial GWT was fairly deep, the mounding profile did not seem to approach the ground surface like in previous tests. It is possible that fines may have accumulated against the trench walls, thus restricting the flow to the monitoring wells. In other words, the water in the French drain may have been at the ground surface right after the water was shut off, but the fines accumulation on the trench walls might made it so that water flowing out of the drain was at such a low rate that no appreciable head of water developed in the monitoring wells.

RCA with 2% fines and RCA 4% fines in Figures 4.13 (g) and (h) are near reflections of each other, with RCA with 2% fines having a slightly quicker dissipation rate. RCA with 4% fines appears to have ponding lasting longer than 72 hours around wells 1 through 3.

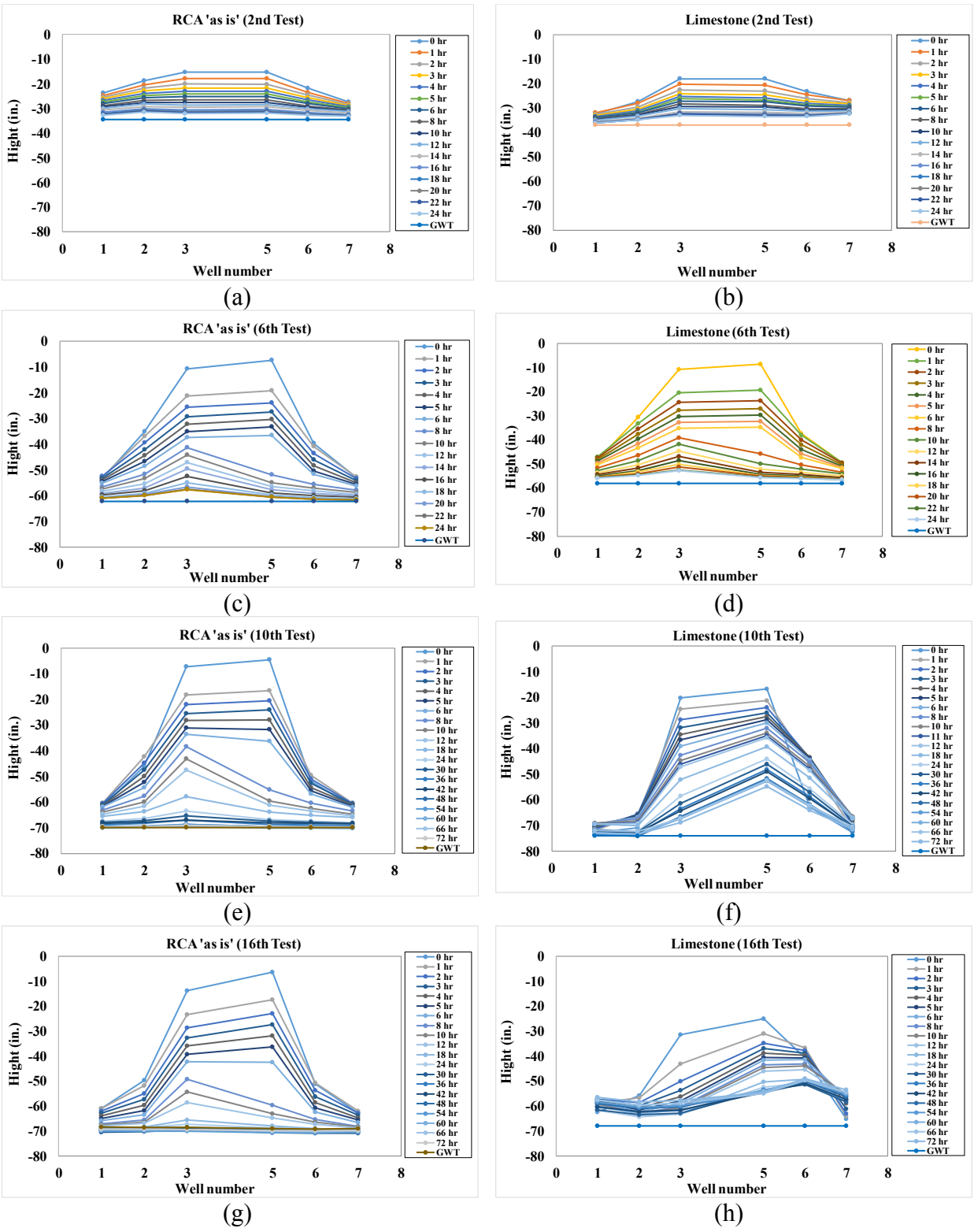

Figure 4.12: Mounding profiles for Stage 1

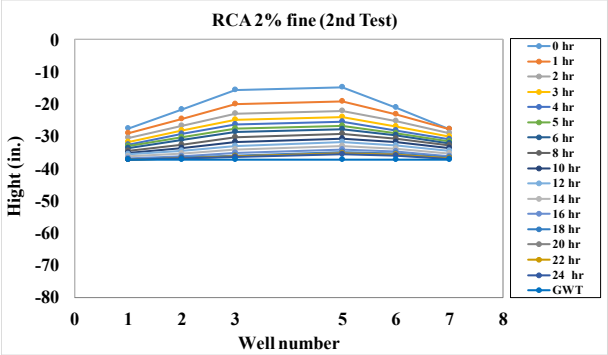

(a)

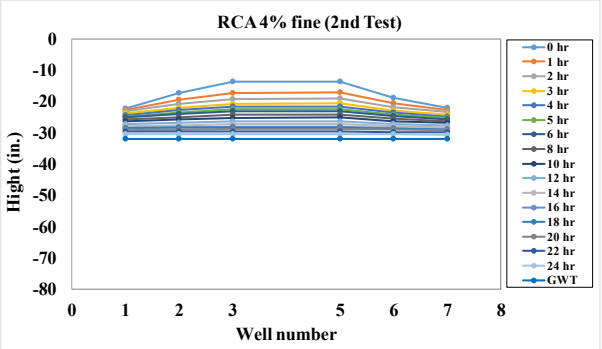

(b)

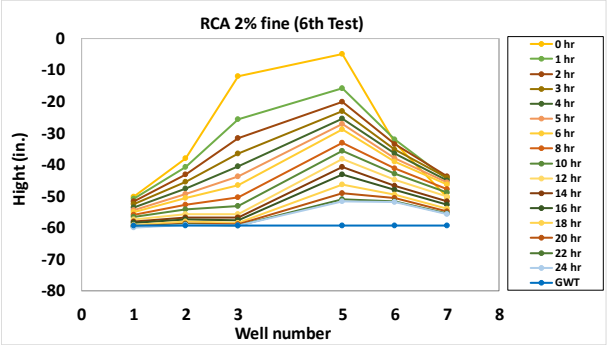

(c)

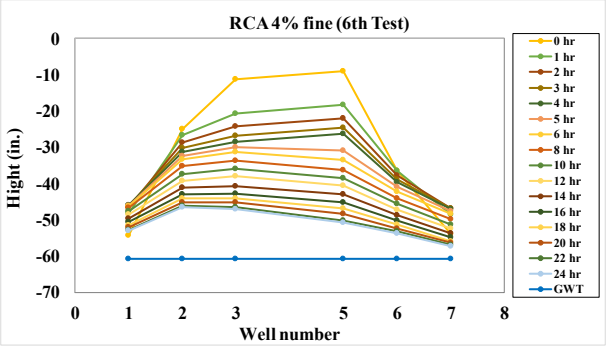

(d)

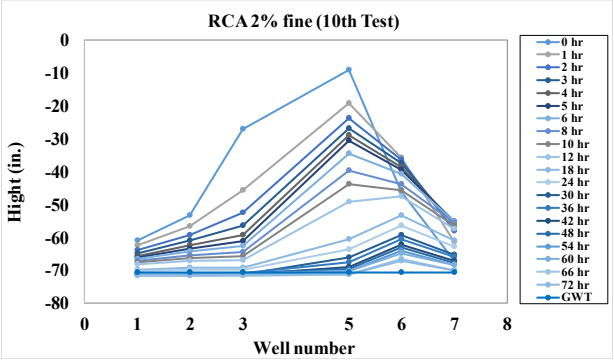

(e)

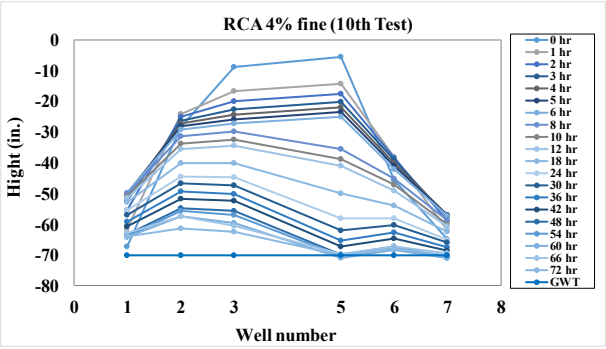

(f)

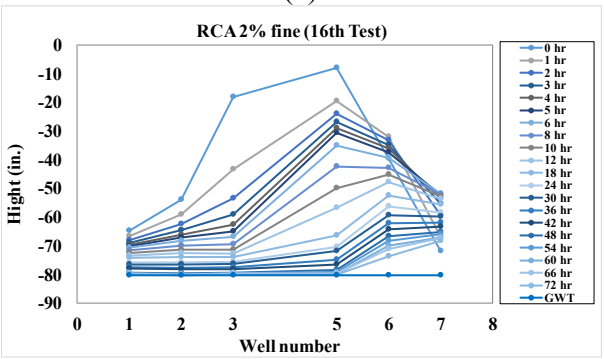

(g)

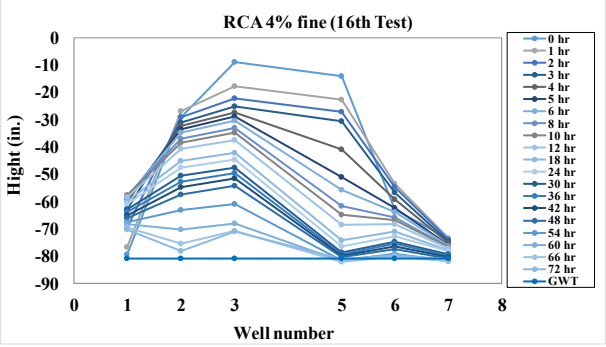

(h)

Figure 4.13: Mounding profiles for Stage 2

4.5. Camera Inspection

A camera was used to inspect the inside of each French drain over the duration of the experiment. The Logitech webcam (C930e) with 1080p HD capability, shown in Figure 4.14, was used. The camera and a portable light were attached to an extendable rod and inserted into the pipe of each French drain during inspection. The purpose of the camera investigation was to ensure that aggregate was not eroding into the horizontal drainage pipe, as well as to detect any scaling on the interior walls of the pipe, possibly indicating precipitation or re-cementation of the aggregate fines. The camera inspection was performed every three months on all four French drains and served as a qualitative performance indicator (see Figures 4.15 through 4.18).

Figure 4.14: Camera to inspect inside pipe

Upon the camera inspection, it was concluded that no surrounding aggregate deposited into the pipes (see Figures 4.15 through 4.18); however, the crowns of the pipes seemed to be within the root zone of the overlying vegetation, which can be seen entering the pipes. Based on observations made during exhuming the geotextile samples, some roots traveled between the 1-foot overlaps in the geotextile, and even in some locations punctured the geotextile. However, the presence of the roots was not severe enough to hinder the exfiltration of water.

(a) French drain RCA 'as is'

(b) French drain RCA with 2% fines

(b) French drain RCA with 4% fines

(d) French drain limestone

Figure 4.15: Camera inspection images (inside pipes) at 3 months

(c) French drain RCA 'as is'

(b) French drain RCA with 2% fines

(d) French drain RCA with 4% fines

(d) French drain limestone

Figure 4.16: Camera inspection images (inside pipes) at 6 months

(e) French drain RCA 'as is'

(b) French drain RCA with 2% fines

(f) French drain RCA with 4% fines

(d) French drain limestone

Figure 4.17: Camera inspection images (inside pipes) at 9 months

(a) French drain RCA ‘as is’

(b) French drain RCA with 2% fines

(b) French drain RCA with 4% fines

(d) French drain limestone

Figure 4.18: Camera inspection images (inside pipes) at 12 months

4.6. Geotextile Permittivity Testing Results

4.6.1. Permittivity Testing Results of the Filter Fabric before Installation

Geotextile (polypropylene nonwoven fabric) was obtained from ACF Environmental Inc., and the material specs are summarized in Table 4.3. The geotextile permittivity from the manufacturer showed a minimum average roll value of 1.6 sec^{-1}. Drainage geotextiles, as required by 2016 FDOT Standard Specifications for Road and Bridge Construction, Section 985-2.2, are required to have a minimum permittivity of 0.5 sec^{-1} (D-3a) for the least restrictive D-3 geotextile listed. Product certification, in accordance with 2016 FDOT Standard Specifications for Road and Bridge Construction, Section 985-3.2, was verified by the FDOT State Materials Office and it was verified that the samples of the geotextile provided met all the requirements for type D-3 French drain filter fabric application.

Table 4.3: Technical data sheet N060 nonwoven geotextile

Property	Min. Avg. Roll value	Test Method
Grab tensile strength	160 lbs	ASTM D4632
Grab tensile elongation	50%	ASTM D4632
CBR Puncture	410 lbs	ASTM D6241
Trapezoid tear strength	60 lbs	ASTM D4533
UV Resistant @ 500 hrs	70%	ASTM D4355
Apparent opening size (AOS)	70 US Sieve	ASTM D4751
Permittivity (sec^{-1})	1.6 (sec^{-1})	ASTM D4491
Flow rate	110 gpm/ft^2	ASTM D4491

The researchers conducted permittivity testing on unused geotextile samples to confirm the geotextile permittivity from the manufacturer of 1.6 sec^{-1}. Exhumed samples collected after completion of field testing are compared with the control samples. The reduction in geotextile permittivity can be used as a means to quantify any clogging that may have occurred within the French drains over the experiment period. Figure 4.19 shows a schematic diagram of geotextile permittivity testing. The apparatus design is in general compliance with ASTM 4491.The design philosophy of the apparatus is to construct a flow system where nearly all the head loss of the system occurs as a result of the water flowing across the geotextile sample. This is achieved by having the cross-sectional area of the geotextile being the smallest cross-sectional area normal to flow within the system. Having a system designed this way makes the geotextile the controlling element for flow rate. Use of pipes and pipe fittings with significantly smaller cross-sectional areas than the geotextile should be avoided because these components may produce local head losses and possibly control the flow rate of the entire system, resulting in erroneous permittivity values. The diameter of the geotextile samples used in this device is 3 inches. The head difference across this system is created by adjusting the flow rate at the inlet (the faster the flow rate the higher the buildup of head) while maintaining a permanent lower elevation head at the weir.

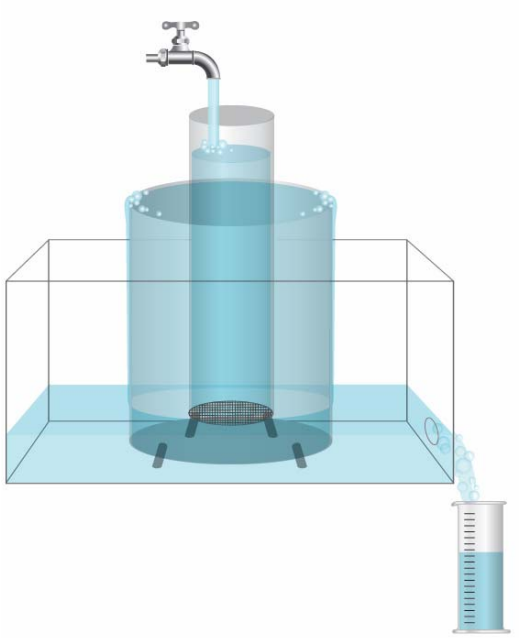

Figure 4.19: Test setup for determining geotextile permittivity

Prior to placing the geotextile samples within the apparatus, they are soaked for a minimum of 24 hours to allow the water to penetrate the pores. De-aired water was not used for permittivity testing because a value reflecting field conditions is desired. Water supplied by the fire hydrant (potable water line) which subsequently cascades across the No. 4 aggregate upon filling up the French drain, contains and produces entrapped air, respectively. Entrapped air in the water reduces the permittivity of the geotextile, thus the conservative approach was taken to measure the permittivity of the geotextile samples in this state. Upon placing the geotextile in the apparatus, both sides of the geotextile surface are inspected to insure excessive bubbles are not present. Water is then supplied at a rate to obtain the desired head difference across the system. As required in ASTM 4491, the permittivity is determined under a head difference of 50 mm. Three control geotextile samples were tested. Three flow rates per geotextile sample (three samples/trials) were used to calculate an average permittivity value for that given geotextile, as shown in Table 4.4. The standard deviation (SD) between the three samples was also calculated. The results show that the geotextile permittivity when used with air entrapped water is slightly lower at 1.1 sec^{-1} as compared to the manufacture's value of 1.6 sec^{-1} using de-aired water. The apparatus constructed for this experiment was able to obtain values of 1.6 sec^{-1} for the geotextile only for the first 30 seconds of testing, before the geotextile had time to build up microbubbles in the pore structure of the geotextile. All values in Table 4.4 are for when the microbubble pore structure and flow rates reached steady-state.

Table 4.4: Permittivity values of nonwoven geotextile samples

	Trial 1 (n = 3)	*Trial* 2 (n = 3)	*Trial* 3 (n = 3)	Overall Average (n = 9)	SD
Permittivity (sec^{-1})	1.09	1.10	1.12	1.10	0.01

4.6.2. Permittivity Testing Results of the Filter Fabric After 12 Months

Upon completion of the groundwater mounding discharge and flow rate monitoring phase of the French drain experiment, parts of each French drain were exhumed, and geotextile samples were taken. Four samples from each trench (top, middle, bottom of the side and underneath) were obtained for the permittivity testing. Geotextile samples taken from the in situ French drains are present in Figure 4.20.

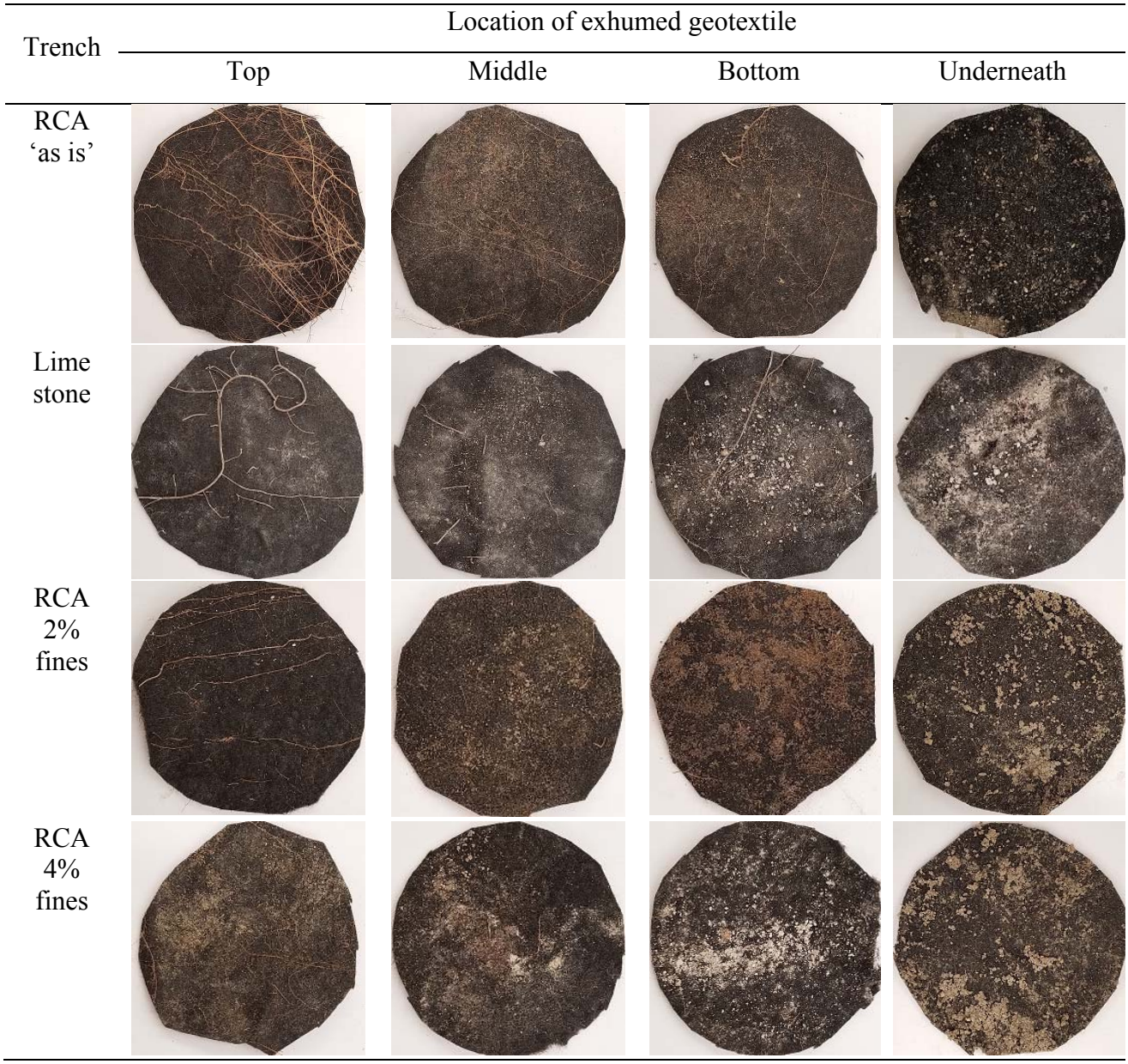

Figure 4.20: Geotextile samples exhumed from French drains

Comparing the permittivity values of the in situ and unused geotextile samples can provide insight into the level of clogging within each French drain. The exhumed samples were tested with the same test setup seen in Figure 4.19 and under the same test procedure. Four exhumed geotextile samples were tested for each French drain. Three flow rates per exhumed geotextile sample were used to calculate an average permittivity value for a given geotextile. Table 4.5 summarizes the permittivity values of each sample taken from the field.

Table 4.5: Permittivity values of unused and in situ nonwoven geotextiles

	Permittivity (sec^{-1})			
	Top	Middle	Bottom	Underneath
Unused geotextile	1.10*	1.10*	1.10*	1.10*
RCA 'as is'	0.98	0.80	0.75	0.59
Limestone	0.97	0.79	0.65	0.44
RCA with 2% fines	0.91	0.82	0.69	0.53
RCA with 4% fines	0.88	0.78	0.64	0.41

(* permittivity for the unused geotextile regardless of location in French drain)

Permittivity ratio was proposed to quantify the level of "clogging" in geotextiles. Permittivity ratio was defined as the ratio of the permittivity of the exhumed geotextile to that of the permittivity of the control geotextile (1.10 sec^{-1} in this study). The permittivity ratio of each exhumed geotextile can be calculated by using the equation below:

$$\text{Permittivity ratio (\%)} = \frac{Permittivity\ of\ In{-}situ\ Geotextile*}{Permittivity\ of\ Unused\ Geotextile}$$

(* After 12 months of field simulation)

The ratio for an unclogged geotextile is equal to 1.0, indicating no change in flow capacity of the geotextile. The comparison of permittivity ratio for each sample is presented in Figure 4.21. For the exterior drains, the reduction of permittivity for RCA 'as is' is similar to limestone for the locations of Top and Middle; however, limestone shows larger reduction than RCA 'as is' in the locations of Bottom and Underneath. Because limestone has more fines (about 2.2%) than RCA 'as is' (about 0.8%), fines migrate downward and build up along the bottom portion of the French drain. The photos of the in situ geotextiles (Bottom and Underneath) of limestone (see Figure 4.20) clearly show more fines in comparison with exhumed geotextiles of RCA 'as is'. In case of the interior drains, both RCA with 2% and 4% fines exhibit overall reduction in permittivity ratio, but RCA 4% fines shows a larger reduction than RCA with 2% fines. Unlike the exterior drains, higher fines content (4% in this study) caused clogging along the all depths.

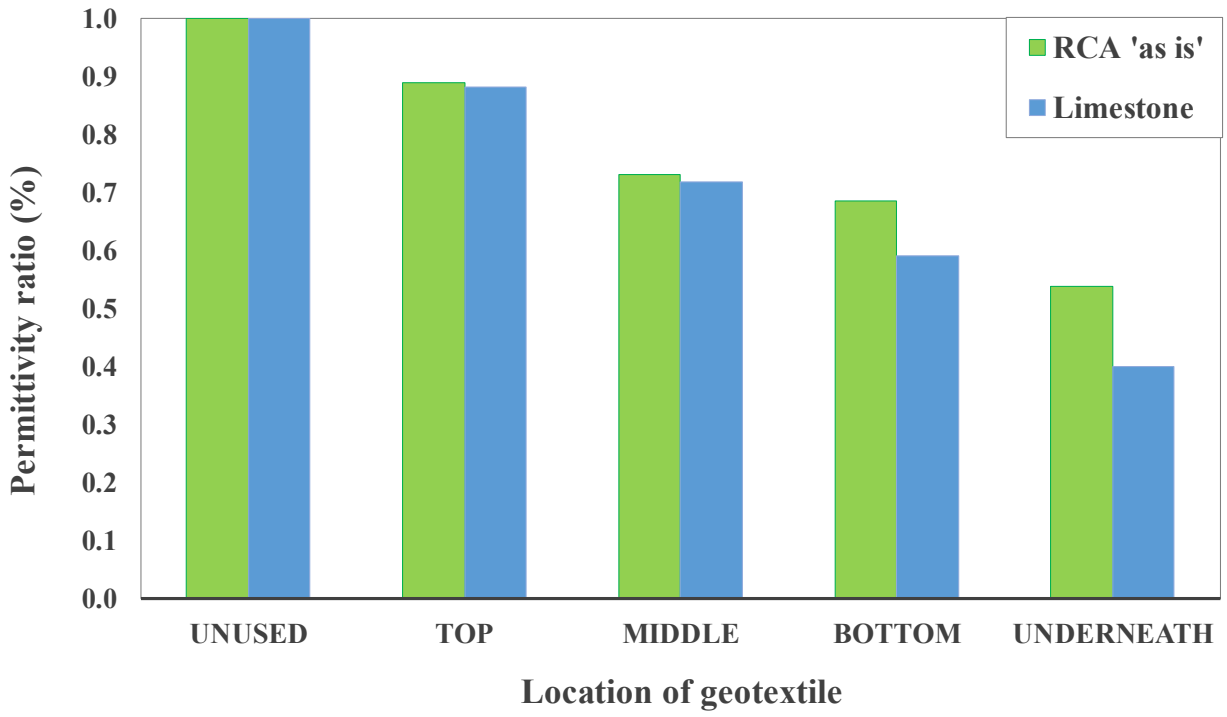

(a) Exterior drains

(b) Interior drains

Figure 4.21: Permittivity ratio of in situ geotextiles

5. RCA MATERIAL CHARACTERIZATION

5.1. Evaluation of Field Geochemical Reaction of In Situ RCA

A field RCA model was developed to evaluate the short- and long-term chemical clogging potential of in situ RCA such as re-cementation and calcite precipitation. RCA No.4 aggregates used for RCA French drain were wrapped by geotextile and placed underground with 2-ft cover depth and kept under in situ condition with different periods of time (at 6, 12, and 18 months). A petrographic examination method (e.g. XRD) was then performed on the aggregate samples taken from the field at 6, 12, and 18 months.

5.1.1. Material and Test Description

In situ RCA field model setup

For the RCA field model, four different types of aggregate were prepared and embedded underground in a loose condition. The aggregate types included: virgin limestone, RCA 'as is' (0.8% fines), and RCAs with additional 2% and 4% fines. Three specimens for each setup were prepared for testing at 6, 12, and 18-month intervals. The schematic diagram of the test setup is shown in Figure 5.1. Figure 5.1 (a) shows the depth profile (cross-sectional view) of the *in situ* RCA test setup. Figure 5.1 (b) shows the top view of the *in situ* RCA test setup. The volume of aggregate placed in each setup was 1.57 cubic ft. All aggregate specimens were wrapped in geotextile and placed into the same soil type as the constructed French drains. Non-woven D-3 geotextile was purchased from ACF Environmental Inc. and approved by the State Materials Office (SMO). The samples in each row shown in Figure 5.1 (b) were tested at different times. For example, Specimens 1-1 through 1-4 were tested at 6 months and Specimens 2-1 through 2-4 were tested at 12 months. Specimens from 3-1 through 3-4 were tested at 18 months.

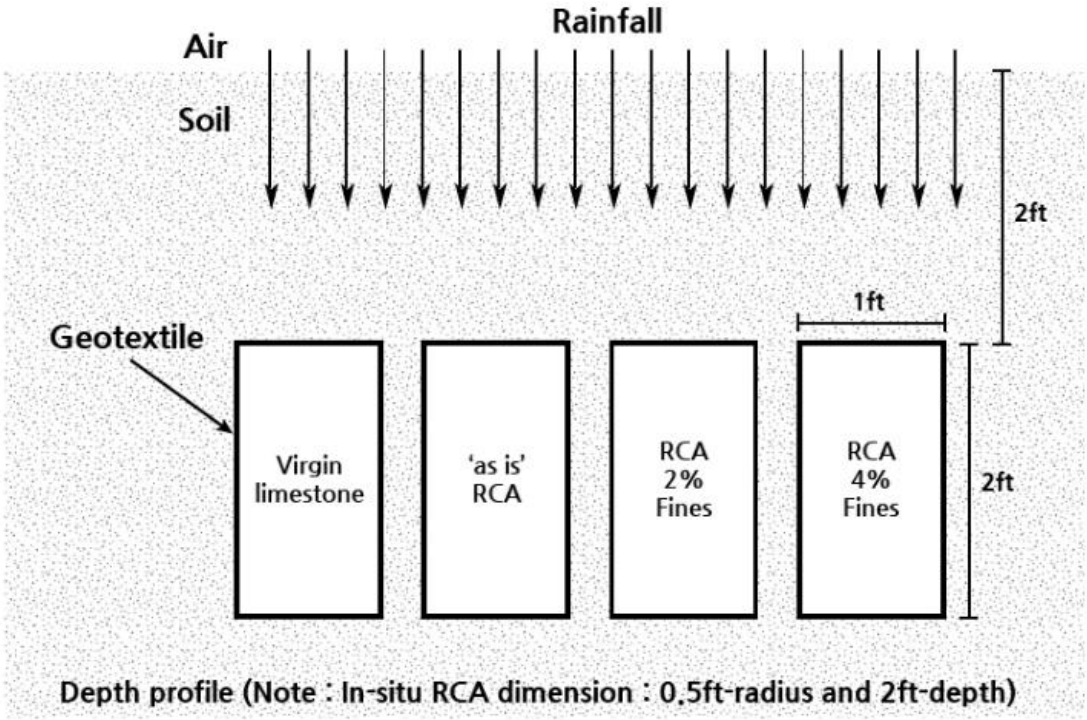

(a) Depth profile (cross-sectional view) of the *in situ* RCA test setup

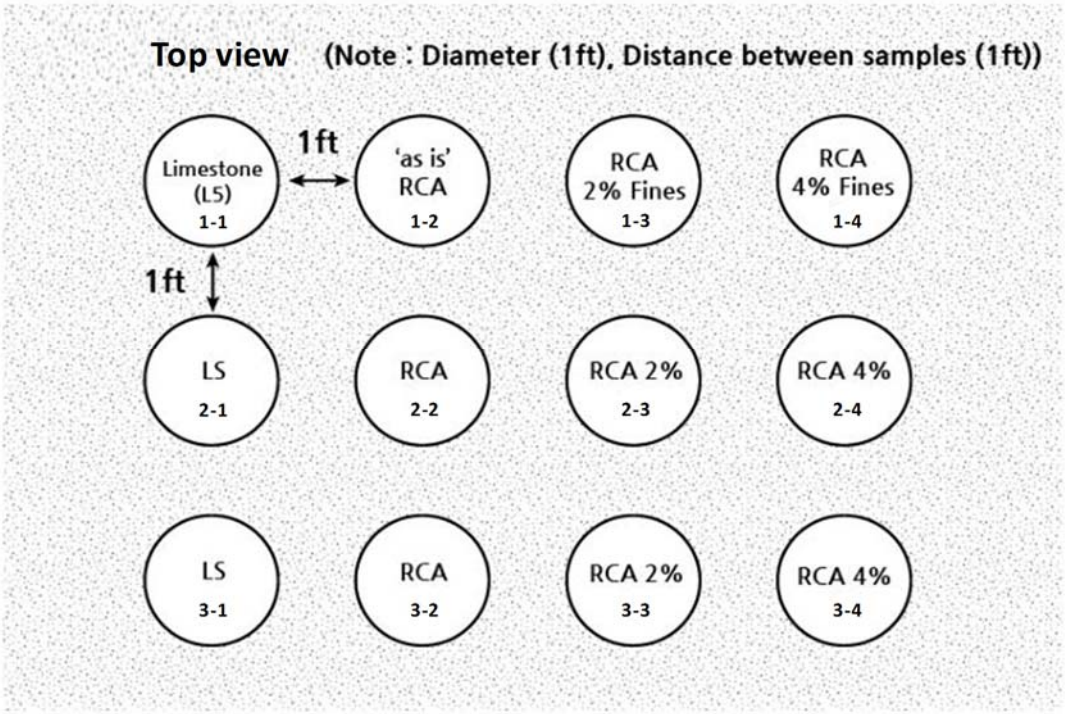

(b) Top view of the *in situ* RCA test setup (note: Specimen IDs are presented in each circle)

Figure 5.1: *In situ* test setup for evaluating the recementation and calcite precipitation (tested after 6, 12, and 18 months)

Materials

Limestone and RCA samples ('as is', 2% and 4% additional fines) were kept under *in situ* conditions for 6, 12, and 18 months respectively and were prepared for evaluation of the potential for short- and long-term re-cementation and calcite precipitation. The samples conditioned for 6, 12, and 18 months were removed from the ground and the aggregates were pulverized for the XRD test. XRD was used to identify crystalline structures in the RCA, which provided information on the basic chemical/mineralogical components of RCA. Figures 5.2, 5.3 and 5.4 show limestone and RCA samples in geotextile removed from the ground after 6, 12, and 18 months. Visual inspections did not show any noticeable changes between limestone and RCA samples.

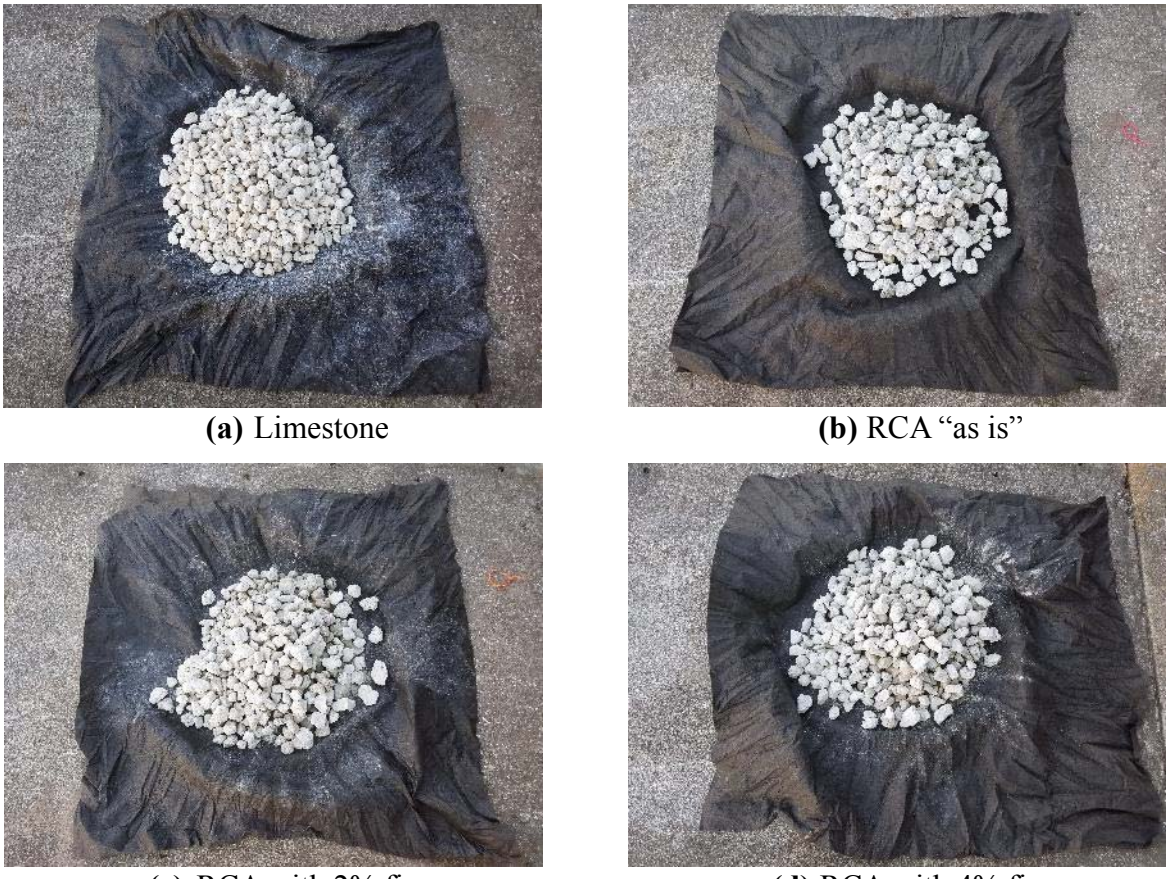

(a) Limestone **(b)** RCA "as is"

(c) RCA with 2% fines **(d)** RCA with 4% fines

Figure 5.2: Limestone and three different types of RCA after 6-month period

(a) Limestone

(b) RCA "as is"

(c) RCA with 2% fines

(d) RCA with 4% fines

Figure 5.3: Limestone and three different types of RCA after 12-month period

(e) Limestone

(f) RCA "as is"

(g) RCA with 2% fines

(h) RCA with 4% fines

Figure 5.4: Limestone and three different types of RCA after 18-month period

5.2. XRD Analysis

Powder X-ray diffraction (XRD) analysis was conducted on all aggregate samples for further investigation. To perform XRD analysis, the samples conditioned for 6, 12, and 18 months were removed from the ground and pulverized to fine particles by using a ball mill. The powder samples were then chemically/mineralogically characterized by XRD according to ASTM C295. The powdered *in situ* samples for 6, 12, and 18-months are shown in Figures 5.5, 5.6, and 5.7. The sample with blue mark indicates the pulverized limestone. Samples with pink, orange and yellow marks represent that those samples are RCA 'as is', RCA with 2% fines, and RCA with 4% fines, respectively.

Figure 5.5: Ground limestone and RCAs (as is, 2% fines, and 4% fines) at 6-months.

Figure 5.6: Ground limestone and RCAs (as is, 2% fines, and 4% fines) at 12-months.

Figure 5.7: Ground limestone and RCAs (as is, 2% fines, and 4% fines) at 12-months.

The results of XRD Analysis

The results of the XRD test on all samples at 6, 12, and 18-months are shown in Figures 5.8 through 5.10. The key components investigated in the analysis were calcite ($CaCO_3$) and portlandite ($Ca(OH)_2$) because the purpose of this test was: (1) to determine the level of calcite precipitation due to portlandite in RCA which may cause clogging of a geotextile filter and (2) to evaluate the relative amount of calcite in RCA. Although the solubility of portlandite is higher than calcite, calcite can also be a donor of calcium cations which can cause calcite precipitation. Different types of crystal structures (for examples, calcite, portlandite and quartz, etc.) were identified by the XRD diffraction angle (x-axes of Figures 5.8 through 5.10, 2θ).

According to the Klug (1974) and Moore (1989) formulas, the intensity (y-axes of Figures 5.8 through 5.10) of the XRD result offers information about the percentage of each crystal structure in the mixture. Based on this assumption, the intensities of calcite and portlandite in limestone and RCA samples (as is, 2%, and 4% fines) were compared with each other to evaluate the relative quantity of calcite as well as portlandite. The XRD setup was the same for all samples.

As shown in figures 5.8 through 5.10, limestone had the highest amount of calcite among all samples because the main chemical compound of limestone is calcite. For RCA samples, the only variable among samples was the different percentages of RCA fines. There was no significant difference in the amount of calcite between RCA 'as is' and RCA with 2% fines. The intensity differences on the amount of calcite at 6, 12 and 18-months were less than 100. Intensities of RCA 'as is' on calcite are around 5,400, 6,000, and 6,010 at 6, 12, and 18-months. On the other hand, RCA with 4% fines produced a relatively high amount of calcite compared to the previous two samples (RCA 'as is' and 2% fines) based on XRD results. Intensities of RCA with 4% fines on calcite were around 7,000, 7,360, and 7,400 at 6, 12, and 18-months, respectively.

In addition, there was no significant difference in the amounts of portlandite from RCA 'as is' and RCA with 2% fines. For instance, the intensity differences in the amount of portlandite between RCA 'as is' and RCA with 2% fines at 6, 12 and 18-months were less than 100. Intensities of RCA 'as is' on portlandite were around 1,783, 1,770, and 1,710 at 6, 12, and 18-months. By contrast, RCA with 4% fines showed a relatively lower value of portlandite in the XRD data compared to the previous two samples (RCA 'as is' and 2% fines). Intensities of RCA 4% fines on portlandite are 1,300, 1,200 and 1,190 at 6, 12, and 18-months.

Larger surface area creates a greater rate and amount of concrete carbonation which is involved in the chemical reaction, which in turn increases the formation of calcite from portlandite. The XRD data showed that there was portlandite in all RCA samples. RCAs with 2% and 4% fines provided more surface area per unit mass due to the presence of fines when compared to RCA 'as is'. RCAs with 2% and 4% fines have a higher chance to be transformed from portlandite to calcite, resulting in a higher amount of calcite as well as a lower amount of portlandite.

XRD data measured at 18 months illustrated no significant difference in the intensity of portlandite and calcite between RCA 'as is' and RCA with 2% fines. On the other hand, RCA with 4% fines exhibited the highest levels of calcite and the lowest levels of portlandite. Portlandite is a byproduct of cementation hydration. Reduced portlandite in RCA with 4% fines supports the conclusion that little calcite precipitation has occurred in the *in situ* RCA.

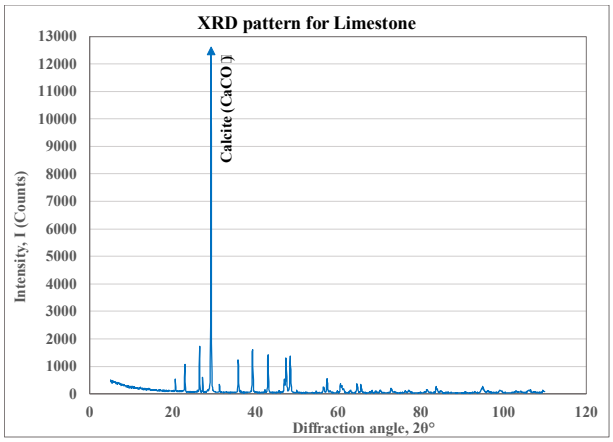

(a) Limestone

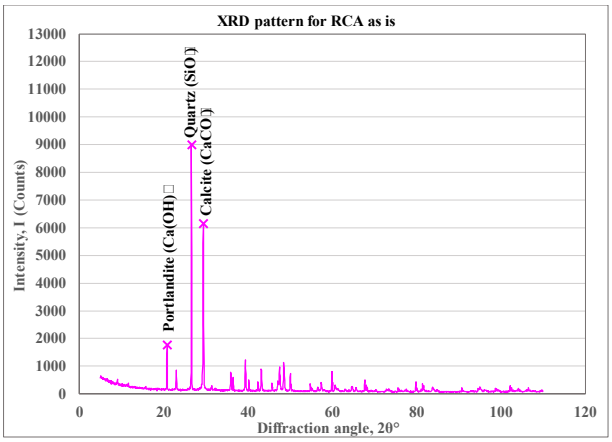

(b) RCA 'as is'

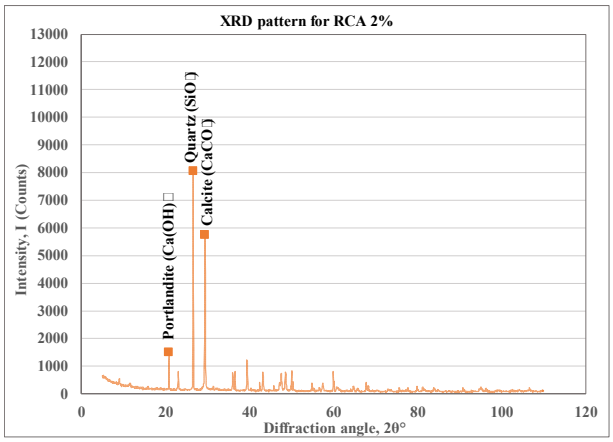

(c) RCA with 2% fines

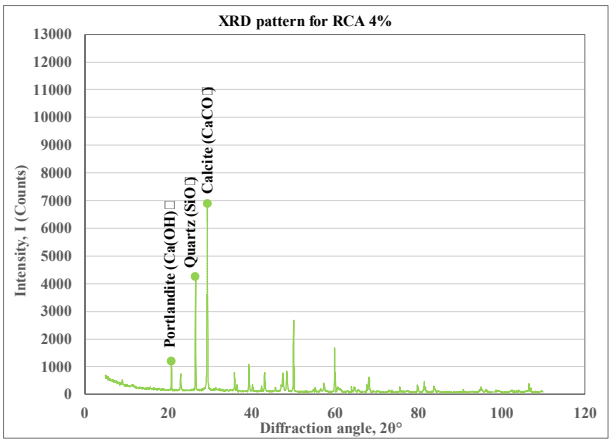

(d) RCA with 4% fines

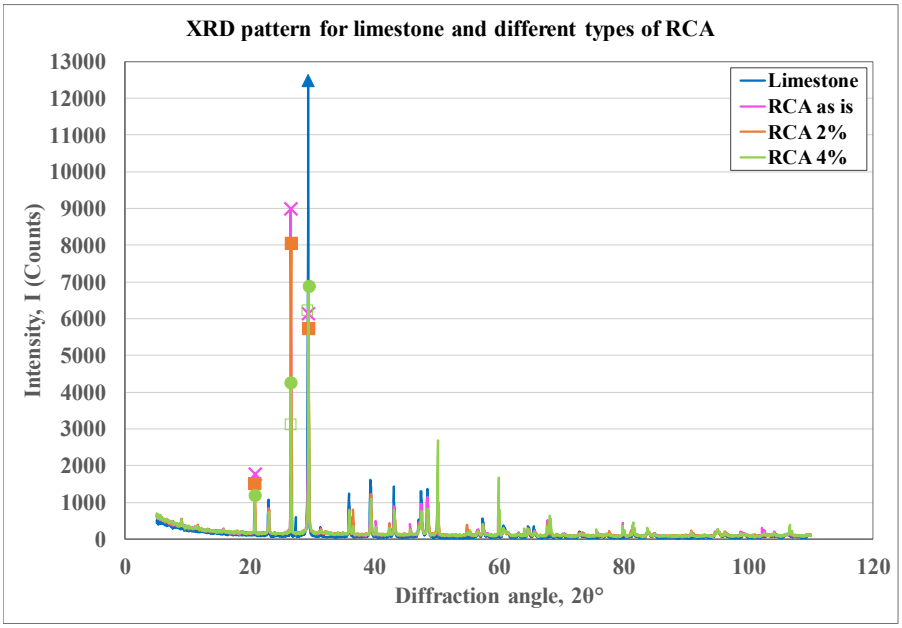

(e) Comparison of XRD results on all samples

Figure 5.8: XRD results of ground limestone and RCAs at 6-months

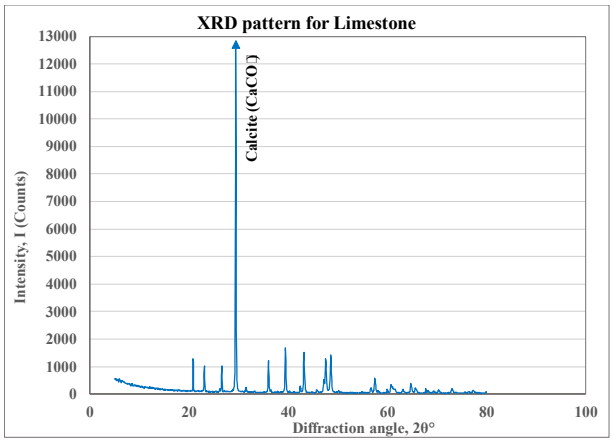

(a) Limestone

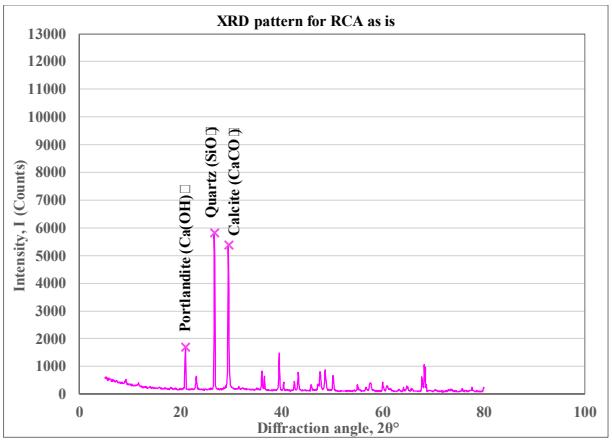

(b) RCA 'as is'

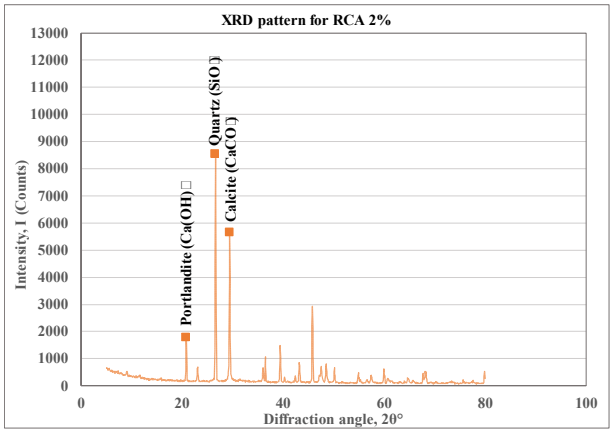

(c) RCA with 2% fines

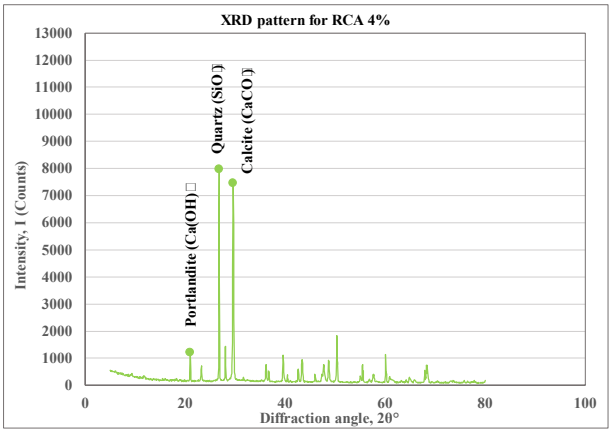

(d) RCA with 4% fines

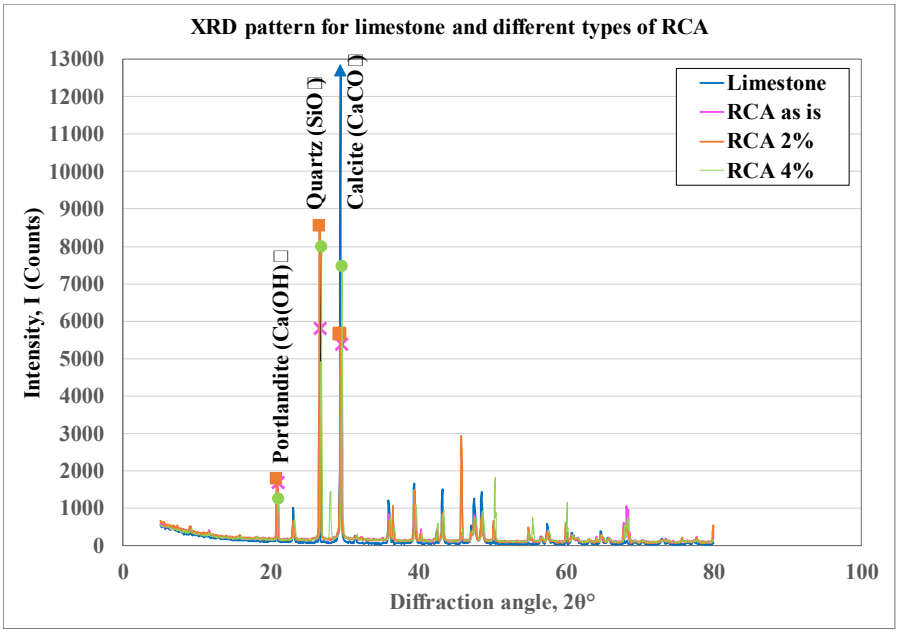

(e) Comparison of XRD results on all samples

Figure 5.9: XRD results of ground limestone and RCAs at 12-months

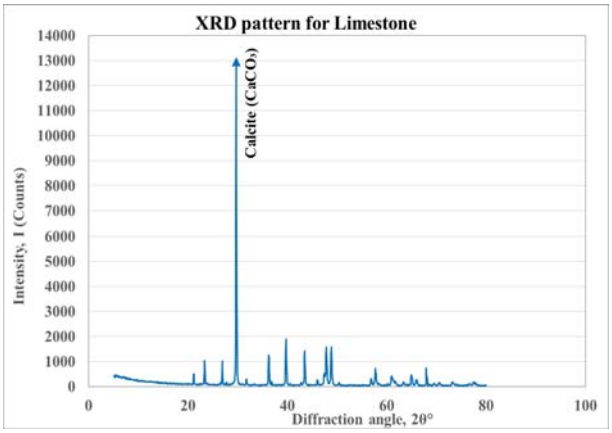

(a) Limestone

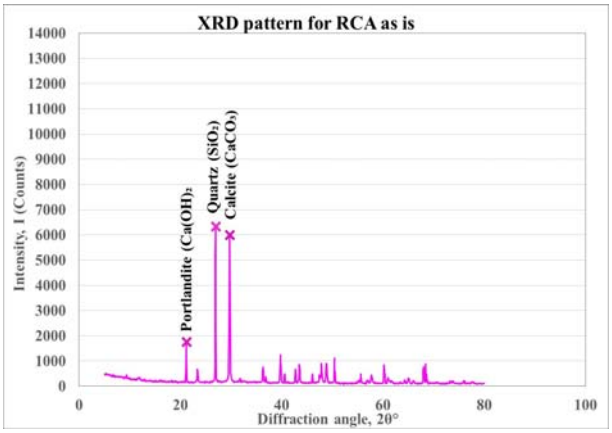

(b) RCA 'as is'

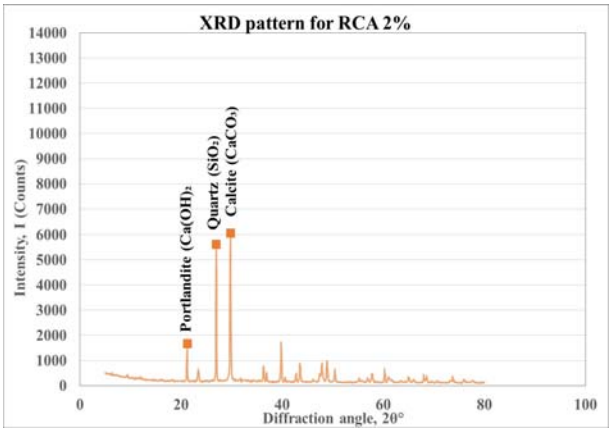

(c) RCA with 2% fines

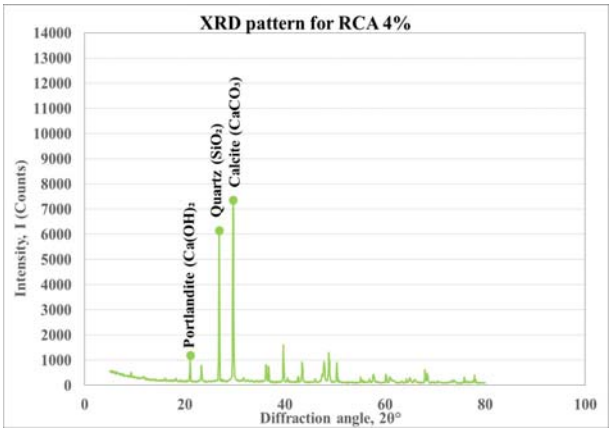

(d) RCA with 4% fines

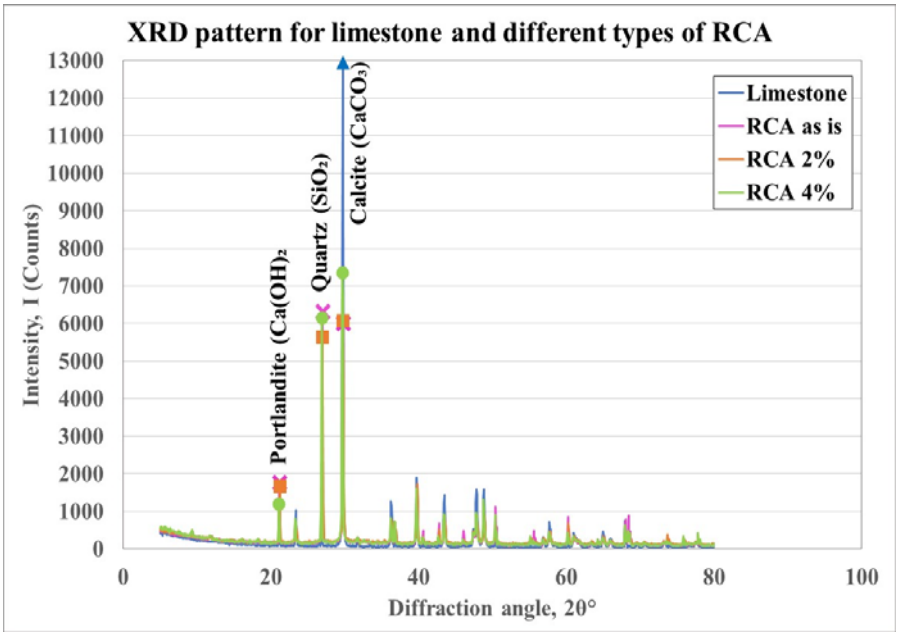

(e) Comparison of XRD results on all samples

Figure 5.10: XRD results of ground limestone and RCAs at 18-months

5.3. Findings

The research has compared XRD results for each sample. The RCA source, production process, and storage condition significantly vary, and these source material variations can affect the XRD results. Thus, the intensities of calcite and portlandite are normalized by the intensity of quartz, which is the major component of sand in concrete. Types and minerals of coarse aggregate vary significantly but sand is a standard material in concrete mixtures.

Figures 5.11 and 5.12 show the XRD results on calcite and portlandite, with the different elapsed times (6, 12, and 18 months). Figure 5.11 indicates that limestone samples had the highest calcite intensity at all times among all samples because its main chemical compound is calcite. In addition, the limestone showed no noticeable change of intensity with different elapsed times. For the RCA samples, the results showed a slight increase in calcite with increasing elapsed time (see Figure 5.11). However, this increase is not significant considering the range of variations by material and test. RCA with 2% fines shows a similar level of calcite, while RCA with 4% fines shows somewhat higher calcite peaks than other samples. This data (see Figure 5.11), suggests that RCA with 4% fines with large surface area and more portlandite may have produced faster and higher calcite precipitation than other RCA aggregate. Figure 5.12 shows the XRD intensity of portlandite for RCA samples. The XRD results show a tendency for decrease in portlandite with the increasing elapsed times. This decreasing tendency indicates that carbonation of portlandite in RCA samples was occurring with time.

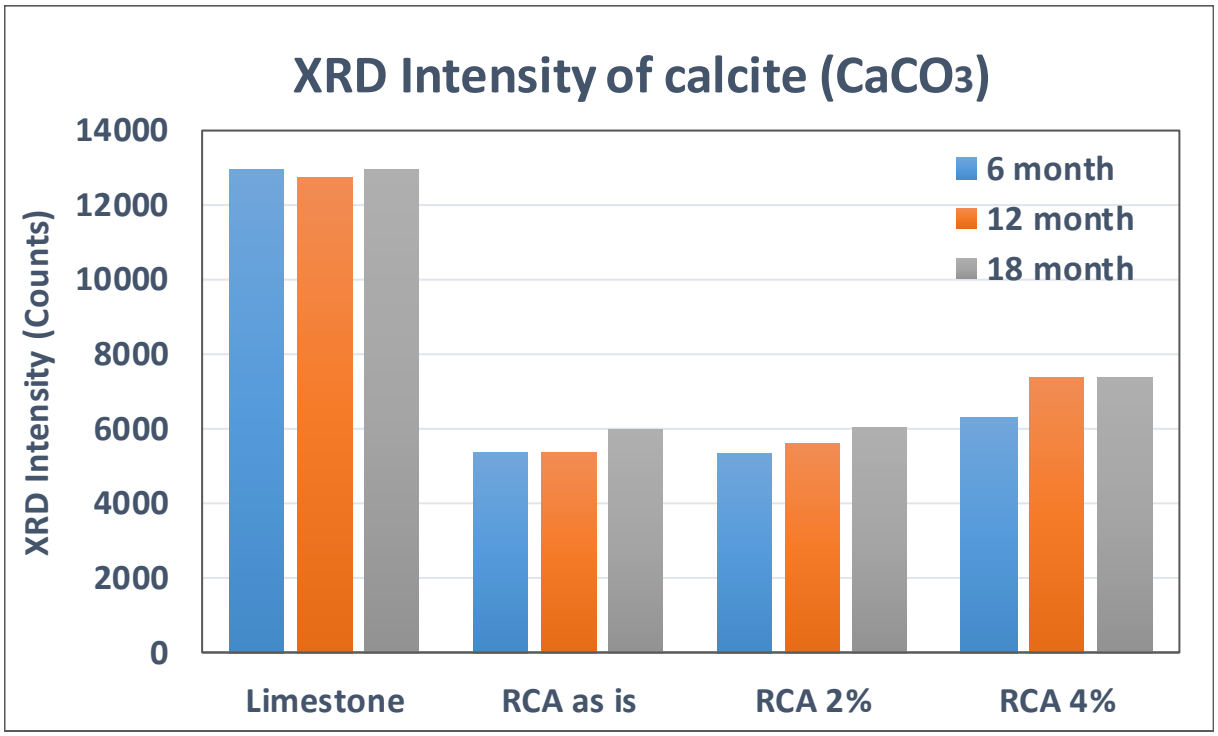

Figure 5.11: Comparison of XRD intensity results (calcite)

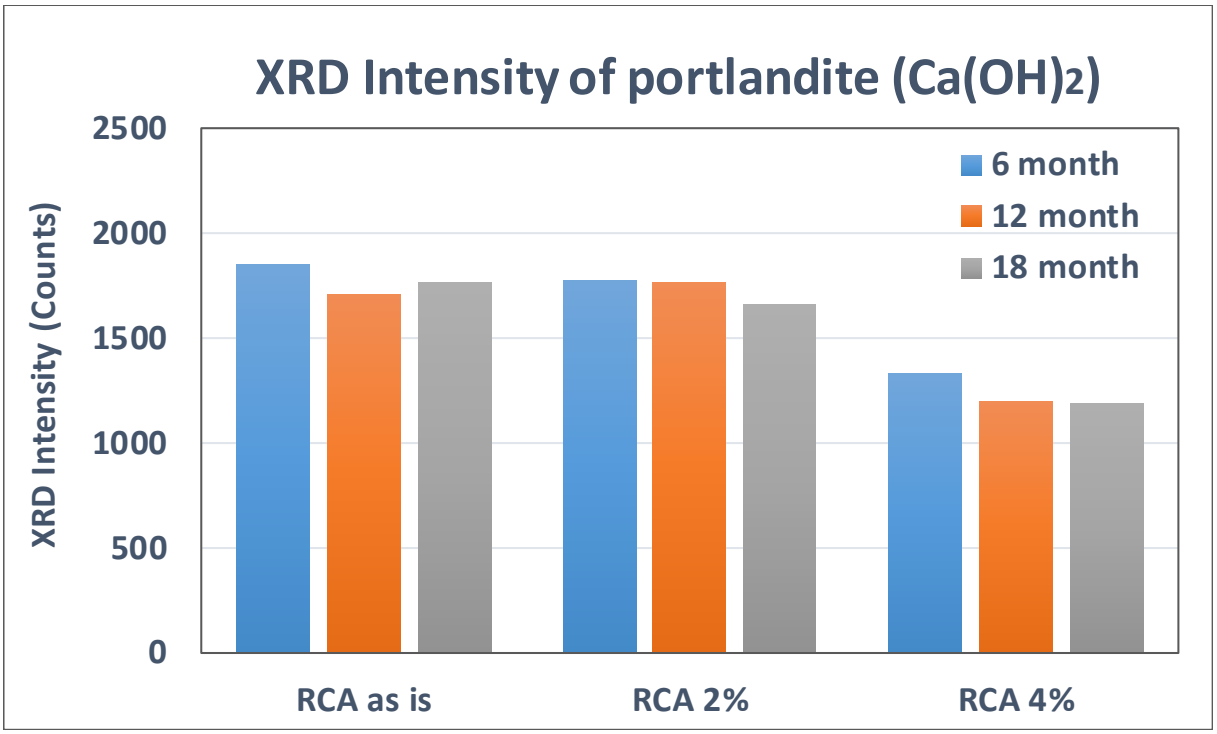

Figure 5.12: Comparison of XRD intensity results (portlandite)

5.4. Discussion

It is important to note that XRD is mainly used to identify crystalline minerals and the XRD intensity is an indirect indicator to estimate the amount of those crystalline minerals. Thus, the XRD results may show a trend but not exact amounts of calcite and portlandite. In addition, the "inherent" test variation (due to moisture, temperature, operator's skill, etc.) is reported as about 10%.

Based on the results of XRD test, the research has concluded the following:

1. Calcite in RCA slightly increases with the elapsed time (due to carbonation). Although limestone shows higher calcite than all RCA samples, it does not show an appreciable change with time.

2. RCA 'as is' and RCA with 2% fines exhibit similar performance, showing a similar level of calcite at all times.

3. RCA with 4% fines shows the highest calcite and the lowest portlandite among the RCA samples. RCA fines having large surface area and portlandite can be a major factor producing precipitation. RCA with more than 4% fines of RCA should not be permitted in French drain systems.

6. CONCLUSIONS AND RECOMMENDATIONS

6.1. Conclusions

This study was aimed at evaluating the effects of RCA on the field drainage performance of French drain.

The following conclusions have been made:

- Based on the field monitoring over 1 year, the drainage performance of RCA French drain is mainly controlled by in situ soil conditions (e.g. groundwater table, permeability of surrounding soils, etc.) and the amounts of excessive fines in the drain system; however, the aggregate type does not appear to be a major factor affecting the exfiltration drainage performance of French drain.

- Upon camera inspection of the French drain systems it was concluded that no surrounding aggregate or precipitation deposited into the pipes. However, the crowns of the pipes seem to be within the root zone of the overlying vegetation, which can be seen entering the pipes. It is assumed that the roots were traveling between the 1-foot overlaps in the geotextile or alternatively, but less likely, have punctured the geotextile. But, the presence of the roots was not enough to interrupt the flow of water.

- When comparing RCA 'as is' (0.8% fines) with limestone (2.2% fines) it was observed that RCA performed better than limestone regarding flow rate (i.e. steady-state exfiltration rate at full storage) and maximum discharge rate (i.e. recovery period). To take into account the effect of the 1.4% fines difference between RCA 'as is' and limestone, the impact of fines between RCA with 2% fines and RCA with 4% fines was used. The 2% fines difference between RCA 2% and RCA 4% caused a reduction in flow rate of 17.8% based upon $Q_{avg-max}$. Even if RCA was extrapolated to contain 2.2% fines and was reduced the full amount assuming 2% fines increase (even though it would actually be a 1.4%) this would result in a $Q_{avg-max}$ value of 6.68(1-0.178) = 5.49, still above the $Q_{avg-max}$ for limestone of 5.38. Thus, when taking into account the fines difference between RCA 'as is' and limestone French drains, it can be seen that RCA performs similar if not better than limestone.

- The reduction of flow rate and discharge rate of French drain consisting of limestone is not only the material difference, but also the fines content. An increase in fines content shows a noticeable decrease in flow rate. When comparing RCA 'as is' (0.8% fines) with limestone (2.2% fines), this 1.4% difference in fines content resulted in a 19.5% reduction in $Q_{avg-max}$. When comparing RCA with 2% fines with RCA with 4% fines, this 2% difference in fines content resulted in a 17.8% reduction in $Q_{avg-max}$. Thus, approximately a 1.5 to 2.0% increase in fines content within the range of 0% to 4% fines results in a 20%

decrease in flow rate.

- In the discharge monitoring experiment, RCA with 2% fines and RCA with 4% fines (both interior drains) have much greater discharge rate than limestone and RCA 'as is' close to the maximum storage water level because the two interior drains have double-sided drainage paths. However, the discharge rate of the two interior drains seems to diminish quicker than the exterior drains as the water level within the drains decreases because the RCA fines migrate and deposit at the bottom and bottom-side walls. More fines on the bottom of the drain will cause a reduction in the permittivity of geotextile at the bottom; as a result, the bottom permittivity becomes more influential on the discharge rate of the drain systems. This indicates that the effect of fines may have more of an impact on the initial dissipation stage rather than the latter dissipation stage.

- On the basis of the correlation between flow rate measurement and groundwater table depth, both the initial GWT and fines content affect the drainage performance of French drains. The flow rate gradually increases in proportion to the depth of the initial GWT for both exterior and interior French drains. The slope of the data between flow rate and GWT trends seem to be due to the French drain drainage conditions, whereas the vertical offset of the lines seems to be due to the fines content. Both exterior French drains have a similar response to changes in the groundwater table depth, as shown by the near parallel slopes of the data. The interior French drains also share similar slopes with each other, but the slopes are flatter when compared to the exterior drains. This flatter slope behavior of interior drains may indicate that the drainage performance of French drain, which contains more fines contents, might be hindered by clogging at the bottom and sidewalls of French drain despite the relatively deep depth of initial GWT during dry session.

- Calcite in RCA slightly increases with the elapsed time (due to carbonation). Although limestone shows higher calcite than all RCA samples, it does not show an appreciable change with time. RCA 'as is' and RCA with 2% fines exhibit similar performance, showing a similar level of calcite at all times. RCA with 4% fines shows the highest calcite and the lowest portlandite among the RCA samples. RCA fines having large surface area and portlandite can be a major factor producing precipitation.

- The permittivity test results show that RCA with 4% fines show higher reduction in permittivity measurement after 12-month field conditioning. In addition, RCA with 2% fines and limestone drains have similar values of permittivity due to probably similar amount of fines content. It is concluded that the fines content is the major controlling factor on the permittivity measurement rather than the aggregate type.

- This study investigated the effects of fine content on the exfiltration drainage performance of French drains through multiple laboratory and field tests (e.g. in-situ flow test, camera inspection, XRD analysis, and permittivity test). It is shown that fines can contribute to

physical clogging and also clogging due to chemical precipitation in the filter fabric. In this study, the fines ranged from 0.8% to 4 % have been used in constructing the field French drains. Among all French drains, the French drain with 4 % fines showed the lowest exfiltration drainage performance, indicating a distinguishable reduction in the flow and discharge rate. In addition, 4% fines of RCA showed higher intensity of calcite in the XRD analysis, indicating higher potential of calcite precipitation. However, considering the general trend of performance reduction over time for all French drains, the reduction performance of 4% fines is still in an acceptable range. It is important to note that the maximum percentage of fines used in this project was 4%. Therefore, it is concluded that more than 4 % fines at a project site should not be permitted in French drain systems.

6.2. Recommendations

- The aggregate sourced for this project was produced using a cone crusher. It is known that this type of crusher generates lower fines content compared to other crushing types (e.g. impact crusher). A low fines generation crushing method is recommended to RCA manufacturing facilities. Fines generated from the RCA manufacturing process may be further reduced by using a blower system to remove fines from the aggregate as it drops from atop of the conveyor belt towards the aggregate stockpile.

- Outdoor storage of aggregate prior to use may be beneficial with respect to: (1) a chance for any un-hydrated cement fines to come into contact with moisture to produce hydration products such as calcium silica hydrate (CSH) and portlandite (CH) and (2) a chance for neutralization of CH with carbon dioxide to transform CH into calcite. Because the solubility of CH in water is 1,000 times higher than calcite, it is desirable to neutralize CH into calcite to avoid the calcium ion donation needed for calcite precipitation on the geotextile (solubility: $CaCO_3$ (5.5×10^{-6}), $Ca(OH)_2$ (3.3×10^{-3}) . Moreover, any rain event can wash out fines and reduce the fines content of RCA.

- If the RCA manufacturing process yields a relatively high fines content and no space and time available for rain-wash, or neutralization, then it is recommended to add washing (e.g. pressure washing) to the manufacturing process.

6.3. Recommended Future Work

- Long-term monitoring (e.g. longer than 1 year) is recommended so that the drainage performance can be compared and analyzed under similar seasonal effects, such as similar ground water table, soil moisture condition, etc., and also the long-term performance model of the RCA French drain can be developed.

- Fines generation resulting from transportation, discharging and placing of RCA prior to construction may need to be determined in advance of the use of RCA in the French drain. Thus, the total amount of fines generation of RCA from each step of French drain construction can be predicted and managed. RCA source variability needs to be identified prior to RCA use in the French drain because the physical properties and mineral compositions of RCA affect the drainage performance of the French drain. Petrographic analyses can be used to develop the material specification for the maximum level of un-hydrated cement grains (e.g. C_2S, C_3S, C_3A, etc.), portlandite, calcite, etc.

REFERENCES

Alfakih, E., Barraud, S., Martinelli, I. (1999). A study of stormwater infiltration system feasibility and design. *Water Sci. Technol*. 39 (2), 225–231.

Argue, J.R., Pezzaniti, D. (2006). Infiltration Systems in Australian Runoff Quality, *Engineers Australia*, Sydney, Australia (Chapter 11).

Barrett, M.E., Irish-Jr L.B., Malina-Jr J.F. and Charbeneau R.J. (1998). Characterization of highway runoff in Austin, Texas, area. *J.Environ.Eng.*,124, 131-137.

Barrett, M.E., Taylor, S. (2004). Retrofit of storm water treatment controls in a highway environment. In: NOVATECH 2004, *Proceedings of the Fifth International Conference of Sustainable Techniques and Strategies in Urban Water Management*, pp. 243–250.

Bauve, J. M., Kotuby-Amacher, J., and Gambrell, R. P. (1988). The effect of soil properties and a synthetic municipal landfill leachate on the retention of Cd, Ni, Pb, and Zn in soil and sediment materials, *J. WPCF*, 60(3), 379-385.

Barraud, S., Gautier, A., Bardin, J.P., Riou, V. (1999). The impact of intentional stormwater infiltration on soil and groundwater. *Water Sci. Technol*. 39 (2), 185–192.

Bertrand-Krajewski, J.L., Chebbo, G. and Saget, A. (1998). Distribution of pollutant mass vs volume in stormwater discharges and the first flush phenomenon. *Water Res.*, 32, 2341-2356.

Bennert, T. and Maher, A. (2008). *The Use of Recycled Concrete Aggregate in a Dense Graded Aggregate Base Course*, Department of Civil & Environmental Engineering, Center for Advanced Infrastructure & Transportation (CAIT), Rutgers, The State University of New Jersey, Piscataway, NJ.

Bouwer, H. (2002). Artificial recharge of groundwater: hydrogeology and engineering, *Hydrogeology* 10 (1), 121–142.

Branscome, J., and Tomasello, S. R., (1987). *Field Testing of Exfiltration Systems* (Technical Publication 87-5). South Florida Water Management District (SFWMD)

Bruinsma, J. E., Peterson, K. R., and Snyder, M. B. (1997). Chemical approach to formation of calcite precipitate from recycled concrete aggregate base layers, *Transp. Res. Rec.*, 1577(1997), 10–17.

Braga, M. A., Silvestre, D. J., Brito, J. (2017). Compared environmental and economic impact from cradle to gate of concrete with natural and recycled coarse aggregates, *Journal of Cleaner Production*, 162 (20), 529-543.

Burton, G.A., Pitt, R.E. (2002). *Stormwater Effects Handbook—A Tool box for Watershed Managers*, Scientists, and Engineers. Boca Raton, FL, Lewis Publishers.

Canters, L. W., and Knox, R. C. (1985). *Septic tank system effects on ground water quality*, Chelsea, Mich, Lewis Publishers Inc.

Duchene, M. and McBean, A. E. (1992) Discharge Characteristics of Perforated Pipe for Use in Infiltration Trenches, *Water Resources Bulletin*, No. 92016.

Estanqueiro, B., Silvestre, J.D., de Brito, J., Pinheiro, M.D. (2016). Environmental life cycle assessment of coarse natural and recycled aggregates for concrete. *Eur. J. Environ. Civ. Eng.* 22 (4), 429-449.

Fathifazl, G., Abbas, A., Razaqpur, A.G., Isgor, O.B., Fournier, B., Foo, S. (2008). Recycled aggregate concrete as a structural material. *Canadian Civil Engineer*, 24.5 (Winter): 20-23

Gupta K. and Saul A.J. (1996). Specific relationships for the first flush load in combined sewer flows. *Water Res.*, 30, 1244-1252

Galli, J. (1992). *Analysis of Urban BMP Performance and Longevity in Prince George's County, Maryland 92711*. Prince George's County Department of Environmental Resources, USA.

Gerhardt, R. A. (1984). Landfill leachate migration and attenuation in the unsaturated zone and nonlayered coarse-grained soils, *Ground Water Monitoring Rev.*, 4(2), 56-65.

Goodrich, J.A., Phipps, D.W., Gorden, G.Z., Mills,W.R. (1990). Bottom plugging daynamics in recharge basins. In: *Proceedings of the Conference on Irrigation and Drainage*, Durango, CO, USA, pp. 369–376.

Hiller, J.E., et al. (2011). *Efficient Use of Recycled Concrete in Transportation Infrastructure*, Report RC-1544 to Michigan Department of Transportation. January 2011.

Ishizaki, K., Masahiro, L., Guangheng, N., Takeshima, M. (1996). Background of rainwater infiltration technology. In: *Proceedings of the Seventh International Conference on Urban Storm Water Drainage*, Hanover, Germany

Kim, J., Nam, B., Behring, Z., and Al Muhit, B. (2014). Evaluation of recementation reactivity of recycled concrete aggregate fines, *Transp. Res. Rec.*, 2401, 44–51.

Korre, A. and Durucan, S. (2009) Final Report: Aggregates Industry Life Cycle Assessment Model: Modelling Tools and Case Studies, EVA025, *Waste & Resources Action Programme*.

Knoeri, C., Mengual, E. S., and Althaus, J. H. (2013), Comparative LCA of recycled and conventional concrete for structural applications, *The International Journal of Life Cycle Assessment*, 18 (5), 909–918.

Klug, H.P. and L.E. Alexander. (1974). *X-ray diffraction procedures for polycrystalline and amorphous materials*[M]：New York, John Wiley＆ Sons.

Kim, J. (2013). *Structural and Material Health Monitoring of Cementitious Materials Using Passive Wireless Conductivity Sensors*, Ph.D. Dissertation, Department of Civil, Architectural and Environmental Engineering, University of Texas at Austin.

Lindsey, G., Roberts, L., Page, W. (1992). Inspection and maintenance of infiltration facilities. *J. Soil Water Conservation*. 47 (6), 481–486.

Lee, J.H. and Bang, K.W. (2000). Characterization of urban stormwater runoff. *Water Res.*, 34, 1773-1782.

Lee, B.C., Matsui, S., Shimizu, Y. & Matsuda, T. (2010) Characterizations of the First Flush in Storm WaterRunoff from an Urban Roadway, *Environ Technol*, 26(7), 773-782.

Langergraber, G., Haberl, R., Laber, J., Pressl, A. (2003). Evaluation of substrate clogging processes in vertical flow constructed wetlands. *Water Sci. Technol*. 48 (5), 25–34.

Muethel, R. W. (1989). *Calcium carbonate precipitate from crushed concrete*, Michigan Dept. of Transportation, Materials and Technology Division, Lansing, MI.

Moore, D. M. and R. C. Jr. Reynolds. (1989). *X-ray diffraction and identification and analysis of clay minerals* [M]：London, Oxford University Press.

Mikkelsen, P.S., Hafliger, M., Ochs, M., Tjell, J.C., Jacobsen, P., Boller, M. (1996). Experimental assessment of soil and groundwater contamination from two old infiltration systems for road run-off in Switzerland, *Sci. Total Environ*. 189–190, 341–347.

Mindess, S., Young, J. F. and Darwin, D. (2003). *Concrete,* Upper Saddle River, NJ, Prentice Hall.

Mehta, P. K. and Monteiro, J. M. (2006). *Concrete: Microstructure, Properties, and Materials*, New York, NY, McGraw-Hill.

Nam, B. H., Behring, Z., Kim, J., and Chopra, M. (2014). *Evaluate the use of reclaimed concrete aggregate in French drain application,* Rep. No. FDOT-BDK78-977-12, Florida Dept. of Transportation, Tallahassee, FL.

Nightingale, H. I. (1989). Artificial recharge of urban storm-water runoff. Artificial Recharge of Ground Water, *Proc., International Syrup*., A. I. Johnson and Donald J. Finlayson, eds., ASCE, New York, N.Y., 211-220.

Nozi, T., Mase, T., Murata, K. (1999). Maintenance and management aspect of stormwater infiltration system. In: *Proceedings of the Eighth International Conference on Urban Storm Drainage*, Sydney, Australia, vol. 3, pp. 1497–1503.

Poon, C. S., Qiao, X. C., and Chan, D. (2006). The Cause and Influence of Self-Cementing Properties of Fine Recycled Concrete Aggregates on the Properties of Unbound Sub-Base, *Waste Management*, 26(10), 1166-1172.

Paige-Green, P. (2010). Preliminary evaluation of the reuse of cementitious materials, *Proc., 29th Annual Southern African Transport Conf.*, Document Transformation Technologies, Centurion, South Africa, 520–529.

Pokrajac, D., Deletic, A. (2002). Clogging of infiltration drainage systems. In: International Conference on Sewer, *Operation and Maintenance*, Bradford, UK.

Pratt, C.J., Powell, J.J.M. (1993). A new UK approach for the design of subsurface infiltration systems. In: *Proceedings of the Sixth International Conference on Urban Storm Drainage*, Niagara Falls, Ont., Canada, 1, pp. 471–476.

Raimbault, G., Nadji, D., Gauthier, C. (1999). Stormwater infiltration and porous material clogging. In: *Proceedings of the Eighth International Conference on Urban Storm Drainage*, Sydney, Australia, vol. 2, pp. 1016–1024.

Reddi, L.N., Ming, X., Hajra, M.G., Lee, I.M. (2000). Permeability reduction of soil filters due to physical clogging. Geotech. *Geoenviron. Eng*. 126 (3), 236–246.

Row, R.K., Armstrong, M.D., Cullimore, D.R. (2000). Particle size clogging of granular media permeated with leachate. Geotech. *Geoenviron. Eng*. 126 (9), 775–786.

Rinck-Pfeiffer, S., Ragusa, S., Sztajnbok, P., Vandevelde, T. (2000). Interrelationships between biological, chemical, and physical processes as an analog to clogging in aquifer storage and recovery (ASR) wells. *Water Res*. 34 (7), 2110–2118.

Sansalone, J.J. and Buchberger, S.G. (1997). Partitioning and first flush of metals in urban roadway storm water, *J.Environ.Eng.*,123, 134-143.

Song, Y., Ooi, S.K., Hellebrand, E. and Muenow, D. W. (2011). Potential for Tufa Precipitation from Crushed Concrete Containing Coarse Basaltic and Fine Coralline Sand Aggregates, *Environmental and Engineering Geoscience*, 17(1), 53-66.

Schueler, T. R. and M. Helfrich. (1988). Design of Extended Detention Wet Pond Systems, Design of Urban Runoff Quality Controls. *Proceedings of an Engineering Foundation Conference on Current Practice and Design Criteria for Urban Quality Control*, Potosi, Missouri, pp. 180-200.

Simion, I.M., Fortuna, M.E., Bonoli, A., Gavrilescu, M. (2013). Comparing environmental impacts of natural inert and recycled construction and demolition waste processing using LCA. *J. Environ. Eng. Landsc. Manag*. 21 (4), 273-287.

Saint Johns River Water Management District (2010). *Applications handbook: Regulation of*

stormwater management systems chapter 40C-42.

Schueler, T. R. (1987). *Controlling urban runoff: a practical manual for planning and designing urban BMPs. Department of Environmental Programs*, Metropolitan Washington Council of Governments, Washington, D.C.

Snyder, M. (1995). Use of crushed concrete products in Minnesota pavement foundations, Rep. MN/RC-96/12, *Transportation Research Board*, Washington, DC.

Snyder, M., and Bruinsma, J. (1996). A review of studies concerning the effects of unbound concrete bases on PCC pavements drainage, *Transp. Res. Rec*., 1519, 51–58

Tam, V. W. Y. (2008). Economic comparison of concrete recycling: A case study approach, Resources, *Conservation and Recycling*, 52, 821-828.

Tamirisa, R. (1993). *Study of highway base/subbase aggregates that cause depositions of calcareous "Tufa" in drains*, Master's thesis, Dept. of Civil Engineering, Univ. of Toledo, Toledo, OH.

Viraraghavan, T., and Warnock, R. G. (1976). Groundwater pollution from a septic tile field, *Water, Air, and Soil Pollution*, 5(3), 281-287.

Warnaars, E., Larsen, A.V., Jacobsen, P., Mikkellsen, P.S. (1998). Longterm hydrology behaviour of stormwater infiltration trenches in central urban area. In: *NOVATECH '98*, Lyon, France.

Warnaars, E., Larsen, A.V., Jacobsen, P., Mikkelsen, P.S. (1999). Hydrologic behaviour of stormwater infiltration trenches in a central urban area during 23/4 years of operation. *Water Sci. Technol*. 39 (2), 217–224.

Wanielista, M.P. and Yousef, Y.A. (1993). *Stormwater management*, New York, John Wiley & Sons.

APPENDIX A

This appendix presents additional photos of the detailed construction procedure.

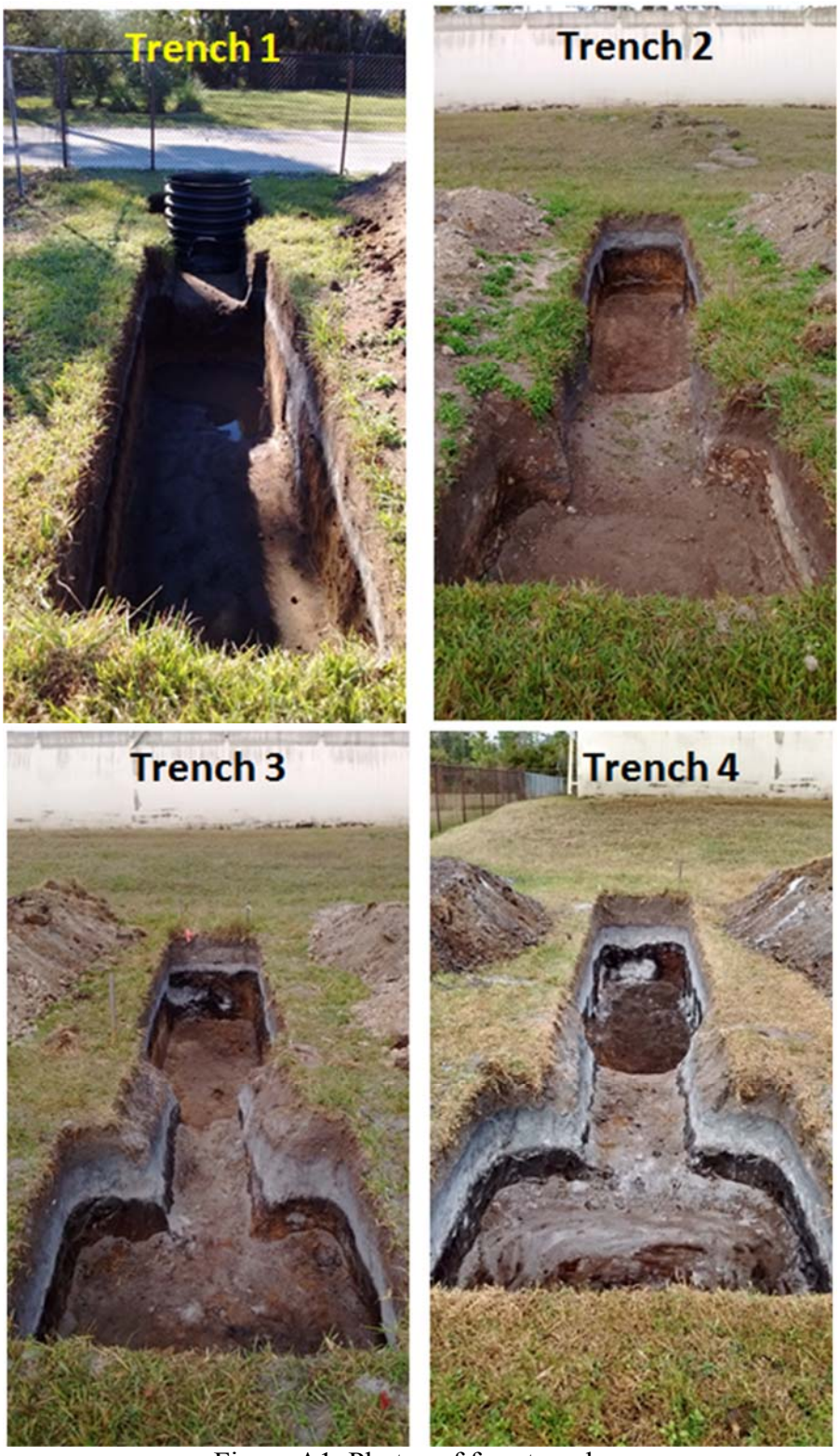

Figure A1. Photos of four trenches

Figure A2. End cap (up) and start of French drain (bottom)

Figure A3. Connection between French drain and sump

Figure A4. Construction of French drain